# DISSERTATION

# Gene Expression In Phenotypically Homogeneous Chondrocytes From Different Articular Cartilage Layers Of Equine Osteoarthritic And Control Joints: Method Validation And Gene Array Analysis


SUBMITTED BY

KATJA FRIEDERIKE DÜSTERDIECK

DEPARTMENT OF CLINICAL SCIENCES


IN PARTIAL FULFILLMENT OF THE REQUIREMENTS

FOR THE DEGREE OF DOCTOR OF PHILOSOPHY

COLORADO STATE UNIVERSITY

FORT COLLINS, COLORADO

SPRING 2007

INFORMATION TO USERS

The quality of this reproduction is dependent upon the quality of the copy submitted. Broken or indistinct print, colored or poor quality illustrations and photographs, print bleed-through, substandard margins, and improper alignment can adversely affect reproduction.

In the unlikely event that the author did not send a complete manuscript and there are missing pages, these will be noted. Also, if unauthorized copyright material had to be removed, a note will indicate the deletion.



ProQuest Information and Learning Company
300 North Zeeb Road
P.O. Box 1346
Ann Arbor, MI 48106-1346

COLORADO STATE UNIVERSITY

OCTOBER 31, 2006

WE HEREBY RECOMMEND THAT THE DISSERTATION PREPARED UNDER OUR SUPERVISION BY KATJA FRIEDERIKE DÜSTERDIECK ENTITLED "GENE EXPRESSION OF PHENOTYPICALLY HOMOGENEOUS CHONDROCYTES FROM DIFFERENT ARTICULAR CARTILAGE LAYERS OF OSTEOARTHRITIC AND CONTROL JOINTS: METHOD VALIDATION AND GENE ARRAY ANALYSIS" BE ACCEPTED AS FULFILLING IN PART REQUIREMENTS FOR THE DEGREE OF DOCTOR OF PHILOSOPHY.

COMMITTEE ON GRADUATE WORK

ROBERT W. NORRDIN

HARI K. IYER

JOHN D. KISIDAY

C. WAYNE C. MCILWRAITH

CHRISTOPHER E. KAWCAK

ADVISER: DAVID D. FRISBIE

DEPARTMENT HEAD: PAUL LUNN

ABSTRACT OF DISSERTATION

GENE EXPRESSION OF PHENOTYPICALLY HOMOGENEOUS CHONDROCYTES FROM DIFFERENT ARTICULAR CARTILAGE LAYERS OF EQUINE OSTEOARTHRITIC AND CONTROL JOINTS: METHOD VALIDATION AND GENE ARRAY ANALYSIS

Osteoarthritis remains a common and debilitating disease in humans, horses and other mammalian species, despite advances in diagnosis and treatment. Hyaline cartilage is considered to play a central role in the pathophysiology of osteoarthritis. The investigation of differences in gene expression in cells from osteoarthritic and control cartilage is expected to yield genes that may play a role in the pathophysiology of osteoarthritis, representing possible new targets for the treatment of the disease.

The goals of this investigation were (1) to develop a methodology to isolate RNA from phenotypically homogeneous cells of various cartilage layers for gene array analysis and (2) to determine differentially expressed genes in these cells in osteoarthritic and control cartilage.

Laser capture microdissection was used to isolate phenotypically homogeneous chondrocytes from frozen sections of adult equine articular cartilage. Total RNA was isolated and its quality was estimated employing capillary electrophoresis. The RNA was amplified by 2 rounds of *in-vitro* transcription and the expression levels of aggrecan, collagen type II, transforming growth factor β (TGF-β) and matrix metalloproteinase 3 (MMP-3) were compared to those from paired cartilage samples, from which RNA had been isolated by an established conventional methodology.

An average of 75 μg RNA was obtained from laser captured, amplified samples. Expression levels in these samples were lower for aggrecan, collagen type II, and TGF-β, but not for MMP-3, compared to those from macroscopic samples. This was a consistent phenomenon, as indicated by similar variances for expression levels obtained with either RNA isolation method. It was concluded that the developed methodology was adequate to produce a sufficient amount of RNA to be used for gene array analysis, given that gene expression levels would be compared among samples that had been processed identically.

Six adult horses, enrolled in a non-competing study employing the carpal osteochondral fragment model for osteoarthritis were used to collect cartilage samples from the dorsal aspect of the radial facet of the 3$^{rd}$ carpal bones. The validated methodology, followed by gene array analysis was used to determine differentially expressed genes from the tangential and the radial layer of articular cartilage from osteoarthritic and control joints.

154 genes were found to be differentially expressed between tangential and radial cartilage layers ($q<0.05$). Tangential and radial layers of cartilage showed 2 different gene expression patterns. The gene expression pattern of chondrocytes from the tangential layer reflected support of cell proliferation, suppression of apoptosis and upregulation of several genes involved in cell-matrix interactions or inflammatory processes. In contrast, the gene expression pattern of chondrocytes from the radial layer was dominated by genes supporting the synthesis of proteins and proteoglycans, suggesting a higher matrix synthetic activity in these chondrocytes compared to those from the tangential layer.

Further, chondrocytes in the radial layer showed gene expression suggestive of anti-calcification mechanisms.

Only 17 genes were found to be differentially expressed between osteoarthritic and control cartilage ($p<0.01$, fold change>1.5). Similar to the comparisons between cartilage layers, different expression patterns were found for osteoarthritic and control cartilage. The expression pattern for osteoarthritic cartilage was similar for the 2 cartilage layers, but changes in expression were more pronounced in the radial than the tangential layer. The gene expression pattern in osteoarthritic chondrocytes indicated the activation of the pro-inflammatory, catabolic NF-κB pathway. It further suggested a response to oxidative stress, but decreased ability to resist apoptosis, as well as downregulation of genes involved in proteoglycan synthesis and energy production compared to control cartilage.

This study was the first to determine gene expression patterns between 2 different layers of osteoarthritic and control articular cartilage. The present results improve our knowledge of zonal dependence of chondrocyte metabolism and its alterations under the influence of osteoarthritis. They provide the basis for future research into the pathophysiology of osteoarthritis, to identify new therapeutic targets for the treatment of this debilitating disease.

Katja Friederike Düsterdieck
Department of Clinical Sciences
Colorado State University
Fort Collins, CO 80523
Spring 2007

## DEDICATION

I dedicate this dissertation to my brother Nikolai in the hope that you will successfully defeat your leukemia, and to my loving husband Russell, who has supported me throughout this experience and who always gives me a better perspective in seemingly desperate moments.

## ACKNOWLEDGEMENTS

I would like to especially thank my advisor Dave Frisbie, as well as my committee members J. Kisiday, C. Kawcak, W. McIlwraith, R. Norrdin and H. Iyer for their support and advice. Thank you for pushing me when I needed it and thank you for all the time you spent to help me and make this dissertation happen.

Further, I would like to especially thank Suzanne Krueger-Koplin from the Macromolecular Resources Facility for helping me by always being available and continuing to motivate me even when things seemed impossible, and for just being a great friend. Also, I extend my thanks to Erin Duffy-Petrilli ,Beth Carbone and Kindra Orr for their everyday help in the lab. I would also like to thank John McGinley from the Cancer Prevention Laboratory and W.J Landis and R Jacquet from the Northeastern Ohio Universities College of Medicine for continuously helping me to make the laser capture part of this dissertation work. I further thank Leni Moldovan from the Davis Heart and Lung Research Institute of Ohio State University for her great advice and work to process the gene arrays, as well as A. Bertone from Ohio State University for allowing us to use her arrays for this dissertation. I would also like to send a huge Thank You to Ann Hess from the Department of Statistics for her hard work and putting up with my 1000 questions even on Labor Day Weekend!

I would like to thank my family in Europe and the USA for bearing with us and supporting us even as we are moving farther away. I also would like to thank my friends in Germany and the USA for always believing in me, and tolerating my long periods of silence, especially Friede: You have taught me that real friendship can survive anything as long as you commit to taking good care of it!

Finally, I would like to thank our dog Bart for making me happy whenever I think of him!

# TABLE OF CONTENTS

# CHAPTER I

## *1 Introduction*

### 1.1 Purpose

The following research was designed to determine genes that participate in chondrocyte metabolism of different layers of articular cartilage from exercising horses, as well as genes that may play a role in the pathophysiology of osteoarthritis. Such genes warrant future investigations of their possible roles in the homeostasis of articular cartilage and in the development of osteoarthritis, as they may represent new molecular targets in the treatment of osteoarthritic joints.

### 1.2 Goals

The goals of this investigation included: (1) The development of a methodology to isolate RNA from microscopic tissue samples of articular cartilage allowing the investigation of gene expression patterns from phenotypically homogeneous cells of various cartilage layers and (2) to determine differentially expressed genes in these cells in osteoarthritic and control cartilage.

### 1.3 Statement of Hypothesis

The hypothesis tested to fulfill the 1$^{st}$ goal was that RNA obtained by employing laser capture microdissection of articular chondrocytes, followed by RNA isolation and linear amplification shows similar gene expression as RNA

that was isolated from larger tissue samples using an accepted conventional isolation method. The hypothesis tested to fulfill the 2nd goal was that gene expression patterns are different between cells from osteoarthritic and control cartilage, as well as between cells from different layers of osteoarthritic or control cartilage.

## 1.4 Specific Aims

### 1.4.1 Method Development (Chapter II)

(1) Laser capture microdissection of adult articular chondrocytes from various cartilage layers.

(2) RNA isolation and quality assessment of RNA from laser capture microdissection samples.

(3) Linear amplification of RNA from laser capture microdissection samples.

(4) Comparison of expression levels of a subset of genes in RNA from laser capture microdissection samples to expression levels in conventionally isolated RNA using real-time PCR.

### 1.4.2 Gene Expression (Chapter III)

(1) Determination of differentially expressed genes in cells from the tangential versus the radiate layer of cartilage.

(2) Determination of differentially expressed genes in cells from osteoarthritic versus control cartilage.

(3) Determination of the influence of osteoarthritis on differentially expressed genes in cells from the tangential versus the radiate layer of cartilage.

## 1.5 Significance, Background & Rationale

### 1.5.1 Significance and Impact of Osteoarthritis

Musculoskeletal disease in horses is a major cause of lameness resulting in pain and loss of function for the affected horse. Lameness was the most common cause for training failure in yearling Thoroughbred horses, with 45% of the horses exhibiting lameness over a period of 6-8 months (Hernandez and Hawkins 2001). A large percentage of lameness' can be attributed to joint associated problems (Jeffcott et al. 1982, Rossdale et al. 1985, Todhunter 1990), of which osteoarthritis is considered the most economically important disease affecting horses (Pool 1996). Economic losses are incurred in the form of expensive treatments, as well as loss of time in training and competition. Thus, it is essential to improve prevention and treatment of this debilitating disease. This can only be achieved based on a thorough knowledge of pathophysiologic pathways of osteoarthritis. This dissertation has validated and implemented new techniques to increase our knowledge of the pathophysiology of osteoarthritis.

### 1.5.2 The Joint as an Organ System

The joint is an organ system made up of several layers of hyaline and calcified cartilage, as well as bone and synovial tissue, which must function as a whole to stand up to long term use. Pathologic change in any one of these tissues can easily lead to the whole organ failing due to osteoarthritis (Pool

1996). For example, isolated cartilage lesions can lead to progressive damage of the articular cartilage resulting in osteoarthritis (Guilak et al. 2004). Deterioration of the hyaline cartilage is considered to be one major characteristic of osteoarthritis (McIlwraith 2005, Benedek 2006). Thus, this study concentrated on the investigation of 2 layers of hyaline cartilage from both diseased and control joints. Paired samples were taken from the same animal, thus decreasing the commonly large variability between animals (Aigner et al. 2001a).

### 1.5.3 Experimental Models of Osteoarthritis

There is much discussion about the inciting causes of osteoarthritis (McIlwraith 1996). Among them is cyclic trauma to either subchondral bone with subsequent sclerosis and decreased ability for shock absorption, or to the soft tissues leading to an inflammatory response. Instability of the joint or changes in joint congruency due to traumatic injuries or developmental defects are also considered as inciting causes. In contrast, the central process of osteoarthritis is generally agreed upon to be the enzymatic degradation of articular cartilage (Malfait et al. 2002, Aigner and McKenna 2002). Biochemically, osteoarthritic cartilage contains a decreased amount of proteoglycans and an increased amount of water. The proteoglycans appear to be abnormal in their structure and degree of aggregation (Mankin et al. 1971, Sweet et al. 1977, Vasan 1980), and the collagen network has been shown to be altered also (Dodge and Poole 1989). In early osteoarthritis, the loss of proteoglycans is attributed to the enzymatic activities of aggrecanases, followed by that of matrix metalloproteinases in the later stages of osteoarthritis, resulting in further

degradation of proteoglycans and also collagen fibrils (Caterson et al. 2000, Nagase and Kashiwagi 2003). The chondrocytes appear to react to degradation and alterations of the matrix by upregulating their proteoglycan and collagen type II syntheses, as determined by biochemical methodologies including the measurement of $^{35}SO_4$ incorporation into normal and osteoarthritic cartilage explants (Collins and McElligott 1960, Eyre et al. 1980, Sandy et al. 1984, Matyas et al. 1995, Smith et al. 2006). But ultimately, the degradation of matrix components exceeds new synthesis by chondrocytes, and progressive cartilage degeneration ensues (Mankin et al. 1971, Poole et al. 1994, Kim et al. 2006). Further, an accelerated advancement of the calcification front into the hyaline cartilage has been observed in experimental models of osteoarthritis, possibly adding to the thinning of hyaline articular cartilage with osteoarthritis (Oegema et al. 1996, Peng et al. 2001).

In summary, the normal homeostasis of articular cartilage matrix appears to be disturbed towards a catabolic state in osteoarthritic joints (McIlwraith and Vachon 1988, Poole et al. 1994). This is likely initiated by an increased activity of aggrecanases (Nagase and Kashiwagi 2003). It seems that the delicate balance between degradation and synthesis, which is present in healthy cartilage, can be disturbed by several different insults, suggesting that cartilage degradation or osteoarthritis represent a "final common pathway" (Ehrlich et al. 1986) of differing etiologies.

Consequently, several different experimental models have been employed to investigate the pathogenesis of osteoarthritis and the response to treatments

for the disease in horses. Most in-vivo models induce synovitis by intra-articular injection of an irritant, such as mono iodoacetate (Gustafson et al. 1992), carrageenan (Owens et al. 1996), filipin (McIlwraith et al. 1979, McIlwraith and Van Sickle 1981), amphotericin B (Suominen et al. 1999), or lipopolysaccharides (Firth et al. 1987, Todhunter et al. 1996). While these models induce synovitis, they lack true clinical relevance due to their non-specifically irritating nature. *In-vitro* models such as the exposure of cartilage explants to IL-1 (Dingle et al. 1987, Dodge and Poole 1989, Tyler 1985, Takafuji et al. 2002, Takafuji et al. 2005) are more disease specific, but inferences to clinical disease can be speculative and should be corroborated by results from in-vivo studies. In contrast, the in-vivo model used in this study is very well suited to make inferences to clinical osteoarthritis in horses. Induction of osteoarthritis is achieved via surgical creation of an osteochondral fragment off the distal dorsal aspect of the radiocarpal bone and the production of a defined amount of bone and cartilage debris from the same site, followed by an incremental controlled exercise regimen (Frisbie et al. 2002). Pathologic, histologic and clinical findings are similar to those seen with early naturally occurring osteoarthritis in horses (Pool 1996, McIlwraith 1998). Characteristics of this model are overt lameness, changes in synovial fluid parameters, focal synovitis, gross cartilage lesions with cartilage fibrillation, chondrocyte necrosis with chondrone formation and decreased staining for glycosaminoglycans (Foland et al. 1994, Frisbie et al. 1997, Kawcak et al. 1997, Frisbie et al. 1998, Kawcak et al. 1998, Frisbie et al. 1999, Frisbie et al. 2002, Frisbie et al. 2003).

### 1.5.4 Gene Expression Analysis of Chondrocytes

The investigation of gene expression at the mRNA level should be regarded as a functional analysis of cell metabolism. The differential expression of certain genes and their post-transcriptional modification determine the metabolism and phenotype of the cell. That cell in turn provides the homeostasis of the surrounding tissue (the extracellular matrix in the case of bone and cartilage). Thus, changes in gene expression due to disease will result in imbalances in matrix homeostasis. In a joint, this will likely result in functional failure of the organ (Aigner and Dudhia 2003). Consequently, understanding the metabolic changes (investigated as changes in gene expression) in cells from normal and osteoarthritic tissues represents an important area of study to improve our understanding of alterations in the cell metabolism under the influence of osteoarthritis. One limitation of studies investigating gene expression patterns *in-vivo* is the fact that it is difficult to repeatedly obtain cartilage samples from the same joint over time without impacting the whole joint by the sampling process, as isolated cartilage lesions can lead to osteoarthritis by themselves (Guilak et al. 2004). Thus, the investigation of gene expression *in-vivo* is limited to one time point in the continuous development of osteoarthritis, and represents just a "snap shot" of what is a dynamic process.

When determining gene expression patterns, it is important to investigate a phenotypically homogeneous cell population (Emmert-Buck et al. 1996), because cells with different phenotypes are expressing different proteins. Thus, comparing gene expression patterns between 2 heterogeneous cell populations

makes it difficult to find subtle differences (Grant et al. 2002, Firestein and Pisetsky 2002). Further, in a phenotypically heterogeneous cell population it is impossible to identify the contribution of different cell types to the expression pattern (Attur et al. 2002a). Normal articular cartilage is made up of 4 layers, which contain chondrocytes of different phenotypes, as well as different patterns of collagen fibers. Further, 3 layers are hyaline in nature, whereas the deepest zone is calcified. Conventional methods of RNA isolation (Chomczinski and Sacchi 1987, Adams et al. 1992, Mallein-Gerin and Gouttenoire 2004) are not suitable to investigate mRNA expression from cells that were selected based on their phenotype or location in the articular cartilage and underlying bone. This is because large numbers of cells are required to obtain sufficient amounts of RNA, and more importantly, cells of interest cannot be separated from unwanted cells under microscopic control. Thus, in this study, laser capture microdissection was employed to fractionate cells from frozen sections based on their phenotype. LCM has been used to isolate mRNA from phenotypically homogeneous cells from different zones of physeal cartilage from frozen sections (Landis et al. 2003, Wang et al. 2004, Jacquet et al. 2005, Shao et al. 2006) as well as from paraffin and frozen sections of articular cartilage (Scharschmidt et al. 2001). To the author's knowledge, the present dissertation is the first report to successfully utilize laser capture microdissection on frozen sections of articular cartilage for gene array analysis. Due to the relative acellularity of adult articular cartilage, the RNA extracted from laser captured cells had to be amplified via *in-vitro* transcription. To validate this methodology, gene expression levels of several

low and high copy genes were compared in RNA that was isolated conventionally from large cartilage samples to those from laser captured and amplified samples using real-time PCR. In the subsequent investigation, gene array analysis was used to determine gene expression of over 3000 genes simultaneously.

### 1.5.5 Gene Array Analysis in Osteoarthritis Research

Most studies investigating gene expression profiles with gene array technology in osteoarthritis have employed *in-vitro* models, probably for the ease of RNA isolation and manipulation of the experimental system. These studies proved to be helpful in elucidating the cellular effects of specific mediators such as beta-2 macroglobulin (Zhang et al. 2002) or IL-1β (Takafuji et al. 2005).

Only few studies have used samples from normal and osteoarthritic joints to determine differentially expressed genes in cartilage by means of gene array technology (Aigner et al. 2001a, Aigner et al. 2003, Gebauer et al. 2005, Smith et al. 2006).

Aigner et al. (2001a) found high variability of gene expression levels in cartilage from human knee joints (normal, early stage osteoarthritis from autopsies and late stage from joint replacement samples). This finding from the array analysis was confirmed with qrt-PCR and has been reported previously (Gehrsitz et al. 2001). Collagen expression (especially collagen types II, III, IV) was upregulated in late stage osteoarthritic samples, as was biglycan. Fibronectin was thought to having a regulatory function on matrix metabolism in early osteoarthritis, a theory suggested before (Homandberg and Wen 1998, Homandberg et al. 1998), as it was upregulated in samples representing early

osteoarthritic changes. The expression patterns of the matrix metalloproteinases suggested that MMP-3 may have a role in normal cartilage maintenance rather than during end-stage osteoarthritis, as it was downregulated in samples representing late stage osteoarthritis. In contrast, MMP-2, MMP-11 and MMP-13 were upregulated in late stage OA cartilage, suggesting their role in the later stages of cartilage matrix breakdown. These observations also supported the notion that collagen denaturation is a phenomenon of late stage, rather than early stage OA.

Further, some studies were able to identify proteins that were differentially expressed in normal and osteoarthritic samples, but had not been implemented in the pathophysiology of osteoarthritis, such as the protein Tob1. Gebauer et al. (2005) substantiated Tob1's differential expression using qrt-PCR and immunohistochemistry on similar samples. Subsequent *in-vitro* experiments revealed an inverse correlation between chondrocytes proliferation and Tob1 expression, supporting the hypothesis that this protein played a role in the pathophysiology of osteoarthritis (Gebauer et al. 2005).

Sato et al. (2006) compared gene expression patterns between damaged and undamaged regions of cartilage from late stage osteoarthritic knee joints. They found 3 genes (*CCND1*, *PSAT*, and *S100A4*) involved in cell proliferation to be expressed higher in damaged cartilage regions. Further, several genes involved in the synthesis of matrix collagens as well as in the degradation of matrix proteins and their inhibitors were upregulated in damaged cartilage samples.

Smith et al. (2006) found that mildly affected equine OA cartilage was mostly characterized by upregulation of genes for matrix proteins and by SOD-2, which is an anti-apoptotic protein. Further, proteolytic enzymes and pro-anabolic proteins were also upregulated. This was interpreted as a simultaneous increase in cartilage matrix degradation and matrix protein synthesis. In more affected equine OA cartilage a decrease in expression of proteins needed for transcription was found, as well as of proteins decreasing apoptosis. Further, higher expression of collagen type II and lower expression of proteoglycans was noticed.

Shortcomings of previous gene array studies undertaken to determine differentially expressed genes in osteoarthritic cartilage, include the fact that osteoarthritic and control samples were collected from different individuals (Aigner et al. 2001a, Aigner et al. 2003, Smith et al. 2006), as well as the determination of gene expression levels in chondrocytes from all layers of articular cartilage. This dissertation addressed those shortcomings by utilizing paired samples (control and osteoarthritic) from the same individual at the same time point after induction of the disease, decreasing variability between individuals. Further, the separation of chondrocytes from two different cartilage layers by laser capture microdissection allowed investigating two phenotypically homogeneous cell populations from articular catilage.

Several other studies have employed gene array technology in the investigation of osteoarthritis. Some studies have used it to identify differentially expressed biochemical markers for osteoarthritis in a variety of samples

(cartilage, synovial fluid, peripheral blood) (Knorr et al. 2005). Other studies have examined the value of immortalized human chondrocytes cell lines by comparing their gene expression patterns to those of human chondrocytes (Islam et al. 2001, Finger et al. 2003). Yet another study used gene array technology to determine the efficacy of nimesulide as an anti-apoptosis treatment *in-vitro* (Mukherjee and Pasinetti 2002).

A unique gene expression profile has been established in peripheral white blood cells from horses with experimentally induced osteoarthritis using the proposed osteoarthritis model and gene array technology (Frisbie, unpublished data 2004). Of over 3000 genes represented on the array, 17 were found to be up- or down-regulated in white blood cells of horses with osteoarthritis, compared to baseline values before the induction of osteoarthritis.

### 1.5.6 Future Approaches/Validation

Real-time PCR has been the method of choice to validate the subset of genes that was identified to be differentially expressed on gene array analysis (Attur et al. 2002a). This approach is cost- and time-effective, because usually only a small subset of all genes represented on a gene array are differentially expressed (Frisbie, unpublished data 2004, Attur et al. 2002a). Another methodology of interest would be to perform in situ immunohistochemistry or hybridization techniques (Attur et al. 2002a).

### 1.5.7 Rationale for the Proposed Study

Osteoarthritis is a common debilitating disease in horses with a significant economical impact on the equine industry (Pool 1996, USDA 2000, Hernandez

and Hawkins 2001). The pathophysiology of osteoarthritis is only partially known. However, the development of new strategies for treatment and prevention of this serious disease has to be based on known aspects of its pathophysiology. Thus, this dissertation aims to improve our knowledge of pathophysiologic processes under the influence of osteoarthritis at the molecular level. To achieve this, differentially expressed genes in health and disease, as well as in different layers of hyaline cartilage were determined and placed in context with current knowledge.

# CHAPTER II

## *2 Method Validation*

### 2.1 Introduction

Osteoarthritis remains a common and debilitating disease in humans, horses and other mammalian species, despite advances in diagnosis and treatment. It has been estimated that by the year 2020, close to 60 million Americans will be affected with this disease (Lawrence et al. 1999). In horses, osteoarthritis is considered the most economically important musculoskeletal disease (Pool 1996). Thus, it is important to establish new and better ways to investigate the tissues that are involved in this debilitating condition. To the author's knowledge, this study is the first to validate the use of laser capture microdissection on frozen sections of adult articular cartilage to isolate sufficient amounts of RNA for gene expression analysis utilizing gene array technology.

Gene expression analysis represents a way to gain insight into the cellular metabolism of the tissue of interest. There is ample evidence that under the influence of osteoarthritis, chondrocytes experience changes in metabolism towards increased catabolic activity, resulting in degradation of the cartilage matrix (Attur et al. 2002b, Kurz et al. 2005, Loeser 2006). Changes in metabolism are reflected in changes in gene expression. Thus, differentially expressed genes in osteoarthritic tissues likely play a role in the pathophysiology of the disease.

When analyzing gene expression patterns, it is important to investigate a phenotypically homogeneous cell population (Emmert-Buck et al. 1996), because cells with different phenotypes are expressing different genes. Hence, determining subtle differences in gene expression between 2 heterogeneous cell populations will be difficult (Grant et al. 2002, Firestein and Pisetsky 2002). Articular cartilage is made up of 4 different layers (tangential, intermediate, radiate, and calcified cartilage layer) with phenotypically different chondrocytes in each layer. Conventional methods of RNA isolation (Chomczinski and Sacchi 1987, Adams et al. 1992) are not suitable to investigate gene expression from phenotypically homogeneous chondrocytes, because they do not allow the separation of these cells under microscopic guidance. In contrast, laser capture microdissection (LCM) allows collection of phenotypically similar cells under microscopic control. During LCM, a transparent film (ethylene vinyl acetate polymer) is placed on top of a microscopic section and a low energy laser is activated over the area of interest. The polymer adheres to the microscopic section in the area where the laser hit. When polymer and microscopic section are separated, the adhered area remains on the polymer and is separated from the unwanted part of the tissue section. The separated cells can then be processed for RNA extraction. LCM has been used to investigate gene expression of phenotypically homogeneous cells from different phenotypic layers of physeal cartilage (Landis et al. 2003, Jacquet et al. 2005, Wang et al. 2004, Benoyahu et al. 2005, Shao et al. 2006), but similar reports of LCM use on adult articular cartilage are scarce (Scharschmidt et al. 2001). This is likely because

the cohesive matrix and the acellularity of articular cartilage making LCM of a sufficient numbers of cells challenging. Further, RNA yield from laser captured articular chondrocytes is extremely low, and assessment of RNA quality is difficult. The use of different primers (oligo-dT and random hexamer primers) to reverse transcribe aliquots of the same sample, followed by real-time PCR and determination of differences in Ct values between the aliquots is a cumbersome technique to estimate mRNA lengths in RNA samples. The idea behind this is that the 5' end of the mRNA transcripts should be underrepresented after reverse transcription with oligo dT primers to a degree, corresponding to the extent of degradation of the RNA in the sample (Swift et al. 2000). However, this should not be the case with random hexamer primers. Thus, Ct values should be different between the aliquots in degraded, but not in high quality samples. A newer methodology to estimate RNA quality especially in small samples is based on an electropherogram tracing obtained via capillary electrophoresis. A computer program (2100 Expert software, Agilent Technologies, Palo Alto, CA) can apply an algorithm to the tracing and assign an RNA Integrity Number (RIN), which is a number on a scale of 1 to 10 (1 standing for complete RNA degradation and 10 standing for intact RNA). This represents an easier and more paracticable method to estimate RNA quality in samples from laser capture microdissection.

The goal of this study was to develop a methodology to obtain sufficient amounts of RNA for gene array analysis of phenotypically homogeneous cells from different adult articular cartilage layers.

## 2.2 Materials & Methods

### 2.2.1 Sample Collection

Articular cartilage was taken aseptically within 6 hours post-mortem from femorotibial, femoropatellar and tibiotarsal joints of adult horses (age 2-7 years) that were euthanized at the Colorado State University Veterinary Teaching Hospital for reasons unrelated to this study. They were placed in cryovials for conventional RNA isolation (macroscopic samples) or in OCT (Tissue Tek OCT Compound, Sakura Finetek, Torrance,CA) for RNA isolation from microscopic sections without laser capture microdissection (scrape samples) or RNA isolation with laser capture microdissection (LCM samples). All cartilage samples were snap-frozen in methyl butane on liquid nitrogen and stored at -80°C until further processing.

### 2.2.2 Conventional RNA Isolation (Macroscopic Samples)

RNA was isolated from macroscopic cartilage samples according to the TRIzol® protocol (Invitrogen, Carlsbad, CA), with some modifications. Briefly, the weight of the cartilage samples was recorded before they were manually pulverized in a liquid nitrogen cooled, custom made stainless steel pulverizer. Then the samples were homogenized twice for 30 seconds (Cyclone Virtishear, Virtis, Gardiner, NY) in a total of 0.038ml of TRIzol® (Invitrogen, Carlsbad, CA) per mg cartilage wet weight. Following, a chloroform extraction was performed twice with a total of 0.3ml chloroform/ml TRIzol® reagent used, to separate the RNA from other macromolecules with the aqueous phase. The RNA was then precipitated with 100% isopropanol, washed in 70% ethanol and suspended in

100µl nuclease-free water. A clean-up and DNase digestion (RNase-free DNase, Qiagen, Valencia, CA) was performed using a commercially available kit (RNeasy Mini Kit, Qiagen, Valencia, CA), following the manufacturer's recommendations with slight modifications: Specifically, the samples were loaded twice onto the silica-gel column and also eluted twice. RNA quantity and purity were determined using spectrophotometry (ND-1000 spectrophotometer, Nanodrop, Wilmington, DE), and RNA quality was assessed using capillary electrophoresis (RNA 6000 Nano LabChip®, 2100 Bioanalyzer, Agilent Technologies, Palo Alto, CA).

### 2.2.3 RNA Isolation from Microscopic Sections (Scrape Samples)

Cartilage samples frozen in OCT (Tissue Tek OCT Compound, Sakura Finetek, Torrance,CA) were sectioned at 10µm thickness on a Leica cryostat (Leica 3050, Leica Microsystems, Bannockburn, IL) at a chamber temperature of -37°C and block temperature of -24°C. The sections were mounted on slides using a tape transfer system (CryoJane, Instrumedics, Hackensack, NJ) and stored at -80°C until further processing. Each slide was dehydrated and stained, using a commercially available kit (HistoGene LCM Frozen Section Staining Kit, Arcturus Bioscience, Mountain View, CA). The manufacturer's protocol recommended dehydration of the slides in 75% ethanol, rehydration in RNase-free water, staining with a proprietary nuclear stain (possibly toluidine blue based, R. Norrdin, personal communication), and dehydration in graded ethanol before immersion in xylene. After being air-dried, the sections were scraped off the slides, and up to 4 sections were combined into 1 sample. The scrape

sections were processed according to the manufacturer's instructions of a commercially available RNA extraction kit (PicoPure™ RNA Isolation Kit, Arcturus Bioscience, Mountain View, CA). Briefly, an extraction buffer was used to lyse the cells in the microscopic sections. The resulting lysate was vortexed in an attempt to make larger DNA molecules more accessible for DNase treatment by shearing them. Samples were loaded twice onto a pre-conditioned RNA-purification column and the column was washed and treated with RNase-free DNase (Qiagen, Valencia, CA) to reduce the risk of DNA contamination. Finally, the RNA was eluted twice from the column, resulting in a sample volume of 11-12 µl. The RNA was tested for quality and stored at -80°C until further use.

### 2.2.4 RNA Isolation from Microscopic Samples (LCM Samples)

The remaining cartilage samples frozen in OCT (Tissue Tek OCT Compound, Sakura Finetek, Torrance, CA) were processed similarly to the scrape samples with the following differences: The frozen sections were cut at 5-7µm thickness. Laser capture microdissection was performed immediately after dehydration and staining as described for the scrape samples. Laser capture microdissection was performed on single sections with an Autpoix Unit (Arcturus Bioscience, Mountain View, CA) using 1 CapSure Macro LCM cap (Arcturus Bioscience, Mountain View, CA) per section, according to a protocol from Landis et al. (2003). To minimize RNA degradation, care was taken that capture on each section was terminated within 20 minutes of removing the section from the -80°C freezer. The RNA was isolated similarly to the scrape samples with the following modifications: The caps containing the captured cells were covered

with 50 µl RNA extraction buffer and kept at room temperature for up to 3 hours before being processed further. Up to 4 caps were pooled into 1 sample. The RNA was tested for quality and then stored at -80°C until further use.

### 2.2.5 RNA Quality Control (Microscopic Samples)

#### 2.2.5.1 Capillary Electrophoresis

The RNA 6000 Pico LabChip® Kit (Agilent Technologies, Palo Alto, CA) and the 2100 Bioanalyzer (Agilent Technologies, Palo Alto, CA) were used to estimate RNA quality. Subjective assessment was performed by inspection of the electropherogram as described by Imbeaud et al. (2005), and for a more objective assessment of RNA quality, the RNA integrity number (RIN) was determined using the 2100 Expert software (Agilent Technologies, Palo Alto, CA).

#### 2.2.5.2 Real-time PCR With Different Reverse Transcription Primers

As a second means of RNA quality control, different reverse transcription primers (random hexamers and oligo dT primers) were tested on aliquots of the same sample, followed by real-time PCR to determine possible differences in threshold cycle (Ct) values between the aliquots. Differences in Ct values between the aliquots were expected to indicate degradation of the RNA. Briefly, RNA samples were divided into 2 aliquots and reverse transcribed using the enzyme Superscript™ III (Invitrogen, Carlsbad, CA) and random hexamers or oligo dT as primers. Then, real-time PCR was performed (ABI 7000 real-time PCR system, Applied Biosystems, Foster City, CA) using TaqMan® primers and

probe for the equine gene glyceraldehyde-3-phosphate dehydrogenase (GAPDH).

### 2.2.6 *In-vitro* Transcription Amplification (LCM Samples)

To obtain µg amounts of RNA from the laser captured samples, an *in-vitro* transcription amplification was performed using a commercially available kit (RiboAmp® HS, Arcturus Bioscience, Mountain View, CA). Briefly, the RNA was reverse transcribed using oligo dT primers incorporating the T7 promoter sequence. Double stranded cDNA was obtained with random hexamers as primers. The double stranded cDNA was amplified into antisense RNA using the enzyme T7 RNA polymerase. The whole protocol was then repeated once again. Amplification yield was determined using spectrophotometry (ND-1000 spectrophotometer, Nanodrop, Wilmington, DE), and the amplification quality was estimated using capillary electrophoresis (RNA 6000 Nano LabChip®, 2100 Bioanalyzer, Agilent Technologies, Palo Alto, CA).

### 2.2.7 Reverse Transcription (Macroscopic and Microscopic Samples)

To prepare the RNA samples for real-time PCR, they were reverse transcribed using the enzyme Superscript™ III (Invitrogen, Carlsbad, CA) and oligo dT primers according to the manufacturer's recommendations.

### 2.2.8 Real-time PCR

Real-time PCR was performed with the ABI 7000 real-time PCR System (Applied Biosystems, Foster City, CA) and TaqMan® primers and probes for the equine genes GAPDH, collagen type II, aggrecan, matrix metalloproteinase 3

(MMP3) and transforming growth factor β (TGF-β) (for sequences see Table 1), using half the reaction volume recommended by Applied Biosystems. All samples were run in duplicates or triplicates (final validation experiment). As negative controls, reaction mix without RNA and reaction mix with RNA reverse transcribed without the addition of Superscript™ III were used.

### 2.2.9 Experimental Design and Statistical Analysis

To determine the best conditions for reliable capture of chondrocytes from frozen sections of adult equine articular cartilage, the following modifications of the protocol recommended by the manufacturer of the HistoGene Kit and the Autopix Unit (Arcturus Bioscience, Mountain View, CA) were tested. The frozen section thickness was varied between 4 and 12 µm. Further, during the dehydration and staining protocol, the effect of transferring the section into the 1$^{st}$ ethanol solution within the -80°C freezer was compared to thawing of the sections prior to the first dehydration step. During laser capture, different laser settings and positioning of the CapSure Macro LCM cap (Arcturus Bioscience, Mountain View, CA) were investigated. All subjective observations about the success of the cell capture were recorded.

To assess the quality of RNA obtained from microscopic samples (scrape samples and LCM samples), RNA was analyzed using the RNA 6000 Pico LabChip® on the 2100 Bioanalyzer (Agilent Technologies, Palo Alto, CA). Electropherograms were analyzed subjectively, and RINs were determined using the 2100 Expert software (Agilent Technologies, Palo Alto, CA). To ascertain that the samples did actually contain RNA, some samples were reverse

transcribed and amplified using real-time PCR and TaqMan® system for the equine gene GAPDH.

To determine a possible effect of RNA concentration on the RIN determined with the RNA 6000 Nano or Pico LabChips®, RNA from 4 macroscopic samples (Table 2) with good purity (260/280 ratios >1.9) and quality (RIN determined with RNA 6000 Nano LabChip® >8.0) was used to produce several dilution series. The RINs for the diluted samples with concentrations from 5 to 350 ng/µl the RINs were determined with the RNA 6000 Nano LabChip® Kit (Agilent Technologies, Palo Alto, CA) (Table 3), and for samples with concentrations of 10-5200 pg/µl were determined with the RNA 6000 Pico LabChip® Kit (Agilent Technologies, Palo Alto, CA) (Table 4). An association between RNA concentration and RIN was assessed for both assays using Microsoft Office Excel 2003 (Microsoft, Redmond, WA).

In an attempt to utilize an alternative methodology to assess RNA quality in the microscopic samples, different primers (random hexamers and oligo dT primers) were used on aliquots of the same sample during reverse transcription. The effect of these primers on differences in threshold cycle (Ct) values between the aliquots determined by real-time PCR was expected to be influenced by the quality of the RNA. Conventionally isolated RNA from macroscopic cartilage samples was used to represent samples with known RNA quality (Table 5): the quality of these samples was determined using the RNA 6000 Nano LabChip® Kit (Agilent Technologies, Palo Alto, CA). To obtain partially degraded RNA, 6 of the 18 samples were incubated at 65°C for increasing times (10, 15, 20, 25, 30, 35

minutes), and quality assessment with the Nano LabChip® was repeated. A possible association between the RIN and the differences in threshold cycle (Ct) values between the aliquots was analyzed. Additionally, 11 microscopic samples (2 scrape and 9 LCM samples) were processed similarly with the difference that the RNA 6000 Pico LabChip® Kit (Agilent Technologies, Palo Alto, CA) was used to determine the RIN. Differences in mean threshold cycle (Ct) values between the aliquots were compared to those from the samples with known quality, using a 2 sample t-test (SAS, Cary, NC).

To validate the complete protocol for isolation and amplification of RNA from laser captured articular chondrocytes, 6 cartilage samples were divided into 2 subsamples. The 1st subsample was used to isolate RNA conventionally, and the 2nd subsample was used to isolate RNA from laser capture microdissection samples, followed by 2 rounds of *in-vitro* transcription amplification. Final modifications of the sample processing and laser capture protocol included omission of the rehydration, staining and water wash steps, as well as shortening the xylene step from 5 minutes to 1 minute prior to laser capture microdissection, pooling of 8 instead of 4 caps into 1 sample, and finally, laser capture was terminated 14 minutes after removing the slide out of the -80°C freezer. Further, care was taken in this part of the study, to capture a representative number of cells from all layers of articular cartilage, to reflect the layered nature of the macroscopic samples. All RNA (macroscopic as well as amplified LCM samples) was reverse transcribed as described above and real-time PCR using TaqMan® systems was performed for GAPDH as housekeeping gene, aggrecan and

collagen type II as high copy number genes and MMP3 and TGF-β as lower expressed genes. Statistical analysis was performed using SAS (Cary, NC). The real-time PCR data was log-transformed to obtain normally distributed data. A paired t-test was used to compare mean expression levels of each gene between isolation methods. An analysis of variance was used to determine whether expression ratios between the 4 genes significantly changed with the RNA isolation method. A 2 sample test for variances was used to find differences in variance of each gene's expression level between isolation methods.

## 2.3 Results

### 2.3.1 Optimizing Laser Capture Microdissection

It was determined that reliable capture of chondrocytes from frozen sections of adult equine articular cartilage was possible when sections of 5-7 μm thickness were used. Thinner sectioning frequently resulted in the production of incomplete sections, which was noted as areas void of matrix and cells at 10x magnification (Figure 1). When thicker sections were used for laser capture microdissection, inadequate wetting was noted to occur frequently, resulting in unsuccessful capture of cells (Figure 2).

Reliable capture of chondrocytes was extremely rare when the slides were thawed before the 1$^{st}$ dehydration step (75% ethanol), but cell capture was reliably achieved when the sections were transferred into the 1$^{st}$ ethanol solution within the -80°C freezer and brought to room temperature while being submerged in the 75% ethanol.

The following observations were made when the laser settings were changed. It was necessary to use the highest power setting (100 mW) in order to successfully capture chondrocytes. Lower power settings resulted mostly in inadequate wetting (Figure 2). The optimal setting for the pulse duration was between 800 and 2000 µs. The shorter the pulse duration was chosen, the smaller was the diameter of the laser spot (Figure 3). It was further noticed that the diameter of the laser spot varied within the same section depending on the local section thickness. In visibly thinner areas, the laser spot diameter was smaller than in visibly thicker areas of the cartilage section. The laser spot size could also be enlarged by increasing the number of laser hits in the same location to up to 5 hits. Using more than 5 hits did not seem to increase the laser spot size any further. For some sections with insufficient wetting, however, increasing the number of laser hits per location to 10 or even 20 resulted in adequate wetting. The time interval between laser hits (delay, tested at 0-50 µs) did not appear to have an influence on the success of cell capture. Finally, it was noticed that cell capture was less successful in the peripheral 50 µm of the circular CapSure Macro LCM cap compared to the more central area of the cap. Thus, cell capture was optimal when the cap was placed such that the cartilage section was located in the center of the cap.

Even when cells were captured successfully, full thickness capture (Figure 4) was extremely rare, especially on thicker sections. Thicker sections usually detached completely from the slide when the CapSure Macro LCM cap was removed, whereas thinner sections usually remained on the slide, and only the

captured areas adhered to the cap. When the section detached completely, double-sided tape (Scotch® Magic™ Tape 810, 3M, St. Paul, MN) was pushed lightly onto the cap before being removed again. The unwanted part of the section came off with the tape, whereas the captured areas of the section remained attached to the cap (Figure 5).

### 2.3.2 Quality Assessment and Quantitation of RNA

It was difficult to interpret the electropherograms from microscopic samples (scrape and LCM samples, 45 samples total, Table 6) obtained using the RNA 6000 Pico LabChip® on the 2100 Bioanalyzer (Agilent Technologies, Palo Alto, CA), because of numerous artifacts (Figure 6), as well as the low RNA concentration in these samples. The RNA concentration in all of these samples (1-4 sections or caps pooled per sample) was likely below the lower level of detection for the RNA 6000 Pico LabChip®, which was given at 500 pg/µl by the manufacturer. When the electropherograms without artifacts (21/45 samples total or 46.7% of all electropherograms) were interpreted subjectively, 1 sample was considered degraded, based on the presence of a peak close to the marker peak. Four electropherograms showed small peaks where one would expect to see the 18S and 28S rRNA peaks in addition to a peak close to the marker peak. These samples were suspected to contain RNA with substantially less degradation compared to the sample with just the peak close to the marker peak. The remaining samples (16/21 or 76.2%) without artifacts did not show any peaks and these were considered to contain extremely low amounts or no RNA (Figure 7). In 24 of the 45 samples, it was attempted to obtain an RIN using the

2100 Expert software (Agilent Technologies, Palo Alto, CA). Only 7 of the 24 electropherograms had an RIN assigned by the computer program (range 1-2.9). Changes in sample processing or during laser capture microdissection did not appear to impact the occurrence of artifacts in the electropherograms or the RNA quality – as far as quality assessment was possible.

To ascertain that these samples contained any RNA, some samples were reverse transcribed using the enzyme Superscript™ III and amplified, using real-time PCR (ABI 7000, real-time PCR system, Applied Biosystems, Foster City, CA) and a TaqMan® system for the equine genes GAPDH and collagen type II (Figure 8, for primer and probe sequences see Table 1). Specific amplification was seen for both genes in all samples. The negative controls (water, as well as non-reverse transcribed microscopic samples) did not show signs of amplification.

RINs determined with the Nano LabChip® Kit (Agilent Technologies, Palo Alto, CA) did not appear to be significantly influenced by RNA concentration down to about 10 ng/µl (Figure 9). In contrast, RINs determined with the Pico LabChip® Kit (Agilent Technologies, Palo Alto, CA) decreased with lower concentrations in samples with good quality RNA (Figure 10). Further, in 48 of 90 (53%) electropherograms obtained with the Pico LabChip® Kit, the computer program (2100 Expert software, Agilent Technologies, Palo Alto, CA) failed to assign an RIN.

Incubation of RNA of good quality (RIN determined with the Nano LabChip® 8.1-8.7) at 65°C for 10-25 minutes caused limited degradation of the

RNA (RIN determined with the Nano LabChip® 6.8-7.8). Longer incubation at 65°C (30 or 35 minutes) resulted in more RNA degradation (RIN determined with the Nano LabChip® 4.3 and 4.6, respectively). Thus, the samples representing known RNA qualities had a range of RINs from 8.7 to 4.3 (Table 5). However, when the differences in Ct values between aliquots reverse transcribed with oligo dT primers or random hexamers were regressed over the RIN, no strong association was found ($R^2$=0.05, Figure 11). Further, based on the difference in Ct values, it would not have been possible to distinguish samples with higher quality (RIN > 6.8, range of difference in Ct values: 0-1.84) from those with lower quality (RIN < 4.6, difference in Ct values: 1.75-2.05). For the 11 microscopic samples with unknown RNA quality, RINs were assigned only to 4 of the 11 samples due to artifacts in the electropherograms. RINs ranged from 1.1 to 2.7. The differences in Ct values ranged from 1.61 to 4.59 for the microscopic samples (Table 7). When comparing the differences in Ct values of the microscopic samples to those of the macroscopic samples, 9 microscopic samples showed slightly larger differences in Ct values (Figure 12) and the mean differences in Ct values for the microscopic and the macroscopic samples were significantly different (p = 0.002, Figure 13).

### 2.3.3 Validation of Laser Capture Microdissection, RNA Isolation and Amplification in Comparison to Conventional RNA Isolation

RNA yields for the macroscopic samples ranged from 3 to 26 ng/mg cartilage wet weight and 260/280 nm absorption ratios were 1.9 to 2.1 (Table 8).

When the electropherograms of these samples (obtained with the Nano LabChip®) were assessed subjectively, all samples were of good quality: both rRNA peaks were distinctively visible, with the 28S rRNA peak being higher than the 18S rRNA peak, and the baseline between both peaks being only slightly elevated (Figure 14). The computer program failed to assign an RIN to any of the 6 samples, despite few artifacts in their tracings.

Laser capture of chondrocytes from the articular cartilage was consistently successful. No adverse effects of omitting the steps in water, as well as shortening the time in xylene to 1 minute were noticed. These modifications actually resulted in fewer sections with folds, which in turn improved the success of cell capture. Omission of the staining step made it more difficult to identify the chondrocytes at first, but within several laser capture microdissection sessions, these difficulties subsided.

Determining RNA yield and quality proved to be difficult again, due to artifacts in most of the electropherograms. However, in contrast to previous LCM samples, both rRNA peaks were distinctively visible in 4 of the 6 electropherograms. The 28S rRNA peaks were smaller than the 18S rRNA peaks and the baseline between the peaks appeared mildly elevated (Figure 15). The amount of total RNA isolated per sample (8 caps pooled per sample) was estimated at 2.0-8.0 ng (200-800 pg/µl in 10 µl total volume). Post amplification, the average amplified mRNA yield was 74.9µg/ sample (Table 9) with most amplicons in the 1.0 kb range, based on subjective assessment of the electropherograms without artifacts (Figure 16).

During real-time PCR, none of the negative controls showed any amplification. Expression levels (Figure 17) obtained from the microscopic samples compared to those from macroscopic samples were lower for aggrecan, collagen type II, and TGF-β ($p<0.0001$, $p=0.0004$, $p<0.0001$, respectively), but not for MMP-3 ($p=0.33$). Subsequently, the expression ratios of aggrecan over MMP-3, collagen II over MMP-3 and TGF-β over MMP-3 were significantly different between the 2 RNA isolation methods (all $p<0.01$), but aggrecan, collagen II and TGF-β (aggrecan/collagen II, aggrecan/TGF-β, collagen/TGF-β) had similar gene expression ratios across isolation techniques. No significant difference in variance was demonstrated for any gene using either isolation technique (aggrecan $p=0.61$, collagen type II $p=0.34$, TGF-β $p=0.16$, MMP-3 $p=0.77$).

## 2.4 Discussion

These experiments show that it is feasible to obtain sufficient amounts of RNA to perform gene array analysis from adult equine articular chondrocytes that were isolated with laser capture microdissection. The validated protocol provides means for the comprehensive investigation of gene expression patterns of phenotypically homogeneous cells from different layers of adult articular cartilage.

Meticulous preparation of the frozen sections appeared to be the key for successful capture of articular chondrocytes. As previously described by Jacquet et al. (2005), the sections had to be completely flat, without any folds for the capture to be successful. Unsuccessful capture from sections with folds is most

likely due to the LCM cap not laying flat on the section when it was placed onto a fold. Subsequently, the polymer film was not in contact or close proximity to the tissue at the edges of the fold, preventing adhesion of the polymer to the tissue upon activation of the laser. Flat sections were more easily obtained in thinner sections (5-7 μm) and by omitting the water steps during dehydration and staining. Water appeared to cause swelling of the cartilage sections and they oftentimes detached partially from the slide, resulting in the formation of folds when the sections were dehydrated.

Cell capture was usually unsuccessful when the sections were thawed before the 1$^{st}$ dehydration step. This has been observed by other researchers and it has been speculated that water condensation on the slide occurring while thawing may cause increased adherence of the section to the slide (McGinley JN, and Jacquet R, personal communication).

The capture of articular chondrocytes appeared to be more difficult compared to softer tissues due to the intimate contact of the chondrocytes with their surrounding matrix (Jacquet et al. 2005) and the cohesive nature of the hyaline cartilage matrix. The presence of collagen (mostly type II) in the matrix makes it strong in tension (Temple et al. 2006), likely impeding the separation of captured areas from the unwanted part of the section upon removal of the LCM cap from the slide. This was further supported by the fact that after the capture of multiple areas, the cartilage section usually detached completely from the slide when the LCM cap was lifted up. To cause a brake in the matrix between areas of articular cartilage that were adhered to the cap from those that were not, sticky

tape (Scotch® Magic™ Tape 810, 3M, St. Paul, MN) had to be applied to the section, demonstrating the tensional strength of the hyaline cartilage matrix.

For successful cell capture to occur, the ethylene vinyl acetate polymer film located on the bottom of the LCM cap has to adhere to the underlying tissue section. This is achieved by transferring energy from a near-infrared laser to the polymer. The laser energy is absorbed by the polymer and it subsequently melts and adheres locally to the underlying section. It is further suggested that the polymer film cools down from its melting point at 90°C within 200 ms after the end of the laser pulse, exposing the tissue sections only to very brief time periods of increased temperatures, thus preserving the integrity of DNA, RNA or proteins in the tissue section (Emmert-Buck et al. 1996). Hence, it seems imperative to use laser settings resulting in the least amount of energy transfer to the polymer film and tissue section, without compromising the success of cell capture. The use of excess energy may result in absorption of thermal energy by the tissue section, and subsequent thermal damage of the RNA. The lowest settings that resulted in reliable capture of articular chondrocytes were 100 mW (laser power), 800-2000 µs of pulse duration, 1-5 laser hits per location with a 20 µs delay between hits. Longer delays between laser hits (30-50 µs) slowed down the LCM process significantly, resulting in fewer cells captured in the limited time available for capture.

The assessment of RNA quality or quantity in the microscopic samples (LCM and scrape samples) presented to be challenging. This was due to severe artifacts in 53% of the electropherograms obtained with the Pico LabChip®.

Further, the RNA concentration in the microscopic samples (1-4 caps or sections pooled per sample) was likely below or at the lower level of detection of this assay (500pg/µl), increasing the chance of small artifacts making the RNA signals undetectable. With more concentrated samples, artifacts did not impact the quality of the electropherograms as much, because of the larger scale of the RNA signals (Figure 18). The RNA Integrity Number (RIN), which is a number on a scale of 1 to 10 (1 representing complete RNA degradation and 10 representing intact RNA), is supposed to be a more objective measurement of RNA quality. It is computed by extracting up to 100 quality determining features from the electropherogram trace (Imbeaud et al. 2005). It has been successfully validated against other means of RNA quality assessment for both the Pico and the Nano LabChip® kits (Imbeaud et al. 2005, Kerman et al.2005). In the present study, the RIN was determined reliably for the electropherograms obtained with the Nano LabChip® kit, but in 59% of the electropherograms obtained with the Pico LabChip® kit, the computer program failed to assign an RIN. This was most likely due to the computer program not being able to apply the algorithm for the RIN on electropherograms with significant artifacts. Because of the low RINs that were actually assigned to the microscopic samples, the influence of RNA concentration on the RIN was investigated using dilution series of macroscopic RNA samples with known good quality. It was found that samples with lower RNA concentration had lower RINs assigned than the same samples with higher concentration when the Pico LabChip® was used, but not with the Nano LabChip®. Imbeaud et al. (2005) made similar observations (lower RINs than

expected, electropherograms with unusual migration behavior and shifted baseline values) in samples with RNA concentrations below the lower limit of quantitation for the Nano LabChip® assay (indicated by the manufacturer at 25 ng/µl). Based on the frequency of artifacts in electropherograms in the present study, it was deemed impossible to reliably determine the RNA quality of each individual microscopic sample, when only 4 sections or caps were pooled into 1 sample. Further, it was even difficult to estimate the RNA quality of the LCM or scrape samples in general, but it was assumed that the RNA in these samples was moderately degraded, at best. Based on specific amplification of selected genes during real-time PCR in a subset of these samples it was concluded that these samples did in fact contain RNA, but at a concentration below the lower level of detection for the Pico LabChip® (<500pg/µl).

A different method to estimate RNA quality was investigated by determining differences in Ct values between aliquots of RNA samples that were reverse transcribed with either oligo-dT primers or with random hexamers. The idea behind this was that the 5' end of the mRNA transcripts should be underrepresented after reverse transcription with oligo dT primers to a degree, corresponding to the extent of degradation of the RNA in the sample (Swift et al. 2000). However, this should not be the case with random hexamer primers. Thus, amplification of the resulting cDNA with primers at a certain distance to the 3' end of the transcript should be different between an aliquot of a degraded sample that had been reverse transcribed with oligo dT primers and an aliquot for which random hexamers had been used for reverse transcription. Macroscopic

samples with good and moderate RNA quality were used to find a possible association between RIN determined with the Nano LabChip® and difference in Ct values for the equine gene GAPDH. However, no such correlation was found. The lack of a correlation may be explained by fact that the TaqMan® system for equine GAPDH aligns relatively close to the 3' end of the GAPDH mRNA (< 1200 base pairs upstream to the estimated 3'end), in an area that may still be attached to the poly-A tail of the GAPDH mRNA, even in degraded samples. This explanation is in accordance with findings by Swift et al. (2000), who saw a decrease in amplification with primers annealing 6000 base pairs upstream to the 3' end in samples with degraded RNA. Despite this, most microscopic samples had a greater difference in Ct values than the macroscopic samples, and the means for the 2 sample groups (macroscopic and microscopic samples, respectively) were significantly different. This was possibly a sign for significantly lower RNA quality in the microscopic samples compared to the macroscopic samples, but the methodology did not appear to be sensitive enough to detect a moderate amount of RNA degradation.

Based on the previous assessments, several modifications were implemented for the final validation experiment. Among these were the shortening of the dehydration protocol, omission of staining of the sections, termination of LCM only 14 minutes after the section was thawed and the combination of 8, rather than 4 caps per sample. The modifications resulted in an improvement of the quality of the electropherograms, allowing subjective assessment of RNA quality in 66% of the LCM samples. In these samples, the

RNA was judged to be mildly degraded. In accordance with these findings, it has been reported that staining of frozen sections is associated with a decrease in RNA quality from laser captured samples (Kerman et al. 2005, McGinley JN, personal communication). Kerman et al. (2005) also noticed RNA degradation in frozen sections taking effect after 7 minutes at room temperature. Thus, restricting the time from thawing of the section until the end of laser capture to even less than the 14 minutes used in the present study may help to increase the RNA quality further. In the final validation experiment of the present study, the total RNA yield was estimated to be 2000 – 8000 pg with 8 LCM caps being pooled into 1 sample. To obtain sufficient RNA from LCM samples for gene array analysis in future investigations, 2 rounds of *in-vitro* transcription amplification (IVT) were performed. IVT is supposed to amplify RNA in a "linear" manner, resulting in preservation of comparative mRNA levels (Van Gelder et al. 1990, Eberwine et al. 1992, Baugh et al. 2001, Ginsberg 2005). This is in contrast to PCR based amplification protocols, which amplify transcripts exponentially, possibly skewing the original quantitative relationships between transcripts (Ginsberg 2005, Patel et al. 2005). In the present study, following 2 rounds of *in-vitro* transcription amplification, an average yield of 74.9 µg RNA (amplified mRNA) was achieved. This amount is more than sufficient to perform gene array analysis: 15 µg or more (amplified) mRNA are required to prevent an increase in false-negative calls when the Affymetrix GeneChip® system is used (Moldovan L, personal communication, Patel et al. 2005). A previous report (Patel et al. 2005) obtained similar RNA yields (2.1–180 µg amplified mRNA from

starting amounts of 500 pg – 200 ng total RNA), utilizing the same reagent kit (RiboAmp® HS, Arcturus Bioscience, Mountain View, CA).

The expression levels determined in laser captured, amplified samples were lower in 3 of the 4 genes tested compared to expression levels in macroscopic non-amplified samples. This may reflect a 3' biased, truncated amplification, as the TaqMan® systems of 2 of the 3 genes anneal >1000 base pairs upstream to the 3'end of the RNA. The electropherogram traces without artifacts, taken after 2 rounds of amplification also support this, as they showed most amplicons to be 1000 or fewer base pairs in length. The introduction of a 3' bias is a well known effect of *in-vitro* transcription amplification, but it is thought to exist for all transcripts, allowing the comparison of relative gene expression levels (Ginsberg 2005). However, the TaqMan® system for equine TGF-β anneals about 720-820 base pairs upstream of the 3' end. Thus, 3' biased, truncated amplification does not explain lower expression levels in the laser captured, amplified samples for this gene. It is possible that the TGF-β cDNA folds extensively into secondary structure, and thus impedes reverse transcription, resulting in fewer transcripts that contain the area where the TaqMan® system anneals. Another possibility is that the TGF-β mRNA is less stable than the other mRNA transcripts tested and the mild degradation in the LCM samples affected the TGF-β transcript more than the other transcripts. This would result in fewer TGF-β templates being available to be amplified and subsequent lower expression levels in the laser captured, amplified samples compared to the higher quality macroscopic samples. Greater sensitivity of

certain mRNA transcripts to RNA degradation has been reported previously (Hargrove and Schmidt 1989, Kerman et al. 2005). These reports emphasize the importance of the use of samples with good or at least similar RNA quality for gene expression analysis. In the present study, the differences in expression levels between laser captured amplified samples and macroscopic samples were found to be a consistent phenomenon, supporting the conclusion that the laser capture microdissection and amplification protocol used in this study is valid to use for gene expression analysis of articular chondrocytes with real-time PCR. Further, if gene array analysis is employed, it would be beneficial to utilize 3' biased probe arrays. It is important to realize that expression levels should be compared only between samples that were processed similarly. Additionally, as the expression ratios between 2 different genes may be altered by the amplification even in similarly processed samples, the comparison of expression levels between 2 different genes should not be performed on laser captured, amplified samples.

In conclusion, meticulous preparation of the frozen tissue sections, omission of staining of the tissue sections, expedient laser capture and pooling of multiple cell captures appeared to be vital to obtain a satisfactory quantity and quality of RNA from articular chondrocytes via laser capture microdissection. Assessment of quality and quantity of the RNA using capillary electrophoresis was challenging due to the likelihood of artifacts in electropherograms from samples with such low concentration of RNA. Two rounds of *in-vitro* transcription amplification of RNA samples from laser captured chondrocytes yielded ample

amounts of RNA for comprehensive gene expression analysis and although the amplification changed the expression levels of 3 of the 4 tested genes, the changes in gene expression were similar and consistent among the different samples. Thus, this study successfully validated a protocol that would allow isolating RNA from phenotypically similar articular chondrocytes for gene expression analysis employing either real-time PCR or gene array analysis.

# CHAPTER III

## *3 Gene Expression*

### 3.1 Introduction

Musculoskeletal diseases are a major cause of lameness in horses, resulting in pain and loss of function for the affected animal, as well as significant economic losses for the equine industry. A large percentage of lameness' can be attributed to joint associated problems (Jeffcott et al. 1982, Rossdale et al. 1985, Todhunter 1990), among which osteoarthritis is considered the disease with the greatest economical impact (Pool 1996).

Osteoarthritis results in progressive deterioration of the articular cartilage associated with changes in bony and soft tissues of the affected joint (Ishiguro et al. 2002). Despite the fact that the joint is an organ made up of several different tissues, and that pathologic changes in any of these tissues can lead to organ failure due to osteoarthritis (Pool 1996), the hyaline cartilage is commonly considered to play a central role in the pathophysiology of osteoarthritis. Subsequently, multiple studies have investigated altered gene expression in cartilage from osteoarthritic joints using various methodologies and sample sources (reviewed in Horton et al. 2005).

Gene array analysis represents a methodology to simultaneously investigate the expression of several thousand genes, allowing the comprehensive study of changes in chondrocyte metabolism under the influence

of osteoarthritis (Aigner et al. 2004). The majority of studies have used this technology to examine gene expression of articular chondrocytes *in-vitro*, but some have investigated gene expression patterns in normal and osteoarthritic cartilage in vivo (Aigner et al. 2001a, Aigner et al. 2003, Knorr et al. 2003, Gebauer et al. 2005, Sato et al. 2006, Smith et al. 2006). Most of these studies compared gene expression patterns of articular cartilage between individuals with and without naturally occurring osteoarthritis. However, the results have to be interpreted with caution, as cartilage samples were not matched well with respect to sampling times and location, age, gender or exercise history of the study subjects. Circumventing those concerns, one study (Sato et al. 2006) compared gene expression patterns between histologically intact and damaged regions of cartilage within the same joint. The present study utilizes an established experimental model for osteoarthritis in horses (Frisbie et al. 2002) with pathologic, histologic, and clinical findings similar to those seen with naturally occurring osteoarthritis in the same species (Pool 1996, McIlwraith 1998, Goodrich and Nixon 2006). Additionally, this model allows for the collection of samples from an osteoarthritic and a control joint in the same individual, decreasing the commonly large variability between individuals.

Further, previous reports on global gene expression in articular cartilage have used samples of full thickness hyaline cartilage. However, articular cartilage is made up of 4 different zones with phenotypically distinct chondrocytes (tangential, intermediate, radial and calcified cartilage zones) (Eurell 2004), and changes in gene expression are most easily detected in

phenotypically homogeneous cells populations (Emmert-Buck et al. 1996, Horton et al. 2005). In the present study, the separation of chondrocytes from different zones of articular cartilage, based on their phenotypic appearance was achieved with laser capture microdissection. To the author's knowledge, it is the first study to determine global gene expression patterns in different zones of articular cartilage from osteoarthritic and control joints.

The goal of this study was to determine differentially expressed genes in phenotypically homogeneous cells of 2 different cartilage layers from osteoarthritic and control joints. These genes are likely to be involved in the homeostasis of articular cartilage or in the pathophysiology of osteoarthritis, and may represent future targets for the treatment of this debilitating disease.

## 3.2 Materials & Methods

### 3.2.1 Animals

Six healthy horses (age 2-5 years) were used, that were enrolled in a terminal study employing the carpal osteochondral fragment model for osteoarthritis (Table 10). The study had been reviewed and approved by Colorado State University's Animal Care and Use Committee. At the beginning of the study, all horses were free of carpal effusion and front limb lameness before and after carpal flexion. They underwent bilateral inter-carpal joint arthroscopy during which an osteochondral fragment was created in 1 randomly allocated joint at the distal aspect of the radiocarpal bone, as described by Frisbie et al. (2002). Additionally, a defined amount of osteochondral debris was left in the joint. Post-operatively, the horses were enrolled in a controlled

exercise program on an equine treadmill (Table 11), starting on day 14 after surgery until 70 days post-operative, when they were euthanized. Three of the 6 horses were treated topically (over the joint with the osteochondral fragment) with 7.3 g of a 1% diclofenac sodium cream (Surpass® Cream, Idexx Pharmaceuticals, Greensboro, NC) twice a day from day 14 until day 70 after surgery.

### 3.2.2 Sampling

Full-thickness hyaline cartilage was collected aseptically from the dorsal aspect of the radial facet of both 3rd carpal bones within 10 hours post-mortem (Figure 19). All samples were placed in OCT (Tissue Tek OCT Compound, Sakura Finetek, Torrance,CA) and snap frozen in methyl butane, which was cooled by liquid nitrogen, and stored at -80°C until further processing.

### 3.2.3 Sample Processing

The samples were processed as validated in the preliminary experiments (see chapter II). Briefly, they were sectioned at 5-7 µm thickness on a cryostat (Leica 3050, Leica Microsystems, Bannockburn, IL) and mounted on slides using a tape transfer system (CryoJane, Instrumedics, Hackensack, NJ). The slides were stored at -80°C until further processing.

Laser capture microdissection was performed immediately after dehydration in graded ethanol and xylene (HistoGene LCM Frozen Section Staining Kit, Arcturus Bioscience, Mountain View, CA) on an Autopix Unit (Arcturus Bioscience, Mountain View, CA), according to a protocol by Landis et al. (2003). To obtain samples representing chondrocytes from the tangential

layer of cartilage, only cells located in close proximity to the articular surface with an elongated (parallel to the articular surface) rather than round appearance were captured. For samples representing chondrocytes from the radial layer, only cells deep within the cartilage, arranged in columns perpendicular to the articular surface with a round appearance were captured. Care was taken to terminate the capture on each section within 14 minutes of removing the section from the -80°C freezer. The actual time from thawing the section until covering of the captured cells with extraction buffer and the estimated number of cells captured was recorded.

The RNA was isolated and treated with DNase, according to the manufacturer's instructions of a commercially available RNA extraction kit (PicoPure™ RNA Isolation Kit, Arcturus Bioscience, Mountain View, CA). The following modifications were implemented: The caps containing the captured cells were covered with 35 µl RNA extraction buffer and kept at room temperature for up to 3 hours before being processed further. Eight caps were pooled into 1 sample and the samples were loaded and eluted twice from the RNA-purification column.

Following, the RNA was tested for quality using the 2nd generation Pico LabChip® Kit and 2100 Bioanalyzer (Agilent Technologies, Palo Alto, CA) and then stored at -80°C until further use. Subjective assessment of RNA quality was performed by inspection of the electropherogram as described by Imbeaud et al. (2005), and the RNA integrity number (RIN) was determined using the 2100 Expert software (Agilent Technologies, Palo Alto, CA).

As an additional means of quality control, remaining slides prepared for laser capture microdissection (4-6 per sample) were used to isolate RNA from scrape samples. Briefly, the slides were dehydrated as described for the laser captured samples, left at room temperature for 10 minutes, and then the sections were scraped off the slides and placed into 50 µl of extraction buffer (4-6 sections pooled per sample). RNA was isolated and tested for quality as described for the laser captured samples. The RNA was not used for any other analysis.

The RNA from laser captured samples was amplified as validated in the preliminary experiments, with several modifications to allow for labeling of the transcripts in preparation for gene array analysis with the Affymetrx GeneChip® System (Affymetrix, Santa Clara, CA). The samples were amplified via 1 round of *in-vitro* transcription (RiboAmp® HS, Arcturus Bioscience, Mountain View, CA) and the amplification yield was determined using spectrophotometry (ND-1000 spectrophotometer, Nanodrop, Wilmington, DE). An adequate amount of Poly-A RNA controls (Affymetrix, Santa Clara, CA) was added to each sample, according to the manufacturer's instructions. Following, the samples were reverse transcribed into double stranded cDNA (RiboAmp® HS, Arcturus Bioscience, Mountain View, CA) and stored at -20°C until further processing.

The 2$^{nd}$ round of *in-vitro* transcription amplification was performed with the GeneChip® IVT Labeling Kit (Affymetrix, Santa Clara, CA), according to the manufacturer's instructions. Briefly, the double stranded cDNA was reverse transcribed overnight and the labeled cRNA was purified on a spin column. The purified cRNA was quantified using spectrophotometry (ND-1000

spectrophotometer, Nanodrop, Wilmington, DE) and the quality of amplification was assessed using the Experion RNA StdSens Analysis Kit and Experion Automated Electrophoresis System (BioRad Laboratories, Hercules, CA). Following, the cRNA was fragmented using the GeneChip® Sample Cleanup Module (Affymetrix, Santa Clara, CA), and the success of fragmentation was ascertained by analyzing the samples one last time with the Experion RNA StdSens Analysis Kit and Experion Automated Electrophoresis System (BioRad Laboratories, Hercules, CA). A large peak close to the marker peak was interpreted as successful fragmentation.

Pre-wetted equine-specific Affymetrix GeneChips® (Gu and Bertone 2004) were loaded with the fragmented, labeled cRNA and hybridized according to the manufacturer's instructions (Affymetrix, Santa Clara, CA). Washing and staining of the array was performed on the Fluidics Station 400 (Affymetrix, Santa Clara, CA) using the appropriate fluidics scripts. Then, the arrays were scanned by the Affymetrix GeneChip® Scanner 3000 (Affymetrix, Santa Clara, CA) and the data was collected and processed by the GeneChip® Operating Software (GCOS v1.2.1, Affymetrix, Santa Clara, CA).

### 3.2.4 Statistical Analysis

Gene array data was processed using R in BioConductor (www.biconductor.org, Gentleman et al. 2004). Statistical modeling was performed using "proc mixed" in SAS 9.1 (SAS Institute, Inc., Cary, NC).

#### 3.2.4.1 Quality Control of the Array Data

Quality control was performed on each array by visual inspection of the raw CEL file images. Further, residual plots, box plots and histograms of probe intensities were examined. An RNA digestion plot was analyzed to detect arrays with different RNA digestion patterns. A principal component analysis (PCA) was performed to find chips that represented outliers. Log ratio vs. average log intensity (MVA) plots were inspected and the percentage of probe sets called present was determined for each gene array. The correlations of $\log_2$ perfect match probe intensities between arrays as well as the correlations between the $\log_2$ perfect match and the $\log_2$ mismatch probe intensities from the same array were assessed. Chips with significant artifacts or patterns, or chips that were consistently outliers in the quality control measures were excluded from the subsequent data analysis and treated as missing data.

#### 3.2.4.2 Normalization and Summarization of the Array Data

Background correction, normalization and calculation of the expression value for each gene (probe set data summaries) were performed using the Robust Multi-Array Average (RMA) algorithm (Irizarry et al. 2003) in BioConductor (www.biconductor.org, Gentleman et al. 2004). The RMA method uses only perfect match probe values.

#### 3.2.4.3 Identification of Differentially Expressed Genes

61% of probe sets were determined to be present on at least 1 array and were included in the further analysis. The remaining 39% of probe were omitted from the further analysis. A mixed model with 1 random factor (horse) and 3

fixed factors (disease status, cartilage layer, treatment) and all pair-wise interactions were fit to the RMA expression indices in SAS for each probe set. Let $Y_{ijkl}$ be the RMA expression index for horse *i*, receiving treatment *j*, with disease status *k* for cartilage layer *l*, for a single probe set then

$$Y_{ijkl} = \mu + T_j + D_k + C_l + TD_{jk} + TC_{jl} + DC_{kl} + H(T)_{i(j)} + HD(T)_{ik(j)} + HC(T)_{il(k)} + \varepsilon_{i(j)kl}$$

where $T_j$ is a treatment effect (fixed), $D_k$ is a disease effect (fixed), $C_l$ is a cartilage layer effect (fixed), $TD_{jk}$ is a treatment-disease interaction (fixed), $TC_{jl}$ is a treatment-cartilage layer interaction (fixed), $H(T)_{i(j)} \sim N(0, \sigma^2_{H(T)})$ is a horse effect (random), $HD(T)_{ik(j)} \sim N(0, \sigma^2_{HD(T)})$ is the horse-disease interaction (random), $HC(T)_{il(k)} \sim N(0, \sigma^2_{HC(T)})$ is the horse-cartilage layer interaction (random).

The effect of treatment, disease status (osteoarthritic vs. control cartilage), cartilage layer (tangential vs. radial layer) and their pair-wise interactions were investigated. Differentially expressed genes for these comparisons were ranked based on their q-values, rather than p-values in order to account for multiple testing. The q-value for a particular probe set is the expected proportion of false positives incurred when calling that feature significant (Storey and Tibshirani, 2003). Therefore, using a q-value threshold of 0.05 produces a group of probe sets such that 5% are expected to be false positives. The q-values were calculated separately for each comparison.

When testing for cartilage layer effect, 158 probe sets had q-values less than 0.05. However, for the other comparisons no probe sets yielded q-values that fell below the 0.05 threshold. Thus, for disease effect and the disease by

location effect, probe sets with raw p-values less than 0.01 and absolute $\log_2$ fold-difference of expression greater than 0.585 (corresponding to a 1.5 fold or greater difference in expression) were identified as most likely candidates for differential expression.

### 3.2.5 Annotation

To assign biological functions to the differentially expressed genes, sequences with unknown gene names were compared to sequences within GenBank, EMBL, DDBJ, and PDB, using the Basic Local Alignment Search Tool (BLASTn, Altschul et al. 1997). Homology to sequences with known gene names was inferred when the score was greater than 200 and the E-value smaller than 0.0001. Biological functions associated with each gene name (name for original sequence or inferred by sequence similarity search) were compiled using Entrez Gene (Maglott et al. 2005), the Human Protein Reference Database (Peri et al. 2003), GeneOntology.org (The Gene Ontology Consortium 2000) and the UniProt Knowledgebase (Apweiler et al. 2004).

## 3.3 Results

### 3.3.1 Sample Processing

#### 3.3.1.1 Laser Capture Microdissection

In most cases (176/192 sections or 91.7%), laser capture microdissection resulted in detachment of the complete cartilage section when the cap was removed from the slide. A double-sided tape (Scotch® Magic™ Tape 810, 3M, St. Paul, MN) was gently pushed onto the cap in these cases and the unwanted part of the section came off with the tape when it was removed again. The

estimated average number of cells captured per sample was 1585 (for individual estimations see Table 12, Figure 20). The average time between thawing of the cartilage section and covering of the captured cells with extraction buffer was 13 minutes (Table 13, Figure 21).

3.3.1.2 RNA Quality and Estimated Yield

Fewer artifacts were noticed in the electropherograms, compared to the measurements with the 1st generation Pico LabChip® Kit (see results section in chapter II). The RINs from laser captured samples ranged from 1 to 7.6 with an average of 2.1 (Table 14). Upon subjective evaluation of the electropherograms, the 18S and 28S rRNA peaks were present in most samples (17 of 24 laser captured samples), and no tracing showed a large peak close to the marker peak (Figures 22a,b,c). Total RNA yield per laser captured sample (8 caps pooled per sample) was estimated at 500-6,000 pg with an average of 2,700 pg per sample. In 5 of the 24 laser captured samples the Pico LabChip® assay estimated RNA yields above 10,000 pg per sample and 4 of the 5 electropherograms had small artifacts. The total RNA yields and RINs from the corresponding scrape samples were higher. Yields were estimated at 16,000 to 50,000 pg per sample (4-6 sections per sample) with an average of 31,000 pg. The RINs for the scrape samples ranged from 7.5 to 8.9 (average 8.6). For individual sample's RNA quality control measures and estimated RNA yields see Table 15.

3.3.1.3 RNA Amplification

The amplified mRNA yield after the 1st round of *in-vitro* transcription amplification ranged from 0.376 µg to 1.681 µg with an average of 1.047 µg of

amplified mRNA per sample. The 260/280 absorption ratios ranged from 1.65 to 2.41 with an average ratio of 2.05. The amplified mRNA yield after the 2nd round of *in-vitro* transcription amplification ranged from 5.0 µg to 86.6 µg with an average amplified mRNA yield of 61.1 µg per sample. The 260/280 absorption ratios ranged from 1.802 to 3.288 with an average ratio of 1.9. For measurements on individual samples see Table 15.

### 3.3.2 Gene Array Data

#### 3.3.2.1 Gene Array Diagnostics

No obvious artifacts were noticed in the CEL image files. The image of array 14 appeared much darker than the rest of the images (Figure 23).

Small, circular areas of increased residual values were seen on arrays 1, 7, 8 and 20. Further, array 14 was noted to have generally higher residual values (Figure 24).

Array 1 had higher overall pixel intensities and array 14 had much lower overall pixel intensities compared to the other arrays (Figure 25).

Array 14 was found to have a markedly different digestion pattern. Further, array 7 had a slightly different digestion pattern compared to the other arrays (Figure 26).

In the PCA plot, array 14 was an extreme outlier. The other arrays were clustered in a relatively tight area. This did not change when array 14 was excluded (Figure 27).

In the MVA plots, array 14 showed extreme curvature, and several other arrays (2, 3, 4, 7, 12, 17, 21, 24) were noted to have mild curvature (Figure 28).

Array 14 had only 3.4% of probe sets called present, which was markedly less than for all other arrays (range 23% for array 7, 44% for array 12, Figure 29). Overall, 61% of probe sets on the array were called present on at least 1 array.

Array 14 had a very low correlation with all other arrays (R=0.24-0.28). After excluding array 14, the lowest correlation between the $\log_2$ values for the perfect match probes was 0.695 (between arrays 7 and 11, Table 16). The correlation between the $\log_2$ values for the perfect match probes and those for the mismatch probes from the same array ranged between 0.64 (array 7) and 0.8 (array 13) (Table 17).

Array 14 was excluded from further data analysis, due to consistently appearing as an outlier in the quality control measures.

3.3.2.2 Differentially Expressed Genes

Of a total of 3719 probe sets on the array, 61% or 2263 probe sets were called present on at least 1 array. After using a multiple testing adjustment, 158 genes were found to be differentially expressed ($q<0.05$) between tangential and radial cartilage layers. Four of these were canine probes and they were omitted from interpretation of the data, resulting in a total of 154 differentially expressed genes. Using the q-value cut-off of $q<0.05$, no genes were found to be differentially expressed between control and osteoarthritic samples, dependent or independent of cartilage layer. Further, no genes were found to be differentially expressed between samples from joints that were treated with the diclofenac ointment and those that were not treated, dependent or independent of disease status or cartilage layer.

3.3.2.2.1 Differentially Expressed Genes between Tangential and Radial Cartilage Layer ($q<0.05$, Table 18)

Genes involved in cell cycle, cell proliferation, differentiation, apoptosis

When comparing the gene expression patterns of genes influencing cell proliferation, differentiation and apoptosis, more genes inhibiting cell proliferation and promoting apoptosis than genes with opposite effects were upregulated in the radial layer, compared to the tangential layer. In the tangential layer, more genes promoting cell proliferation and inhibiting apoptosis than genes decreasing cell proliferation and supporting apoptosis were upregulated, compared to the radial layer.

Genes involved in inflammatory mediator synthesis

An inhibitor of phospholipase A was upregulated and prostaglandin synthase, also known as COX2 was downregulated in the radial layer compared to the tangential layer, whereas an enzyme synthesizing leukotrienes was upregulated in chondrocytes from the radial layer compared to those from the tangential layer.

Genes coding for growth factors, transcription factors influencing growth factor expression

Fibroblast growth factor was upregulated in the radial layer compared to the tangential layer. Further, a transcriptional repressor of tumor necrosis factor, epidermal growth factor receptor and platelet derived growth factor was downregulated in the radial layer compared to the tangential layer.

Genes coding for extracellular matrix proteins, their modifiers, extracellular matrix proteases and protease inhibitors, cell-matrix interaction proteins

Chondrocytes from the radial layer were more actively expressing genes coding for non-collagenous matrix proteins than the cells in the tangential cartilage layer. ADAMTS1, an aggrecanase, was upregulated in the tangential layer, compared to the radial layer, as were CD44 and thrombospondin 1, receptors believed to be involved in cell-matrix interactions.

Genes involved in angiogenesis

The antiangiogenic gene thrombospondin 1 was represented with 3 probe sets on the array, and it was consistently upregulated in the tangential layer compared to the radial cartilage layer. As mentioned above, this gene is also implicated to be involved in cell-matrix interactions and matrix homeostasis.

Genes involved in cell protection under stress

In the radial layer, protein stabilizing chaperones were upregulated, compared to the tangential layer, where anti-apoptotic genes and a free radical scavenger were upregulated.

Genes coding for immune response proteins

Several surface receptors involved in immune responses, as well as an endogenous antimicrobial peptide were downregulated in the radial layer compared to the tangential layer. Only a protein involved in cellular IgG and albumin recycling, as well as the lambda chain of the immunoglobulin molecule were upregulated in the radial layer compared to the tangential layer.

Genes involved in cell communication

Two genes, whose proteins may be involved in cell communication were upregulated. Further, an inhibitor of calcineurin, which is a transcription factor enhancing IL-2 expression was downregulated in the radial layer, compared to the tangential layer.

Genes involved in the clotting cascade

An activator of vitamin K was upregulated in the radial layer, compared to the tangential layer.

Genes coding for Intracellular structural proteins, proteins involved in cell and intracellular movement

Several actin binding, organizing and cross-linking genes were expressed differentially between radial and tangential cartilage layers. However, no obvious gene expression pattern was noticeable for either cartilage layer. Myosin was upregulated, whereas tubulin was downregulated in the radial layer compared to the tangential layer.

Genes involved in intracellular iron storage

Two genes encoding the components for ferritin, an intracellular iron storage protein, were upregulated in the tangential layer compared to the radial layer.

Genes involved in intracellular signaling

A total of 7 proteins likely involved in the transmission of different intracellular signals were differentially expressed between the radial and the

tangential cartilage layers. Most of them (5 of 7) were upregulated in the radial layer.

Genes coding for Ion channels

Two genes coding for ATP-driven proton pumps were upregulated in the radial layer, compared to the tangential cartilage layer, as was a calcium channel. A potassium pump was downregulated in the radial layer compared to the tangential layer.

Genes coding for transcription factors involved in skeletal development

A gene coding for a transcription factor which plays an important role during skeletal development was upregulated in chondrocytes from the tangential layer compared to cells from the radial layer. Overexpression of this gene during skeletal development results in skeletal abnormalities as seen in trisomy-16 mice and humans with Down syndrome.

Genes involved in mRNA processing

Two genes involved in mRNA splicing were upregulated in the radial layer, compared to the tangential layer.

Genes coding for transcription factors of unknown function

Several transcription factors of unknown specific function (3 of 4) were upregulated in chondrocytes from the radial layer compared to those from the tangential layer.

Genes coding for ribosomal proteins and other proteins necessary for translation

All genes coding for ribosomal proteins and other proteins necessary for translation that were found to be differentially expressed were upregulated in the radial layer compared to the tangential layer of articular cartilage.

Genes involved in amino acid synthesis and transport of amino acids

All differentially expressed genes involved in endogenous amino acid synthesis and amino acid transport were upregulated in the tangential layer compared to the radial cartilage layer.

Genes involved in intracellular protein transport

All differentially expressed genes involved in protein transport were upregulated in the radial layer compared to the tangential layer of articular cartilage.

Genes involved in protein catabolism

Gene expression of a protein involved in regulated protein catabolism via the ubiquitin cycle was upregulated in the radial compared to the tangential cartilage layer.

Genes coding for intracellular proteases and inhibitors

Cystatin B, an intracellular protease inhibitor was upregulated in tangential chondrocytes compared to radial layer cells.

Genes involved in lipid and steroid metabolism

Three genes involved in lipid and steroid metabolism were differentially expressed, but no obvious pattern was noted for either cartilage layer.

Genes involved in carbohydrate metabolism

Two genes involved in carbohydrate metabolism were found to be upregulated in the radial layer, compared to the tangential layer.

Genes involved in oxidative phosphorylation

A gene coding for a protein supporting oxidative phosphorylation was upregulated and another gene, coding for a protein that neutralizes superoxides was downregulated in the radial layer compared to the tangential layer of articular cartilage.

3.3.2.2.1 Genes Most Likely Differentially Expressed Between Osteoarthritic and Control Cartilage – Dependent on Cartilage Layer as Indicated ($p<0.01$ and $\log_2$ fold change$>1.5$, Table 19)

To determine genes that were most likely differentially expressed between control and osteoarthritic cartilage and to evaluate if this was dependent on cartilage layer, genes with a raw p-value of $p\leq0.01$ combined with a $\log_2$ fold change in expression of $\log_2\geq0.585$ (corresponds to a 1.5 fold or greater difference in expression) were selected. Seven genes were found to fall into these parameters for disease status and 10 genes were found to fall into these parameters for the interaction between disease status and cartilage layer.

Genes involved in cell cycle, cell proliferation, differentiation, apoptosis

Under the influence of osteoarthritis, cyclin D2, a gene absolutely necessary for cell proliferation was upregulated, as was another gene inhibiting cell proliferation (dual specificity phosphatase 1). This gene is also commonly involved in the response to oxidative stress. Two genes believed to have anti-

apoptotic properties were downregulated in osteoarthritic cartilage. This was more pronounced in the radial than the tangential cartilage layer. One of these genes may also support cell proliferation and the other one may be involved in protein folding and assembly.

Genes coding for extracellular matrix proteins, their modifiers, extracellular matrix proteases and protease inhibitors, cell-matrix interaction proteins

A protease inhibitor acting against cathepsin G and other extracellular proteases was upregulated under the influence of osteoarthritis.

Genes involved in cell protection under stress

As mentioned before, a gene involved in the response to oxidative stress was upregulated in osteoarthritic cartilage.

Genes coding for immune response proteins

A gene involved in the transcriptional regulation of the immune response and inhibitor of the NF-κB pathway was downregulated in osteoarthritic cartilage, compared to control cartilage.

Genes involved in the transport of proteins

A gene involved in the transmembranous transport of proteins was upregulated in osteoarthritic cartilage compared to control specimens.

Genes involved in carbohydrate metabolism

Two genes involved in glucose metabolism, 1 coding for a protein of the glycolytic pathway and the other coding for a protein involved in preparation of glucose as building blocks for proteoglycans were downregulated in osteoarthritic

cartilage, and this was more pronounced in the radial than in the tangential cartilage layer.

## 3.4 Discussion

The separation of chondrocytes from the tangential and the radial cartilage layer by laser capture microdissection was consistently successful. Despite having to spend time on determining phenotypic characteristics of the chondrocytes, dehydration and cell capture of each section were performed on average within 13 minutes. It was impossible to determine the exact number of cells captured per slide, because visual inspection of the LCM caps after cell capture was not performed. This step would have added 1-2 minutes to the time interval between thawing of the section and covering the captured cells with extraction buffer, likely resulting in lower quality RNA. Thus, to estimate the number of captured cells, the laser hits were counted and it was assumed that 1 cell was captured per laser hit.

The RNA quality was assessed to be adequate despite low RINs in most laser captured samples. This was justified by the presence of rRNA peaks in 17 of the 24 samples, as well as by the higher RINs in the corresponding scrape samples. Further, no large peaks were found close to the marker peak, as noticed in more degraded samples in the preliminary experiments (Figure 7). Low RINs and missing rRNA peaks in 7 of the 24 electropherograms were attributed to the low concentration in the laser captured samples. Very low RNA concentration in some samples may be explained by the fact that cell capture may have been less than 100% efficient. Visual inspection of the caps after cell

capture would have allowed to use only those caps with very efficient capture, however, RNA quality would have been compromised due to added time of the laser capture process.

The 2 rounds of *in-vitro* transcription amplification resulted in a sufficient amount of RNA for gene array analysis in 23 of the 24 samples. The sample with significantly less RNA compared to the other samples was loaded onto an array anyway, but had to be excluded from the data analysis, because it consistently presented as an outlier during array diagnostics (array 14). Array 7 also had a slightly different RNA digestion pattern, and showed small circular areas of increased residual values on the residual plot. This array was included in the final data analysis, because it did not consistently present as an outlier in the array diagnostics.

Few studies have used gene array analysis to investigate gene expression patterns in normal or osteoarthritic cartilage. Previous investigations analyzed cartilage samples from naturally occurring osteoarthritis, usually utilizing large samples including all hyaline cartilage layers (Aigner et al. 2001a, Knorr et al. 2003, Gebauer et al. 2005, Sato et al. 2006, Smith et al. 2006). In contrast, the present study utilized paired samples from the same animal with experimentally induced osteoarthritis. This approach, combined with the separation of chondrocytes from the tangential and the radial layer was expected to decrease variability in the data and facilitate the discovery of differentially expressed genes. Thus, it was surprising that with adequate statistical corrections to maintain the false discovery rate below 5%, no genes were found to be

differentially expressed between osteoarthritic and control cartilage. Even when less rigorous statistics were applied, only 17 genes were detected to be differentially expressed between osteoarthritic and control cartilage. It is unlikely that this was due to errors in sample processing or data acquisition, as there were 154 genes found to be differentially expressed between tangential and radial layers of the articular cartilage, even with the application of a multiple testing adjustment. Another reason for the lack of differentially expressed genes between osteoarthritic and control cartilage could be the fact that only part of the equine genome was represented on the array. It is possible that genes which were not present on the array were in fact differentially expressed, and this is a clear limitation of the present study, due to the fact that the equine genome has not been completely sequenced yet. However, one would then expect to find similarly low numbers of differentially expressed genes for the cartilage layer effect, which was not the case. Most likely, the small fold differences between expression in osteoarthritic and control cartilage made it difficult to detect significantly differentially expressed genes: few genes had greater than 2-fold differences in expression when comparing osteoarthritic to control cartilage, and more genes showed greater differences in expression when the tangential layer was compared to the radial layer (Figure 30). Another gene array investigation that utilized the same gene array yielded similarly small fold changes, but identified more differentially expressed genes by using a raw p-value cut-off of $p<0.005$ (Smith et al. 2006), which is not considered an adequate multiple testing adjustment (Gottardo et al. 2003).

To the author's knowledge, this investigation was the first to compare global gene expression between 2 different layers of articular cartilage. Chondrocytes from the tangential and the radial layer of articular cartilage are phenotypically distinct and, as hypothesized, their gene expression patterns were found to be distinct, too.

Chondrocytes from the tangential layer showed a gene expression pattern more consistent with cell proliferation and inhibition of apoptosis, whereas the radial layer's expression pattern suggested that cell proliferation may be less prominent and apoptosis may be prevalent in this layer. In contrast, Aigner et al. (2001b) did not detect proliferating chondrocytes in any layer of normal or osteoarthritic adult human articular cartilage by in-situ detection of the cell proliferation-associated antigen Ki-67. Similarly, no apoptotic cells were found in normal cartilage using the TUNEL assay. Nevertheless, the ability of articular chondrocytes to proliferate even within the original cartilage matrix has been demonstrated *in-vitro* after impact loading and was enhanced in a concentration-dependent manner by fibroblast growth factor 2 (Henson et al. 2005). Cells staining positively for proliferating nuclear antigen were seen in the tangential layer of the articular cartilage. Considering these findings, it is possible that the gene expression pattern seen in the present investigation reflects of the tangential chondrocytes' ability to proliferate upon an adequate stimulus (such as mechanical insult), rather than suggesting actual proliferation taking place at the moment of sampling.

Genes believed to be involved in the cellular response to stress exhibited patterns similar to those believed to play a role in cell proliferation: in the tangential layer, anti-apoptotic genes and a free radical scavenger were upregulated, whereas protein stabilizing chaperones predominated the gene expression pattern in the radial layer. Reasons for differences in stress response between tangential and radial layer chondrocytes are unknown, but the existing gradient in oxygen tension between cartilage close to the articular surface (about 10%) and deeper cartilage layers (less than 1%) (Goldring 2006) may make it more likely for free radicals to occur in the tangential layer, possibly explaining the upregulation of a free radical scavenger in this layer compared to the radial layer.

The most convincing difference in gene expression patterns was found for genes involved in protein synthesis and intracellular protein transport. All genes found to be differentially expressed in this functional category were upregulated in the radial layer compared to the tangential layer. Additionally, 2 genes coding for proteins that are involved in mRNA processing were also upregulated in the radial layer. This suggests that chondrocytes from the radial layer synthesize protein more actively than chondrocytes from the tangential layer. One may speculate that this could be related to the maintenance of the larger volume of extracellular matrix in the more acellular radial layer compared to the tangential layer. This theory was supported by the increased expression of extracellular non-collagenous matrix proteins, such as aggrecan, in chondrocytes from the radial layer, compared to the tangential layer in the present study. A similar

zonal expression pattern of aggrecan mRNA has been described in normal human articular cartilage (Aigner et al. 1997). Wong and Carter (2003) suggested that the maintenance of high aggrecan levels in the radial cartilage layer may be due to this layer being loaded mainly under hydrostatic pressure and experiencing less strain, fluid flow and matrix consolidation than the tangential layer of articular cartilage. The upregulation of the anabolic cytokine fibroblast growth factor 2 in the radial layer observed in the present study may fit into this picture, as it has been implicated as a mechanotransducer in the anabolic response of articular cartilage to mechanical loading (Vincent and Saklatvala 2006). Considering the likely increase in protein synthesis in the radial layer over the tangential layer, it was surprising to find that all differentially expressed genes involved in amino acid synthesis and transport, were downregulated in the radial layer. The significance of this observation is unknown.

A gene coding for an enzyme involved in intracellular protein catabolism (ubiquitin-conjugating enzyme E2G 1) was upregulated and another gene coding for an intracellular protease inhibitor (cystatin B) was downregulated in the radial layer, possibly indicating increased protein modification and breakdown in combination with the increase in protein synthesis by chondrocytes from this layer compared to the tangential layer.

However, 2 genes (thrombospondin 1 and CD44) believed to be involved in cell-matrix interactions and thus, in the homeostasis of the extracellular matrix were upregulated in the tangential layer. An unexpected finding, considering the

smaller volume of extracellular matrix to be maintained within the tangential, compared to the radial layer. The specific function of thrombospondin 1 in cartilage is not known, but it may be a major activator of transforming growth factor β as well as other growth factors. In contrast to these findings, thrombospondin 1 mRNA and protein have been localized mainly to the intermediate layer of normal articular cartilage (Pfander et al. 2000). It is possible that the capture of some intermediate layer chondrocytes caused this gene to be falsely upregulated in the tangential layer samples of the present study. The other gene involved in cell-matrix interactions that was upregulated in the tangential layer, CD44, is a hyaluronan binding receptor, facilitating the retention of large hyaluronan/proteoglycan/link protein aggregates (Knudson and Loeser 2002). An experimentally induced decrease in CD44 protein expression and the competitive inhibition of hyaluronan/proteoglycan/link protein aggregate binding in articular chondrocytes drastically decreased the proteoglycan content of the extracellular matrix (Chow et al. 1998, Knudson et al. 2000). However, with the tangential layer experiencing more fluid flow, strain and thus, tensional forces compared to the radial layer, one would expect genes coding for proteins involved in the maintenance of the collagenous protein network to be upregulated, rather than a gene like CD44.

With differences in local biomechanics between the tangential and the radial layer, one might assume that the cells in these layers may also experience different type of forces, possibly resulting in differential expression of genes coding for intracellular structural proteins. However, no obvious patterns were

found among these genes (mostly proteins related to actin filament organization) in this investigation. Similarly, Langelier et al. (1999) did not find a zonal distribution of actin microfilaments in bovine articular cartilage. But they showed that microtubules and vimentin filaments were present in higher numbers within superficial cells compared to cells from the radial layer. In the present study, alpha tubulin was in fact upregulated in the tangential layer compared to the radial layer, supporting the findings by Langelier et al. (1999).

ADAMTS1 was upregulated in the tangential layer of articular cartilage. Consistent with these findings, this protease has been found to be present to a greater extent in the superficial cartilage layers of healthy joints. ADAMTS1 was found to be constitutively expressed in healthy articular cartilage, and was only slightly upregulated in osteoarthritic specimens (Wachsmuth et al. 2004). Another study showed that the articular cartilage of ADAMTS-1 knock-out mice was indistinguishable from cartilage of wild-type mice with respect to morphology, proteoglycan metabolism or effects of antigen-induced arthritis (Little et al. 2005). Thus, it appears that this member of the aggrecanase family does not play a critical role in the pathogenesis of osteoarthritis and its functions in articular cartilage may even be replaceable by other enzymes.

The differential expression of genes involved in the synthesis of prostaglandin suggested an increased synthesis of prostaglandins in the tangential layer compared to the radial cartilage layer. Prostaglandins are potent pro-inflammatory mediators and they are thought to promote proteoglycan catabolism (Goldring and Berenbaum 2004). This finding either reflects an

elevated basal expression of these enzymes in the tangential layer, or it could be a sign of an early inflammatory stimulus in the superficial layers of the articular cartilage, even in the control joints. In the radial layer, a gene coding for an enzyme that is involved in leukotriene synthesis was upregulated compared to the tangential layer. Similarly to prostaglandins, leukotrienes are pro-inflammatory mediators, and they have been shown to upregulate the synthesis of other pro-inflammatory cytokines such as interleukin-1β and tumor necrosis factor α, as well as matrix metalloproteases (Martel-Pelletier et al. 2004). The significance of the zonal distribution of gene expression with indications for higher prostaglandin activities in the tangential layer and higher leukotriene activities in the radial layer is unknown.

Both genes coding for the peptides that make up the protein ferritin were upregulated in the tangential cartilage layer compared to the radial cartilage layer. Ferritin may represent a non-specific acute phase protein which is upregulated in many different cell types in response to the exposure to various cytokines (Richardson and Dodge 2003), and the upregulation in the tangential layer may also suggest an early inflammatory stimulus in the tangential cartilage layer in the present study. However, the significance and function of ferritin in articular chondrocytes is not known (Richardson and Dodge 2003).

Several genes coding for surface receptors involved in immune responses were upregulated in the tangential layer compared to the radial layer. Among them were the lipopolysaccharide receptor CD14 and the toll-like receptor 4. CD 14 is thought to mediate the inflammatory response to lipopolysaccharides. Toll-

like receptor 4 has been reported to be upregulated in osteoarthritic chondrocytes and is likely involved in the pro-inflammatory response to lipopolysaccharides and other stimuli (Kim et al. 2006). A higher prevalence of these receptors on tangential chondrocytes may be physiologically sensible, as these cells may experience inflammatory stimuli earlier than chondrocytes localized deeper within the articular cartilage.

The upregulation of genes coding for proteins that synthesize prostaglandins, others that may be non-specific acute-phase proteins and surface receptors involved in chondrocytic immune responses in the tangential layer of control cartilage was unexpected. These findings may indicate some early inflammatory stimulus to the tangential layer of the articular cartilage of the control joints. Proteoglycan depletion starts in the superficial cartilage layers in early osteoarthritis (Visco et al. 1993) and one may speculate that slight changes in the biomechanics of the control joints due to the horses trying to adapt to low grade pain in the contralateral osteoarthritic joints resulted in early, low grade damage to the cartilage matrix. However, if this was the case, matrix proteinases such as aggrecanase 1 (ADAMTS4) should be upregulated (Caterson et al. 2000) in conjunction with the pro-inflammatory genes. Further, a possible remote effect on the control limb and its joints in the carpal osteochondral fragment model has been addressed to a certain degree by Norrdin et al. (1998), who did not find an effect of the induction of osteoarthritis on morphometric indices of subchondral bone remodeling in the metacarpophalangeal joints of the same or contralateral limbs. These observations would suggest that adaptation to low

grade pain in the osteoarthritic joint did not have an influence on local joint biomechanics of the contralateral limb.

An activator of vitamin K was upregulated in the radial layer compared to the tangential layer. Chondrocytes have been shown to synthesize several vitamin K-dependent proteins, among them matrix Gla protein (Loeser and Wallin 1991). This protein has been shown to inhibit matrix calcification when activated by activated vitamin K (Rutsch and Terkeltaub 2005). Thus, the activator of vitamin K may help to prevent advancement of the calcified cartilage into the radial layer of the hyaline cartilage.

Two genes involved in carbohydrate metabolism were upregulated in the radial layer. Glucose is considered to be the major source of energy and proteoglycan precursors in chondrocytes (Shikhman et al. 2004, Goldring 2006). The upregulation of these 2 genes in the radial layer is consistent with the findings suggesting an increased protein and proteoglycan synthesis within the radial layer compared to the tangential layer.

Two genes coding for proteins that transport protons over cell or intracellular vacuolar membranes were upregulated in the radial layer compared to the tangential layer. These Hydrogen ion ATPases have been shown to be necessary for IL-1 stimulated proteoglycan degradation (Tattersall et al. 2005), but the significance of their zonal gene expression is unknown.

Several genes believed to be involved in cell communication or intracellular signaling were differentially expressed. The specific signaling functions of most of these genes are not known. Other genes in this category

code for proteins of signal cascades that are involved in many different processes. Thus, it is difficult at this time to make inferences about the biological significance of their gene expression patterns.

Similarly, several transcription factors with unknown specific effects were differentially expressed between the 2 cartilage layers, and it would be pure speculation to interpret some biological significance into these expression patterns. Interestingly, a transcription factor involved in skeletal development was upregulated in tangential layer chondrocytes compared to cells from the radial layer. This finding and the lack of knowledge about the specific function of this factor make this gene an interesting target of future investigations.

In summary, chondrocytes from the tangential layer of articular cartilage showed a gene expression pattern supporting cell proliferation and antagonizing apoptosis. Further, genes coding for membrane receptors involved in cell-matrix interactions and ADAMTS1, a constitutively expressed aggrecanase were upregulated. Finally several pro-inflammatory genes and genes involved in immune responses were also upregulated in the tangential layer. In contrast, the gene expression pattern from chondrocytes of the radial layer was dominated by the upregulation of genes involved in mRNA processing, protein synthesis, protein stabilization, intracellular protein transport and regulated protein catabolism, suggesting a higher protein synthetic rate in the radial layer. The upregulation of 2 genes from glycolytic pathways may be associated with the high biosynthetic rate in these cells, as they are likely to aid in providing energy

for biosynthetic activity. Finally a gene possibly involved in preventing calcification in the radial layer was also upregulated.

The gene expression pattern for osteoarthritic cartilage showed downregulation of anti-apoptotic genes as well as genes involved in protein folding and assembly. This was more pronounced in the radial than the tangential layer. A similar observation has been reported by Smith et al. (2006) in full thickness cartilage from equine osteoarthritic palmar metacarpal condyles, utilizing the same gene array. A gene believed to be involved in the cellular response to oxidative stress was upregulated under the influence of osteoarthritis in the present study. Oxidative stress may play a role in shear stress-induced chondrocyte death (Martin and Buckwalter 2006) and in the pathogenesis of osteoarthritis (Terkeltaub et al. 2002). No pattern indicating general promotion or inhibition of cell proliferation was noticed in osteoarthritic cartilage.

A protease inhibitor of cathepsin G and other proteases (α-1-antitrypsin) was upregulated in osteoarthritic cartilage independent of cartilage layer. It is known as the major inhibitor of neutrophil derived elastase, an enzyme with questionable significance for cartilage breakdown in osteoarthritis. Alpha-1-antitrypsin has been shown to bind aggrecanase-1 in vivo, but does not inhibit its proteolytic activity (Yoshida et al. 2005). Thus, the significance of its upregulation in osteoarthritic cartilage is unknown.

A gene coding for an inhibitor of the NF-κB complex was downregulated in osteoarthritic cartilage, which is in agreement with previous reports. The NF-κB pathway is considered to be a central pathway in the pathogenesis of

osteoarthritis. Activation of this pathway for example by IL-1 or TNF-α results in upregulated transcription of genes coding for matrix metalloproteinases, pro-inflammatory cytokines and enzymes, promoting inflammation and the breakdown of collagens in the extracellular matrix (Roshak et al. 2002, Vincenti and Brinckerhoff 2002). Thus, the downregulation of an inhibitor of this pathway in osteoarthritic cartilage is not surprising.

In osteoarthritic cartilage, a gene coding for a protein possibly involved in the transport of other proteins across membranes was upregulated. This may indicate that the osteoarthritic chondrocytes are more actively secreting proteins into the extracellular space than the cells from control cartilage. However, the exact function of this gene product is unknown (Sugasawa et al. 2001).

Osteoarthritic chondrocytes appeared to decrease their energy production via the glycolytic pathway and the activation of glucose molecules to be used for proteoglycan synthesis, as 2 genes involved in these processes were downregulated. This observation was more pronounced in the radial compared to the tangential cartilage layer.

In summary, the gene expression pattern in osteoarthritic chondrocytes indicated the activation of the pro-inflammatory, catabolic NF-κB pathway. It further suggested a response to oxidative stress, but decreased ability to resist apoptosis, especially within the radial layer. This layer also showed greater downregulation of genes involved in proteoglycan synthesis and energy production than the tangential layer. Thus, gene expression in chondrocytes of the radial layer appeared to be altered to a greater degree under the influence of

osteoarthrosis than that of cells within the tangential layer. This may be surprising, because proteoglycan depletion has been reported to occur first within the more superficial layers of osteoarthritic cartilage in one study (Visco et al. 1993), possibly suggesting a greater impact of osteoarthritis on gene expression in the tangential layer.

The present study failed to corroborate previously published expression patterns suggesting increased proteoglycan degradation with fibronectin fragments possibly modulating chondrocyte metabolism in early osteoarthritis (Aigner et al. 2001a), or increases in collagen synthesis and matrix proteases as well as their inhibitors in severely damaged osteoarthritic cartilage (Sato et al. 2006). Similarly, Tob1, which has been identified as an important regulator of cellular processes in late stage osteoarthritis (Gebauer et al. 2005) was not found to be differentially expressed in the present study. Further, none of 17 differentially expressed genes found in leukocytes from horses before and after experimental induction of osteoarthritis, using the same model as in the present study (Frisbie, unpublished data 2004) were found to be differentially expressed in the cartilage specimens analyzed in this investigation. This may be due to the differences in sample sources (peripheral blood leukocytes vs. chondrocytes) between the 2 investigations. In a study utilizing the same gene array as in the present investigation, cartilage with mild osteoarthritic changes showed expression patterns suggesting increased matrix turnover and activation of anabolic pathways, whereas expression patterns from more severely affected cartilage suggested decreased protein synthesis, but increased collagen type II

synthesis and failure to counteract apoptosis. Only the decreased ability to resist apoptosis was found in the present study, especially in the radial cartilage layer. This is likely in part due to the analysis of cartilage samples representing a different stage of the disease. Most previous reports utilized late stage or severely osteoarthritic cartilage samples, whereas the present study analyzed cartilage from an area with well documented early or mild osteoarthritic changes (Foland et al. 1994, Frisbie et al. 1997, Kawcak et al. 1997, Frisbie et al. 1998, Kawcak et al. 1998, Frisbie et al. 1999, Frisbie et al. 2002, Frisbie et al. 2003). The present study was only able to obtain information about gene expression at one single time point after the induction of osteoarthritis, representing just one "cross section" of the continuous progression of the disease. The invasive nature of taking articular cartilage biopsies prohibits the repeated sampling of this tissue. Thus, non- invasive methodologies, such as magnetic resonance imaging are commonly used to accurately study the progression of osteoarthritis (Bruyere et al. 2006, Raynauld et al. 2006). The sampling location in the present investigation on the dorsal aspect of the radial facet of the 3$^{rd}$ carpal bone was chosen to ascertain the sampling of damaged cartilage from osteoarthritic joints, because gene expression patterns appear to differ between samples from damaged areas of cartilage compared to intact or less damaged areas of cartilage from the same joint (Sato et al. 2006, Smith et al. 2006). Another possibility for the discrepancies in gene expression patterns may be the overall low number of genes found to be differentially expressed between control and osteoarthritic cartilage in the present study.

It is important to evaluate gene array data with the knowledge that there are multiple sources of variation during sample preparation, array processing, data acquisition and data manipulation (Parmigiani et al. 2003). To keep sources of variability as low as possible during sample preparation, strict adherence to experimental protocols was practiced. RNA labeling, fragmentation and hybridization as well as data acquisition was performed by 1 experienced investigator in as short a time period as possible. Data manipulation was performed after quality control of the raw data, and 1 array, which had been loaded with a significantly smaller amount of RNA compared to the others was excluded based on consistently presenting as an outlier during quality control steps. Another source of uncertainty for the results of this study may be the annotation of sequences with unknown gene names or unknown biological function. Because very stringent rules were used to find genes that were homologous to the sequence of interest, it is less likely that erroneous gene names were assigned. With this approach, one may actually risk to have missed homologous genes for some sequences, which then had to be excluded from the data interpretation, as no function could be assigned to them. Further, the assignment of a biological function to a sequence based on the inferred gene name was performed using 4 well-known, accepted and reviewed web databases. This approach should yield reliable sequence annotations, increasing the confidence in the results of this study. Bias may however be introduced during the interpretation of the expression patterns, especially when a gene is associated with more than 1 biological function. Unless the protein's

activity in articular cartilage has been investigated extensively, the function(s) of significance for this specialized tissue are chosen subjectively. Thus, the differential expression of genes for future investigations should at least be confirmed using quantitative real-time PCR, which is considered the current gold standard technique to quantitate gene expression (Attur et al. 2002a, Aigner et al. 2003, Gebauer et al. 2005).

By extrapolating the metabolic status of a cell from its RNA expression pattern, a multitude of post-transcriptional means of protein expression will be ignored, unless a concurrent analysis of protein expression is performed. Thus, such interpretation of gene expression has to be regarded as preliminary until follow-up work, investigating the protein expression is done.

Another limitation of this study was the fact that half the horses were treated with an anti-inflammatory ointment over the osteoarthritic joint. However, no differentially expressed genes between treated and untreated joints were detected when the q-value threshold of $q<0.05$ was used, indicating that the effect of the diclofenac ointment on gene expression was minimal.

Genes that were determined to be differentially expressed in the present study and that are confirmed using real-time PCR should be investigated with respect to their specific functions in articular cartilage using explant and cell cultures. Only that information will allow researchers to obtain a more comprehensive understanding of chondrocyte metabolism in health and disease.

In conclusion, laser capture microdissection of phenotypically similar articular chondrocytes from different cartilage layers, followed by gene array

analysis of isolated and amplified RNA yielded different expression patterns for the tangential and the radial cartilage layer, as well as for osteoarthritic and control cartilage. The gene expression pattern of chondrocytes from the tangential layer reflected support of cell proliferation, suppression of apoptosis and several genes involved in cell-matrix interactions or inflammatory processes. In contrast, the gene expression pattern of chondrocytes from the radial layer was dominated by genes supporting the synthesis of proteins and proteoglycans, suggesting a higher synthetic activity of these chondrocytes compared to those from the tangential layer. Further, the chondrocytes in the radial layer showed gene expression suggestive of anti-calcification mechanisms. Different expression patterns were also found for osteoarthritic and control cartilage. The general expression pattern for osteoarthritic cartilage was similar for the 2 cartilage layers, but changes in expression were more pronounced in the radial than the tangential layer.

The gene expression pattern in osteoarthritic chondrocytes indicated the activation of the pro-inflammatory, catabolic NF-κB pathway. It further suggested a response to oxidative stress, but decreased ability to resist apoptosis and downregulation of genes involved in proteoglycan synthesis and energy production.

This study was the first to determine gene expression patterns between 2 different layers of osteoarthritic and control articular cartilage. The present results improve our knowledge of zonal dependence of chondrocyte metabolism and its alterations under the influence of osteoarthritis. They provide the basis

for future research into the pathophysiology of osteoarthritis, to identify new therapeutic targets for the treatment of this debilitating disease.

## 4 Figures

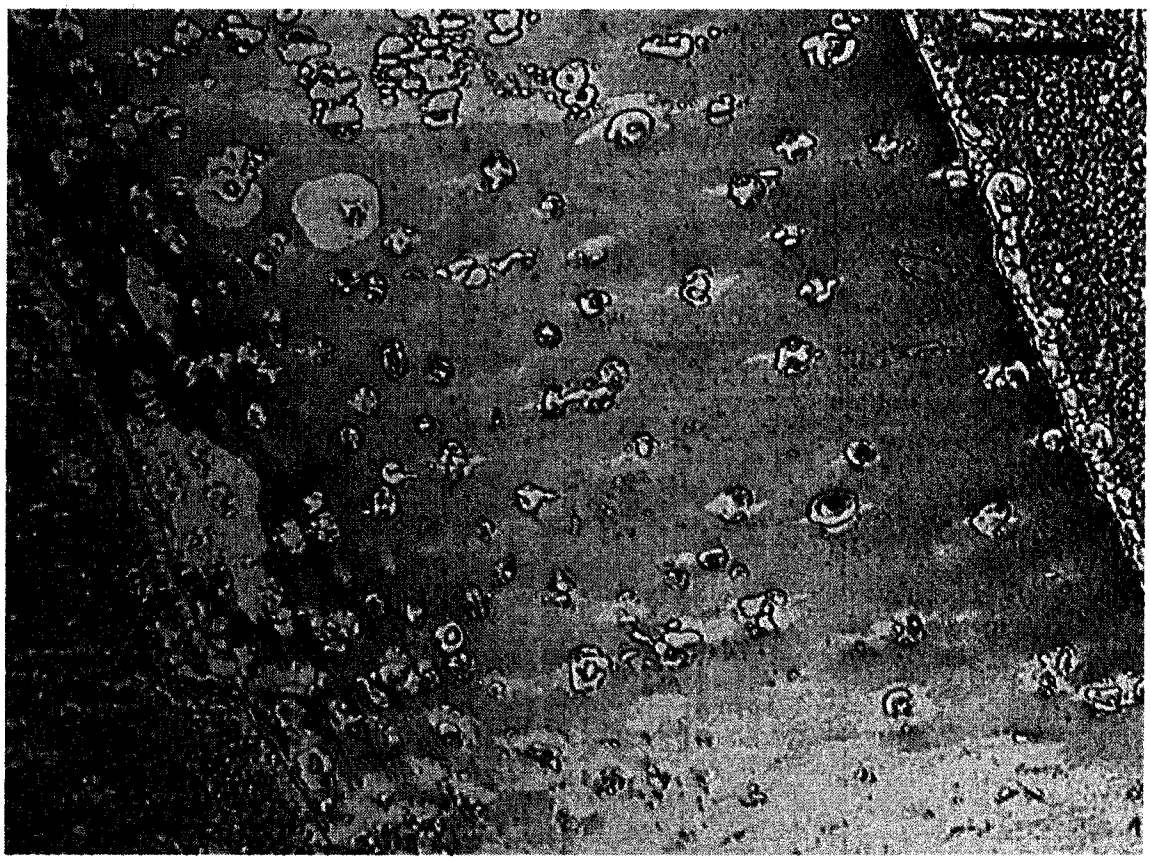

Figure 1: Unstained frozen section (magnification 10x) of equine articular cartilage estimated to be thinner than 5 µm. Note the areas void of matrix and cells towards the bottom of the image. Bar = 120 µm.

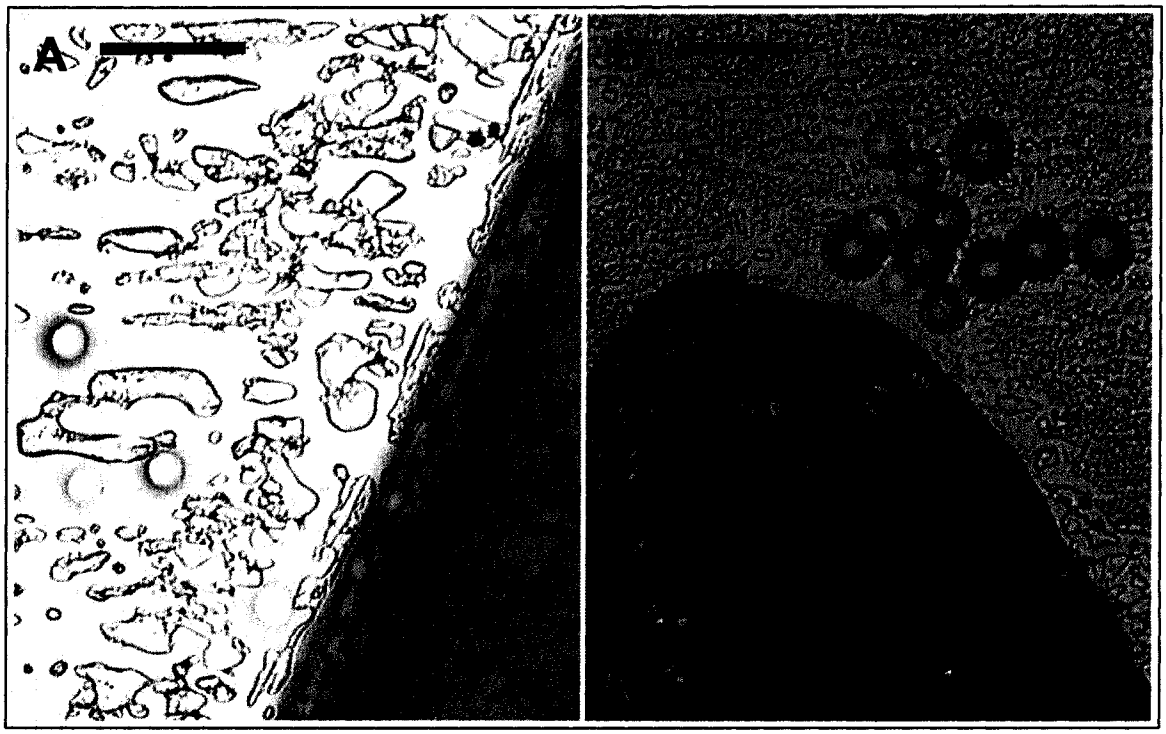


Figure 2: Test fires with the Autopix Unit (Arcturus Bioscience, Mountain View, CA), demonstrating the quality of adherence of the polymer to the slide ("wetting"). (**A**) Inadequate wetting, characterized by a faint circle with fading margins. (**B**) Good wetting with crisp margins. Sections stained with HistoGene LCM Frozen Section stain (Arcturus Bioscience, Mountain View, CA). Bars = 40 µm.

Figure 3: Test fires with the Autopix Unit (Arcturus Bioscience, Mountain View, CA), demonstrating the decrease in spot diameter with shorter laser pulse durations (from left to right: 2000, 1500, 800, 1000 µs). Section stained with HistoGene LCM Frozen Section Stain (Arcturus Bioscience, Mountain View, CA). Bar = 40 µm.

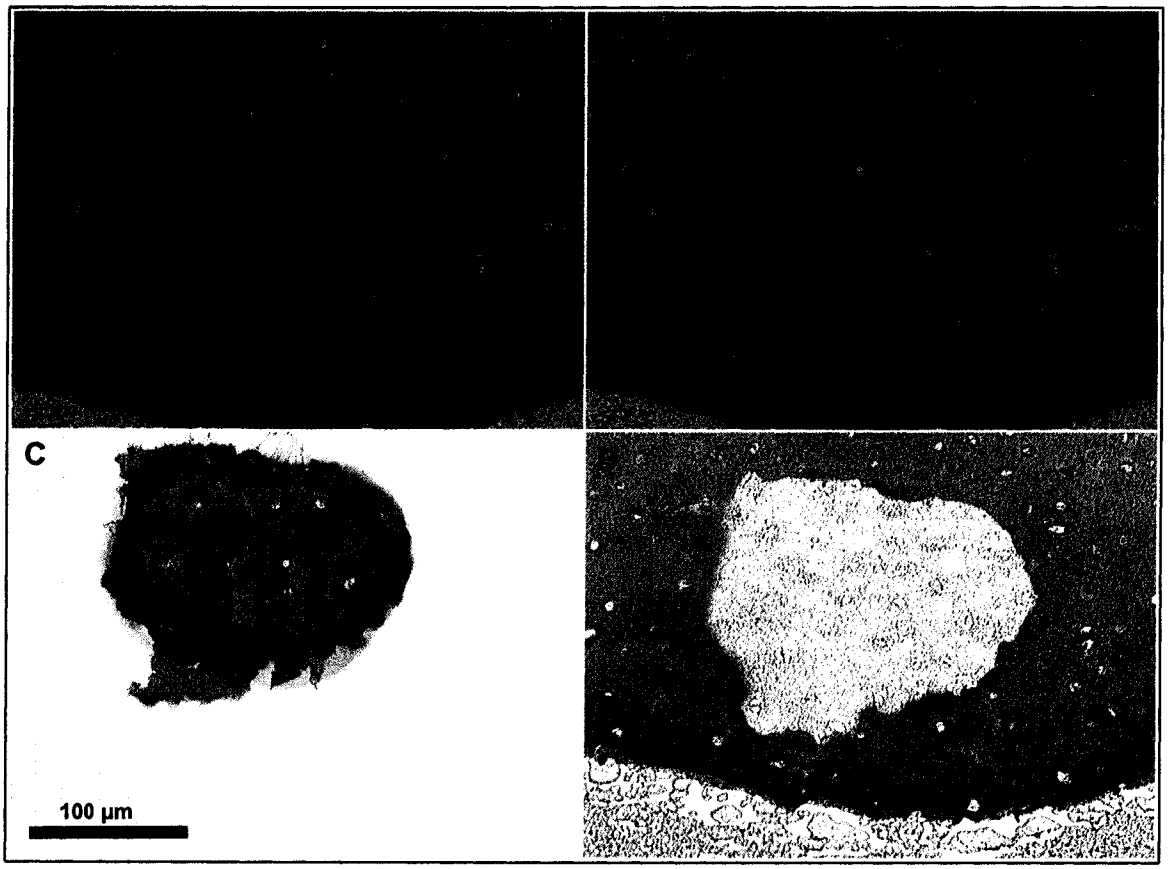


Figure 4: Full thickness capture of an area of articular cartilage. (**A**) The area of interest is marked. (**B**) Appearance of the area of interest after the laser was ignited. The crisp dark margins on the periphery of the area of interest signify good wetting. (**C**) Image of the cap after having been lifted off the section. The area of interest is captured successfully. (**D**) Image of the section after full thickness capture of the area of interest. Sections stained with HistoGene LCM Frozen Section stain (Arcturus Bioscience, Mountain View, CA). Bar = 75 µm.

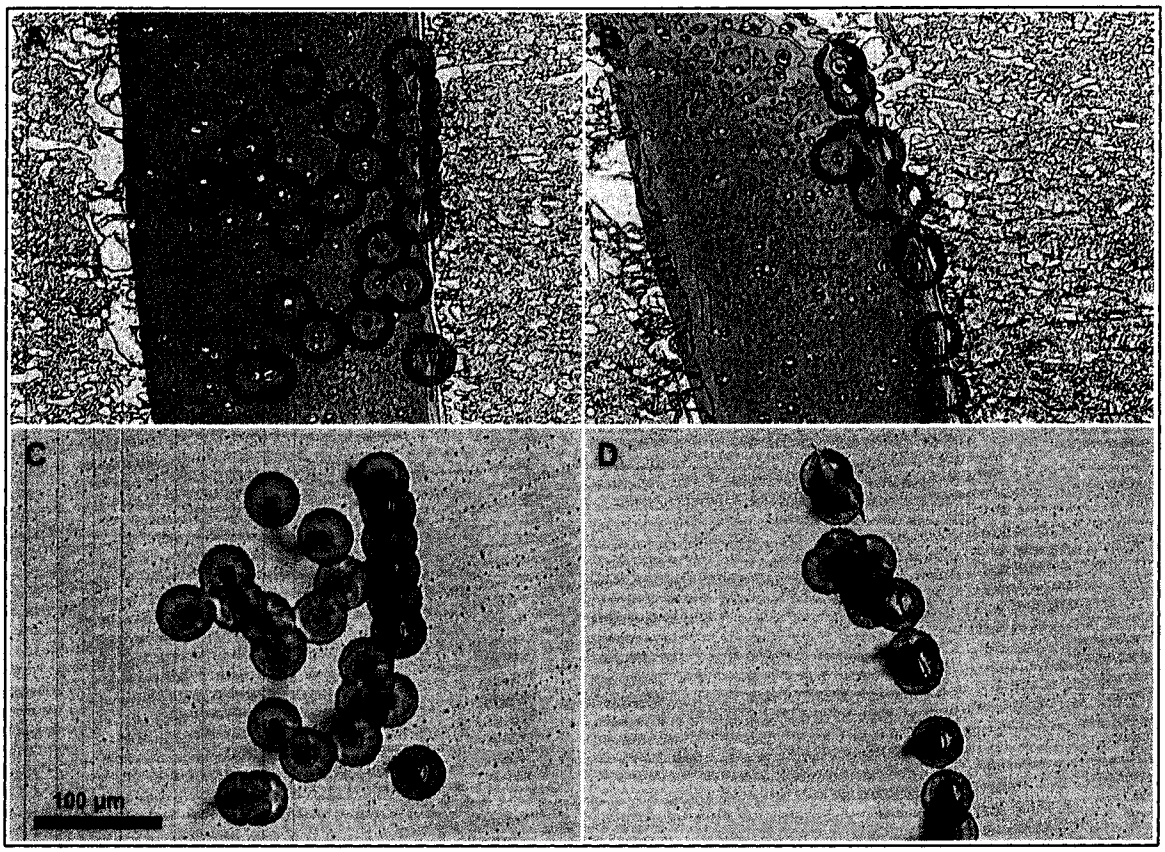


Figure 5: Capture of smaller areas of interest with the use of sticky tape after the complete section lifted off the slide when the LCM cap was removed. (A, B) Areas of interest were lasered. Good wetting is noted. (C, D) The areas of interest remain adhered to the cap after sticky tape was applied to remove unwanted areas of the articular cartilage section. Sections stained with HistoGene LCM Frozen Section stain (Arcturus Bioscience, Mountain View, CA).

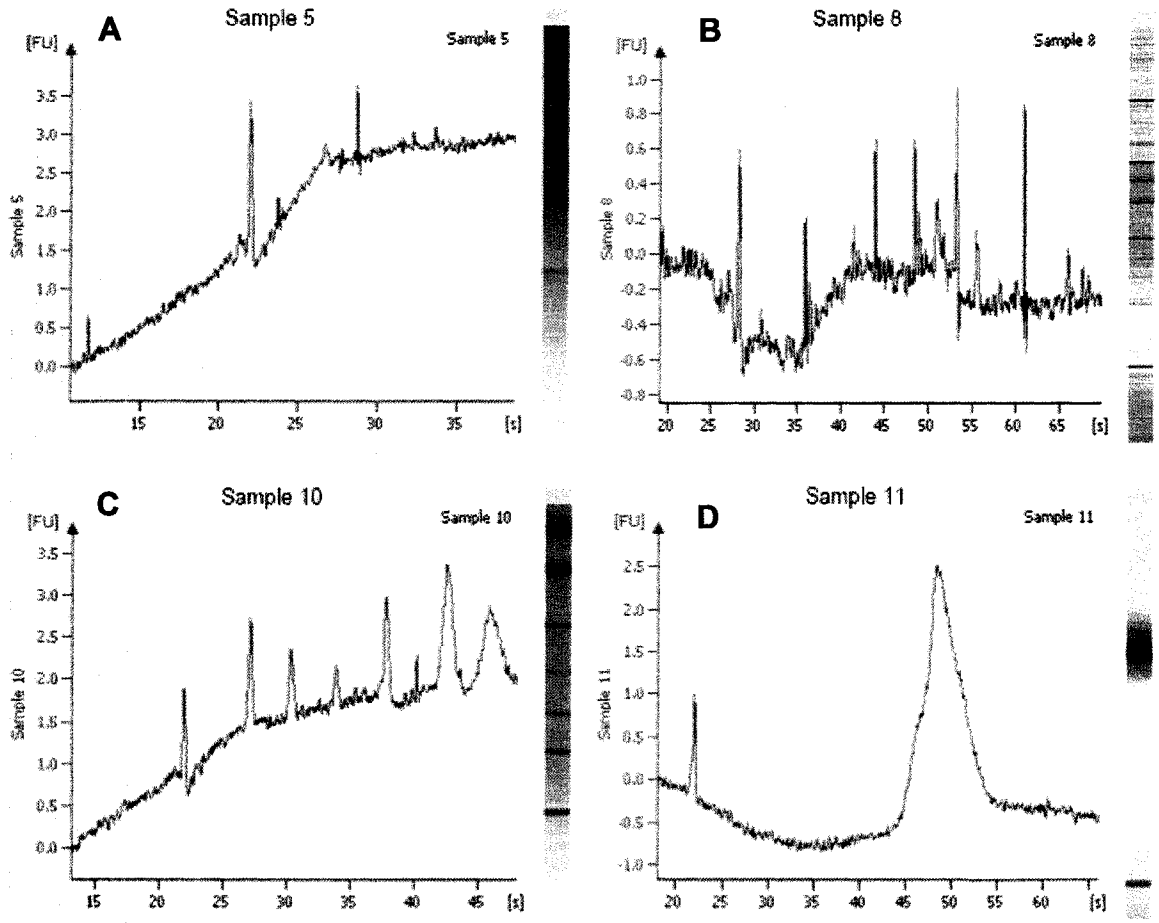


Figure 6: Examples of electropherograms with artifacts: (A, Sample 5) Shifting baseline (B, Sample 8) High noise in baseline values (C, Sample 10) Multiple unexplainable peaks (D, Sample 11) Large singular unexplainable peak. (The y-axis shows the intensity of fluorescence detected (a measure for RNA amount). The x-axis shows the time of detection.)

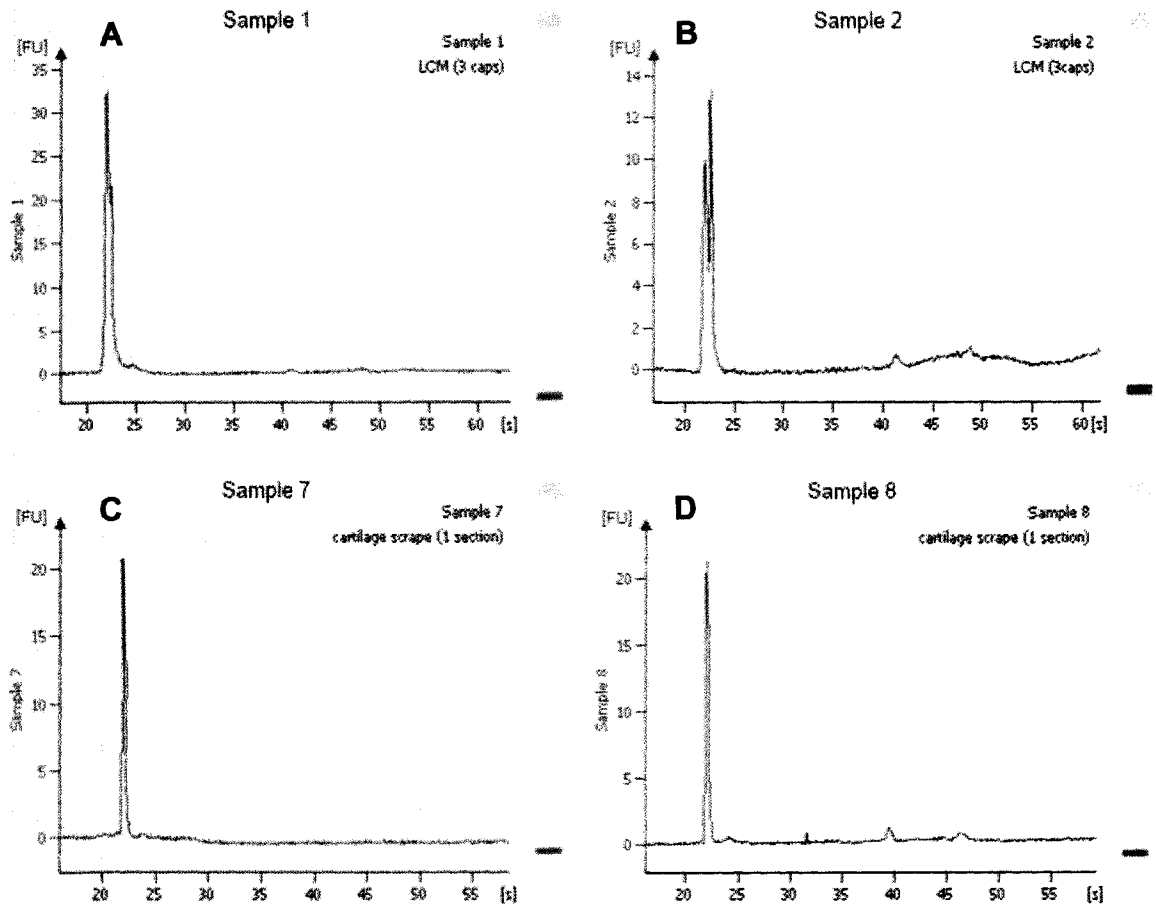


Figure 7: Examples of electropherograms from microscopic samples (scrape and LCM samples) without artifacts. (A, Sample 1) Peak close to the marker peak – degraded sample. (B, Sample 2) Peak close to the marker peak and small peaks where one would expect the 18S and 28S rRNA peaks – RNA is less degraded than in sample 1. (C, Sample 7) No peaks, horizontal baseline – RNA concentration too low to be detected. (D, Sample 8) Small peaks where one would expect the 18S and 28S rRNA peaks – RNA less degraded than in sample 2. (The y-axis shows the intensity of fluorescence detected (a measure for RNA amount). The x-axis shows the time of detection.)

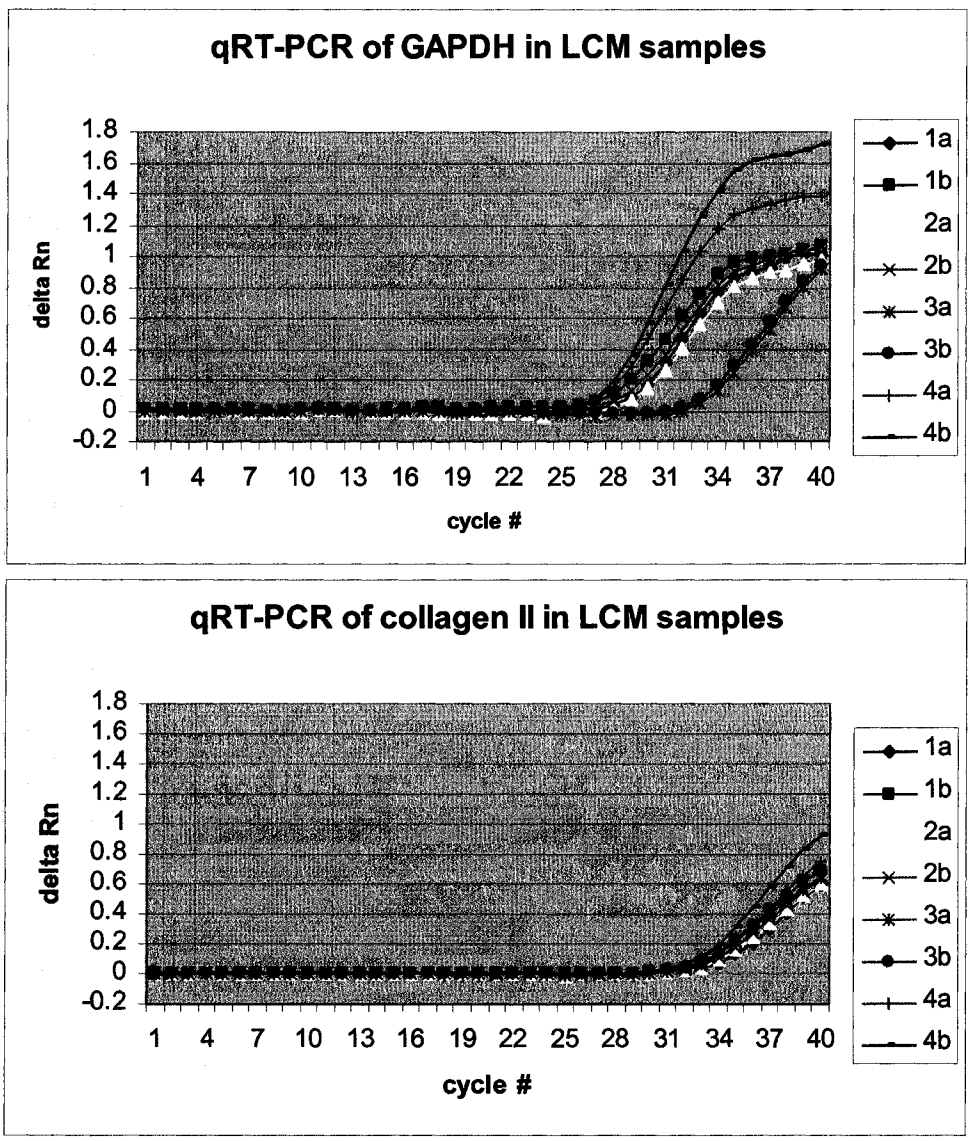


Figure 8: Real-time PCR for equine GAPDH and collagen type II in LCM samples (4 samples run in duplicates shown). Specific amplification of both genes in all samples confirms the presence of mRNA in the LCM samples. (Y-axis shows normalized reporter fluorescence (accumulating fluorescence of the reporter dye minus fluorescence of a reference dye: delta Rn), x-axis shows the number of the PCR cycle.)

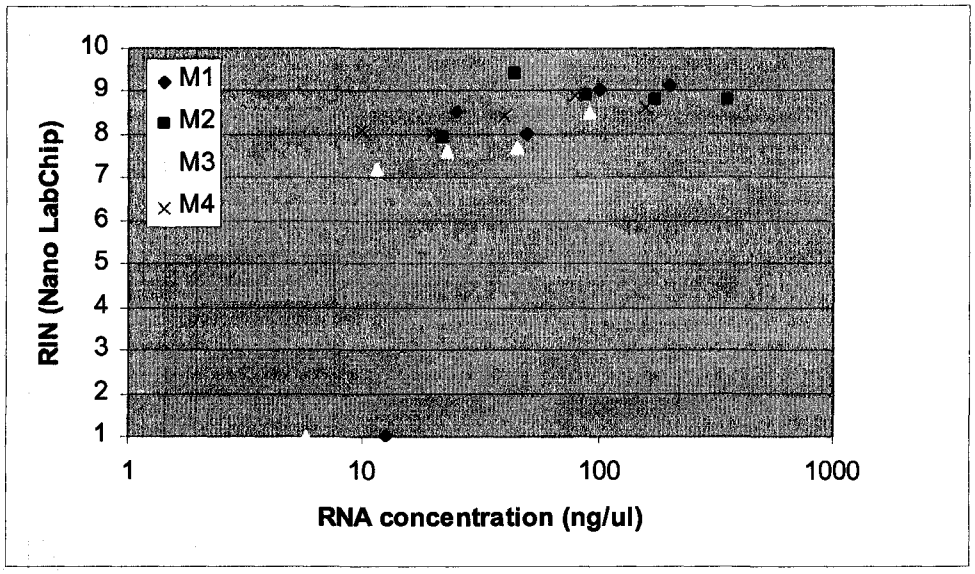


Figure 9: RINs determined with the Nano LabChip® Kit (Agilent Technologies, Palo Alto, CA) from 6 macroscopic samples did not appear to be significantly influenced by RNA concentration down to about 10 ng/µl. (The y-axis shows RNA integrity number, the x-axis shows the RNA concentration in ng/µl.)

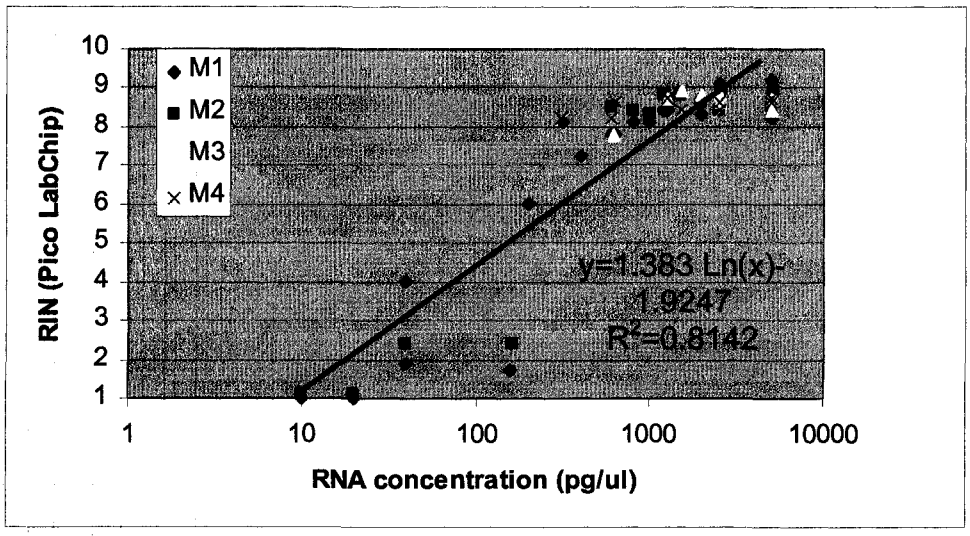


Figure 10: RINs of diluted macroscopic samples with good RNA quality determined with the Pico LabChip® Kit (Agilent Technologies, Palo Alto, CA) decreased with lower concentrations. (The y-axis shows RNA integrity number of each sample, the x-axis shows the RNA concentration in ng/µl.)

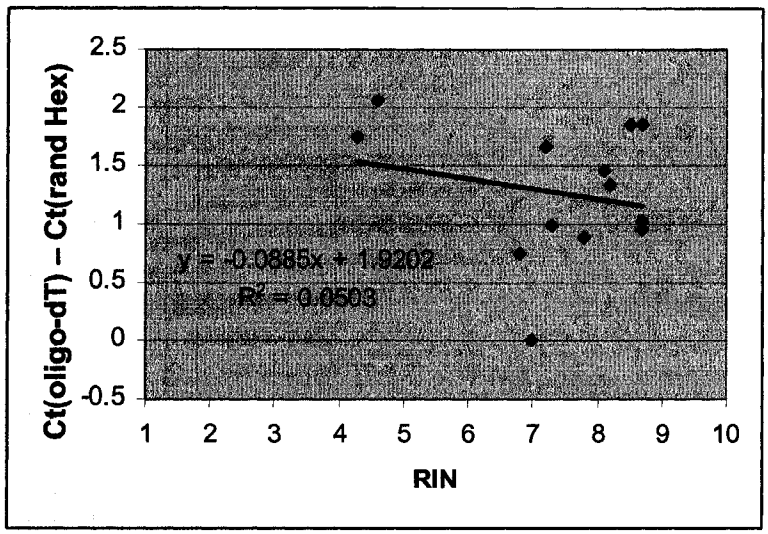


Figure 11: Differences in Ct values between aliquots of samples with known RNA qualities that were reverse transcribed with either oligo dT primers or with random hexamers. No strong association between differences in Ct values and RINs was found. (The y-axis shows the difference in Ct-values for aliquots reverse transcribed with oligo-dT primers minus Ct-values for aliquots reverse transcribed with random hexamer primers. The x-axis shows RNA integrity numbers.)

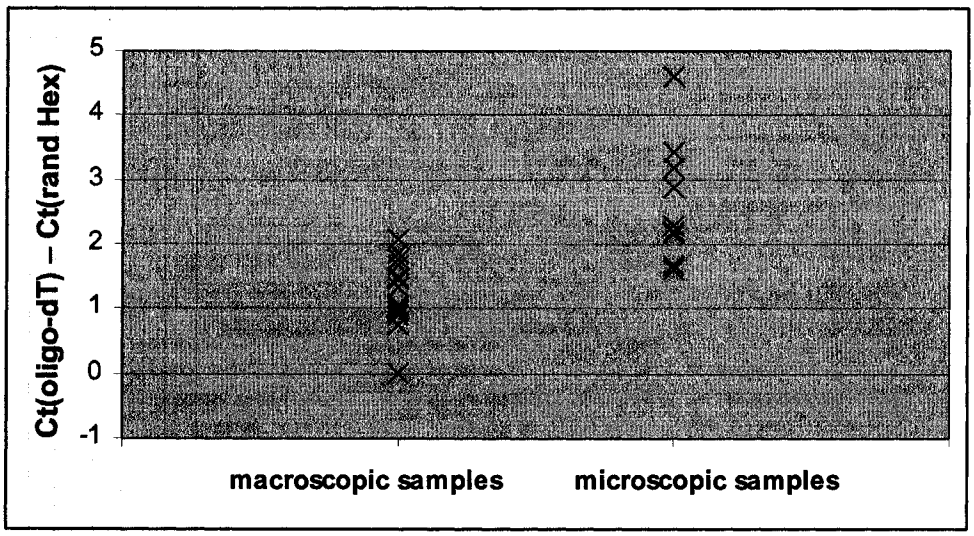


Figure 12: Differences in Ct values between aliquots of RNA samples that were reverse transcribed with either oligo dT primers or with random hexamers. The macroscopic samples had known RNA quality (RINs 4.3-7.8), and the microscopic samples had unknown RNA quality. (The y-axis shows the difference in Ct-values for aliquots reverse transcribed with oligo-dT primers minus Ct-values for aliquots reverse transcribed with random hexamer primers. The x-axis shows the 2 different sample groups.)

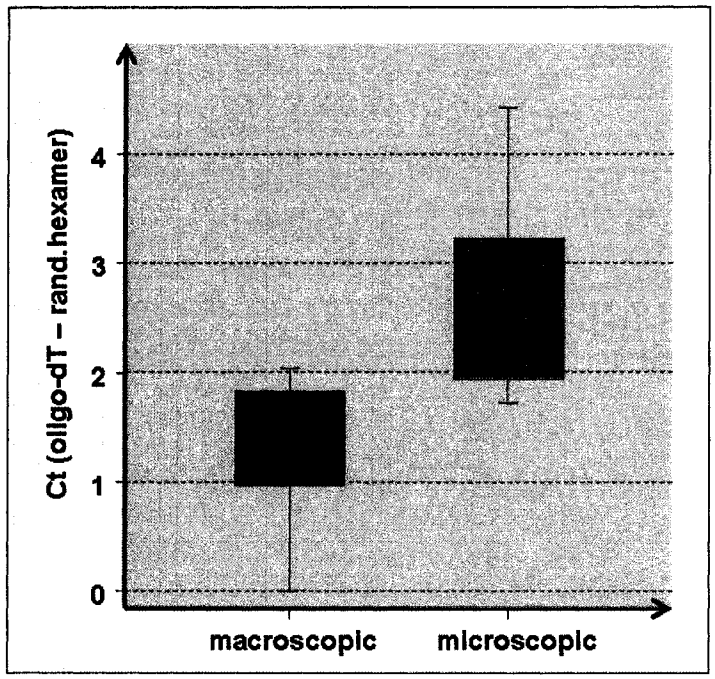


Figure 13: Differences in Ct values between aliquots of RNA samples (macroscopic and microscopic samples) that were reverse transcribed with either oligo dT primers or with random hexamers. The differences in Ct values were significantly greater compared to those in the macroscopic samples ($p=0.002$). (The y-axis shows the difference in Ct-values for aliquots reverse transcribed with oligo-dT primers minus Ct-values for aliquots reverse transcribed with random hexamer primers. The x-axis shows the 2 different sample groups.)

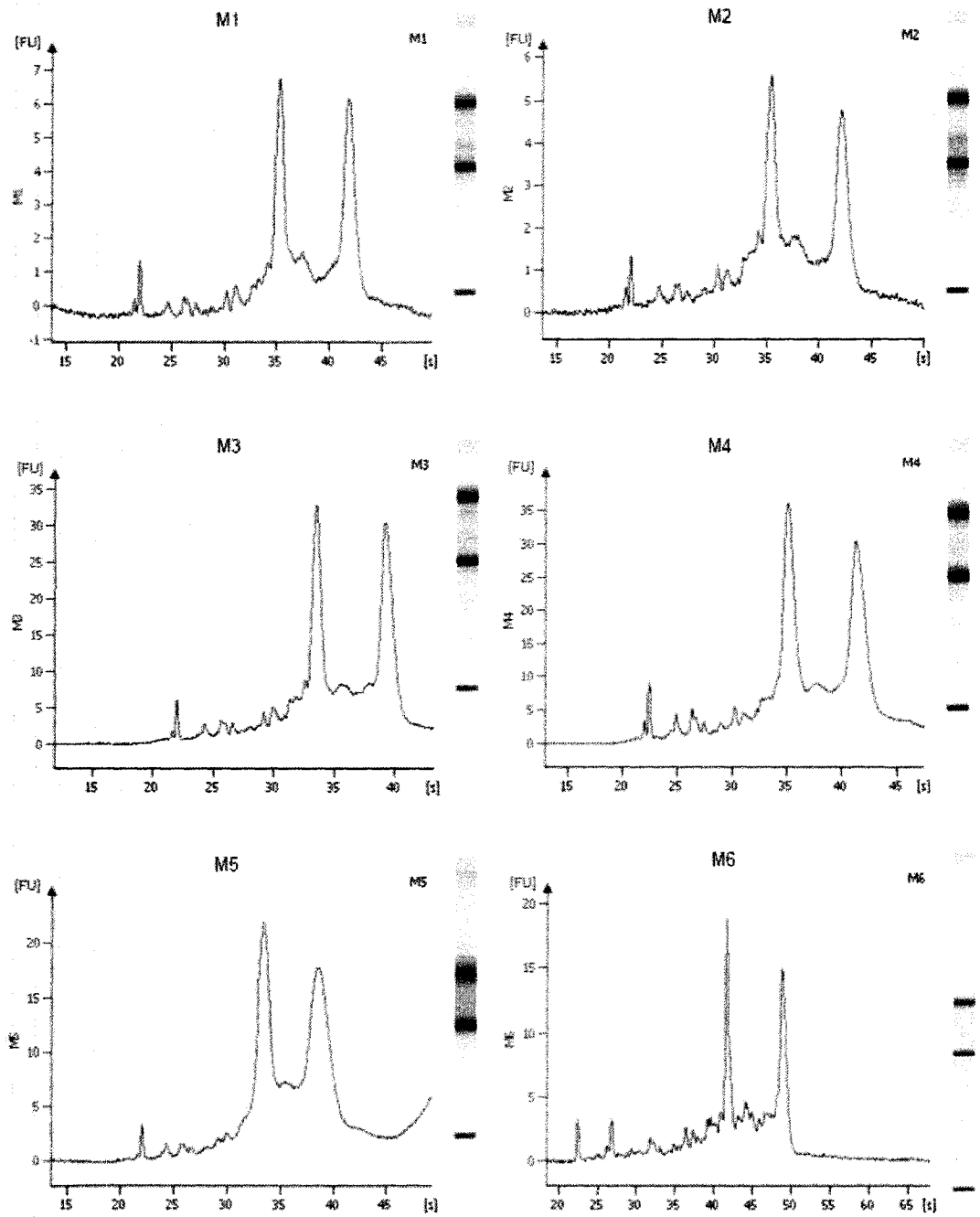


Figure 14: Electropherograms of RNA from macroscopic samples produced in the final validation experiment. Note the 2 distinct rRNA peaks with only moderate elevation of the baseline in the area between the peaks and no large peak close to the marker peak. (The y-axis shows the intensity of fluorescence detected (a measure for RNA amount). The x-axis shows the time of detection.)

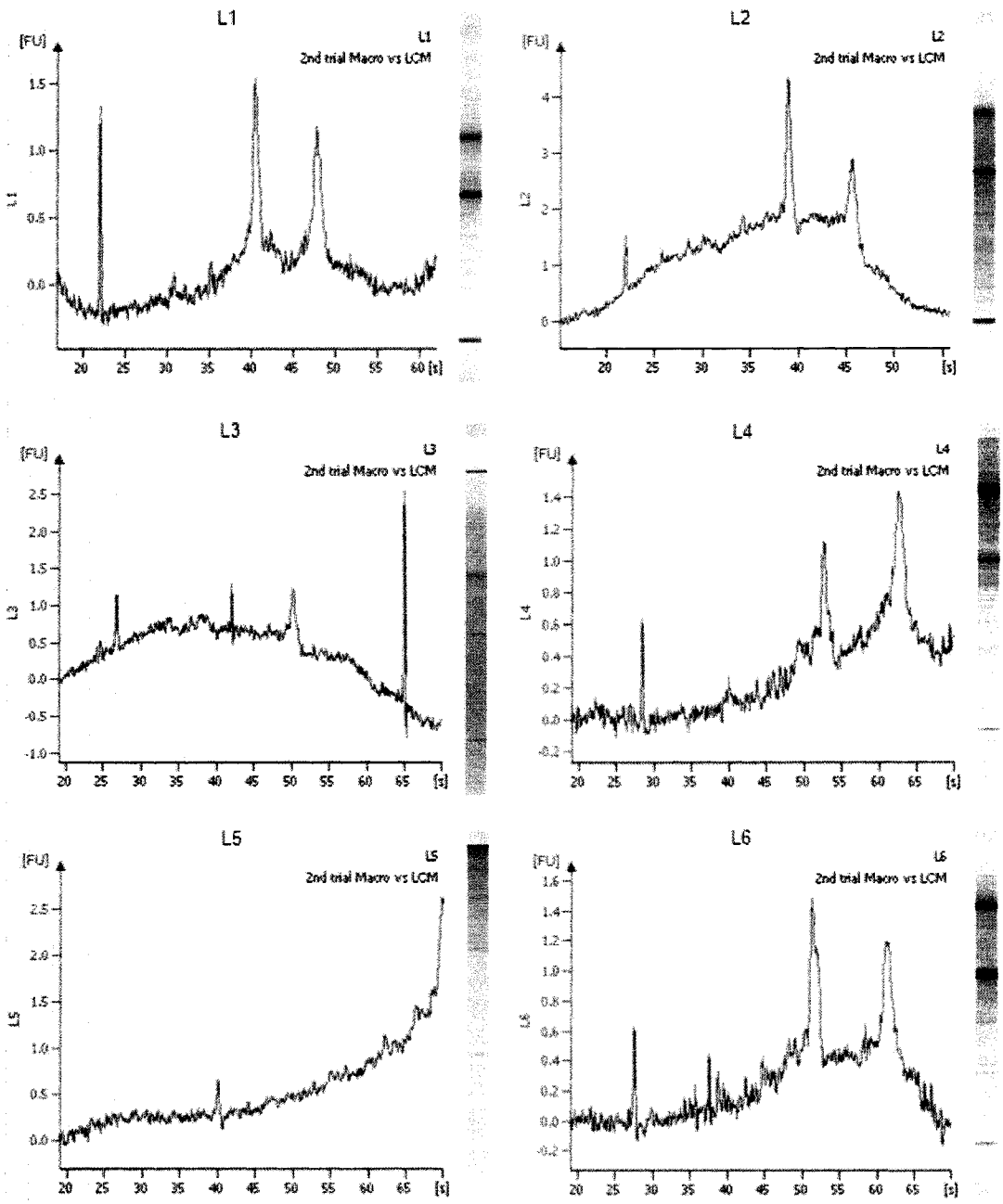


Figure 15: Electropherograms of RNA from LCM samples produced in the final validation experiment. (The y-axis shows the intensity of fluorescence detected (a measure for RNA amount). The x-axis shows the time of detection.)

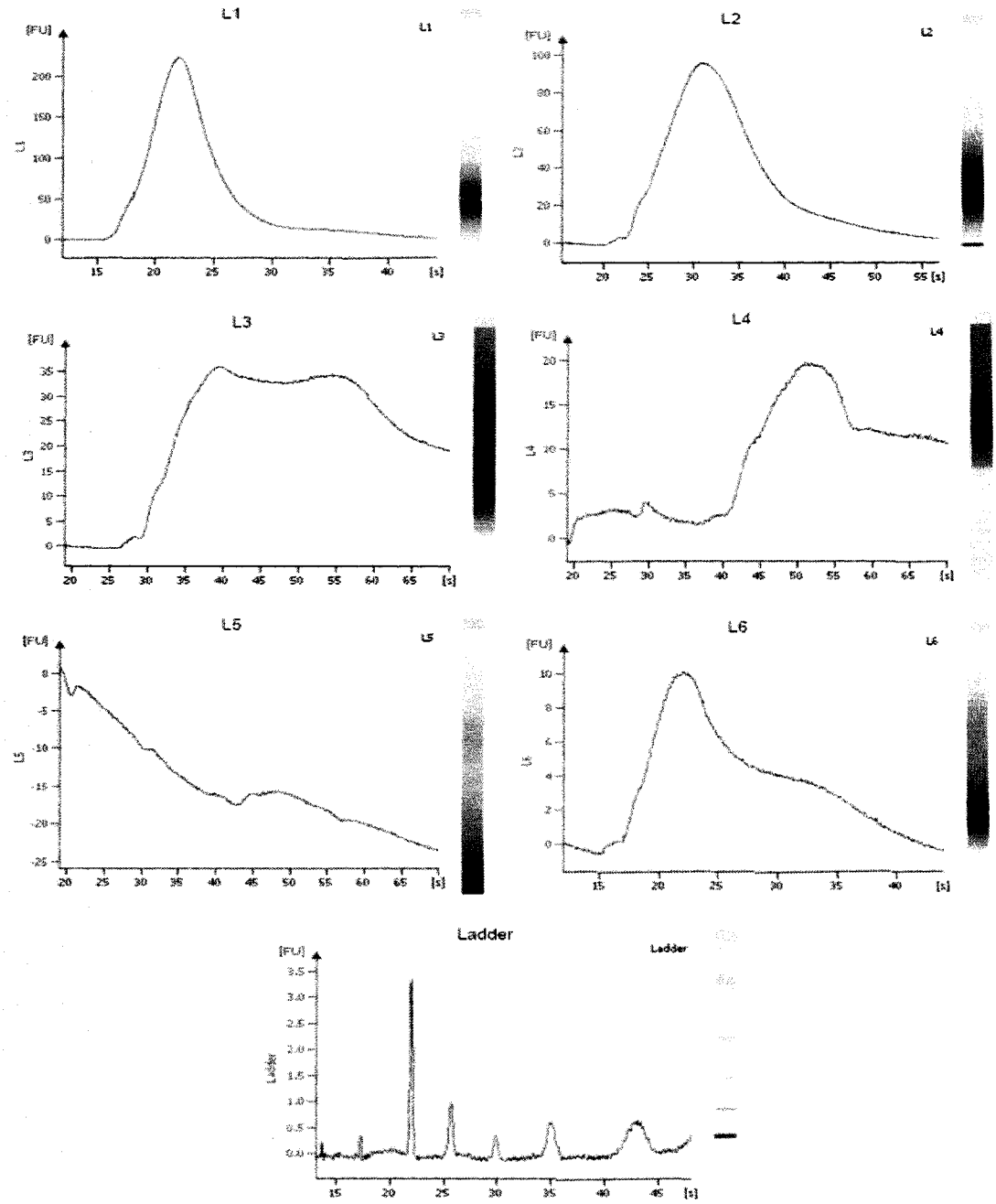


Figure 16: Electropherograms of RNA from LCM samples after 2 rounds of *in-vitro* transcription amplification. (The y-axis shows the intensity of fluorescence detected (a measure for RNA amount). The x-axis shows the time of detection.)

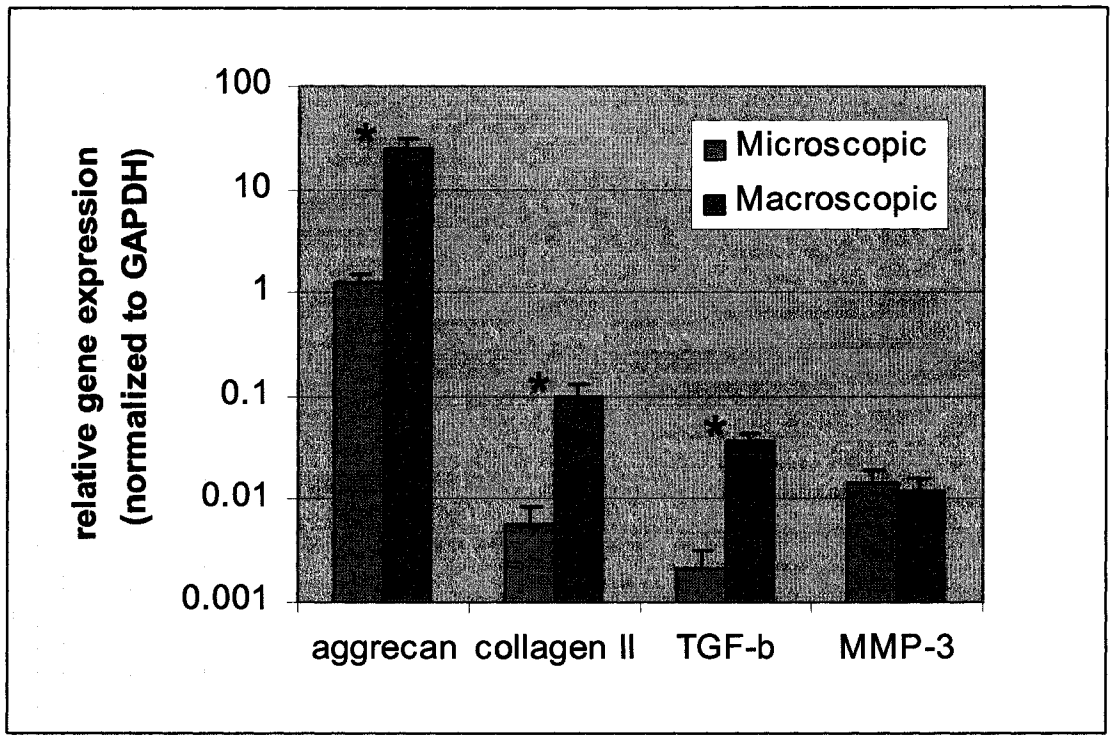


Figure 17: Expression levels normalized to GAPDH obtained from paired macroscopic (conventional RNA isolation) and microscopic samples (RNA isolated from laser captured cells and amplified in 2 rounds of *in-vitro* transcription). Error bars represent standard error, and asterisks indicate significant differences between isolation methods for the same gene. (The y-axis shows the level of relative gene expression normalized to the housekeeping gene GAPDH, and the x-axis shows the 4 different genes tested.)

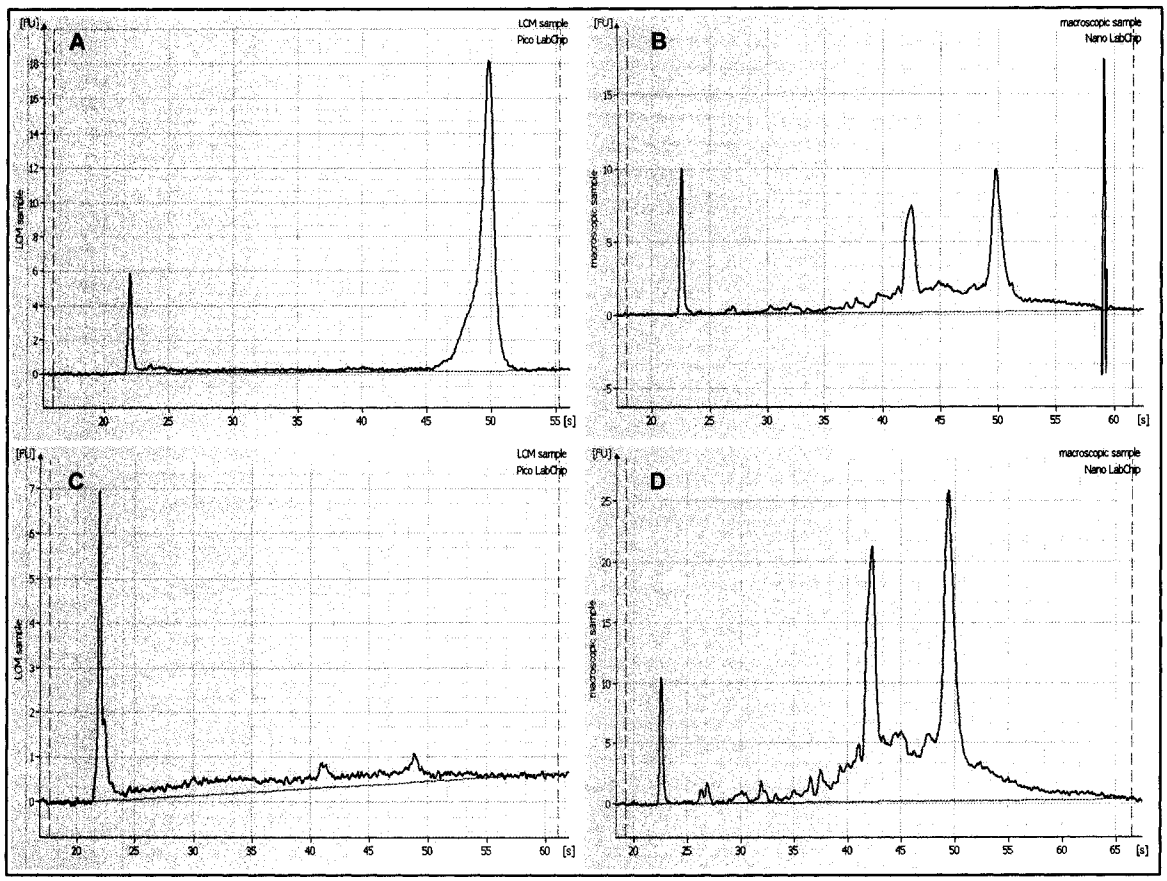


Figure 18: Electropherograms from samples with low RNA concentration (A, C) and high RNA concentration (B, D). The impact of artifacts on the electropherogram tracing is much greater in the lower concentrated sample compared to the sample with higher RNA concentration. (**A**) Electropherogram of an LCM sample with an unexplainable large peak, resulting in rescaling of the y-axis and difficulties to assess the signals from the sample RNA. (**C**) Electropherogram of an LCM sample without artifacts. Notice the larger scale of the y-axis compared to (A). (**B**) Electropherogram of a macroscopic sample with an artifact of similar size as the one in (A). Note that the signals from the sample RNA are still well visible. (**D**) Electropherogram of a macroscopic sample without artifacts. (The y-axis shows the intensity of fluorescence detected (a measure for RNA amount). The x-axis shows the time of detection.)

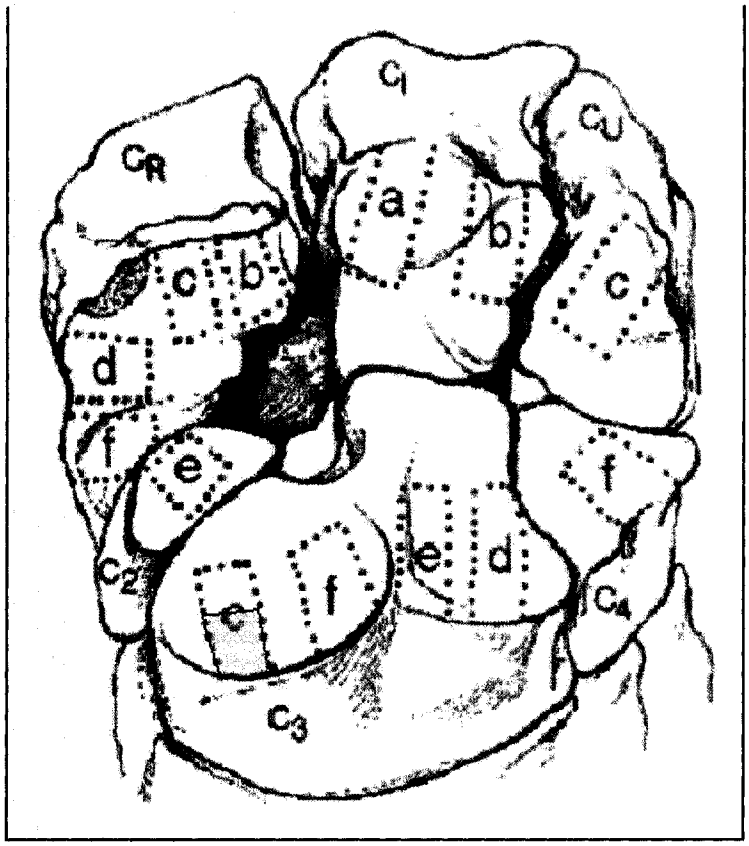


Figure 19: Sampling location (pink area) of full-thickness hyaline cartilage from the dorsal aspect of the radial facet of the 3rd carpal bones for the gene array analysis experiment.

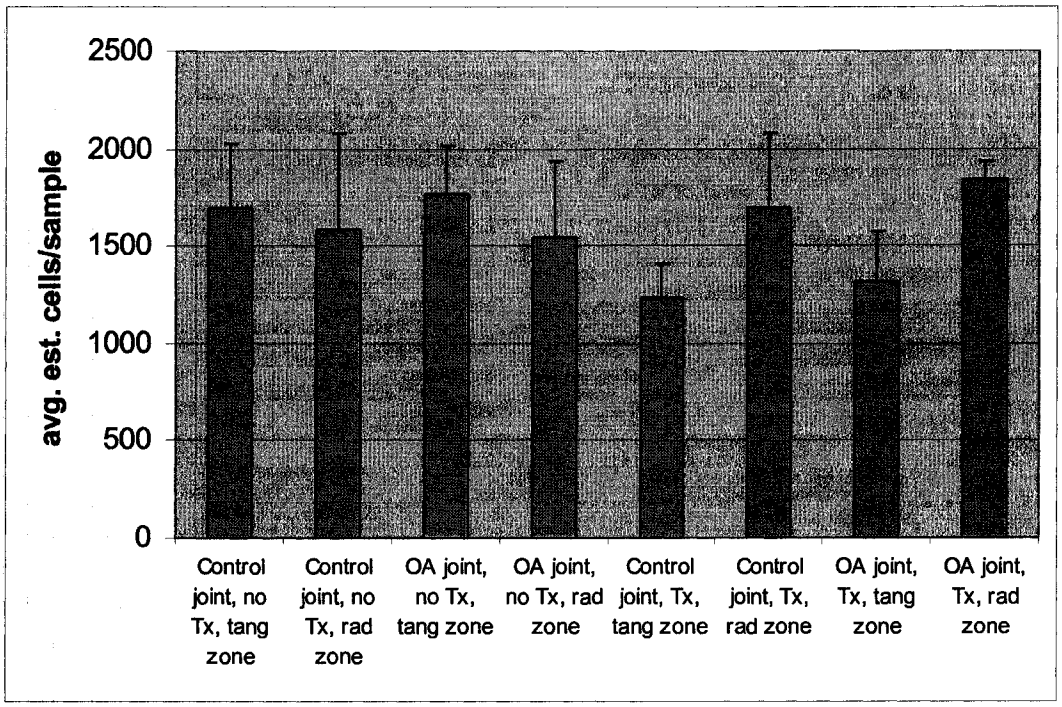


Figure 20: Estimated average cell numbers per sample by group. (The y-axis shows the average estimated number of cells that were captured per sample. The x-axis shows the different sample groups. OA joint: osteoarthritic joint, Tx: treatment with diclofenac ointment, tang zone: tangential layer of articular cartilage, rad zone: radial layer of articular cartilage. Error bars represent standard deviation.)

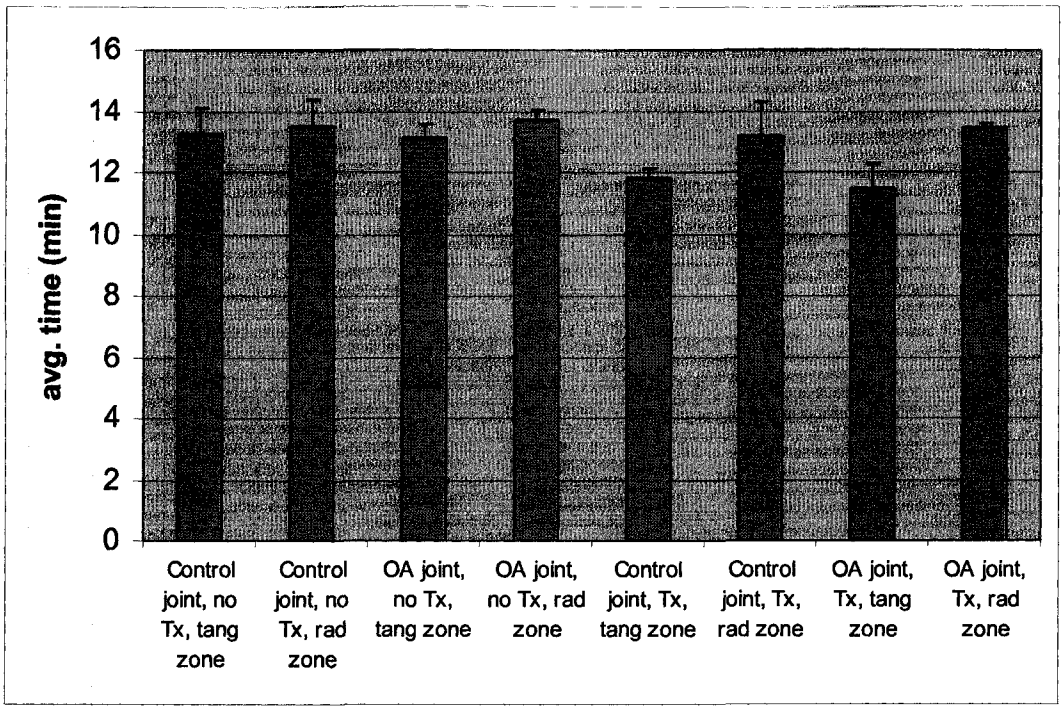


Figure 21: Average time in minutes from thawing the section to covering the captured cells with extraction buffer for each group. (The y-axis shows the average time from thawing of the slide until covering the captured cells with extraction buffer. The x-axis shows the different sample groups. OA joint: osteoarthritic joint, Tx: treatment with diclofenac ointment, tang zone: tangential layer of articular cartilage, rad zone: radial layer of articular cartilage. Error bars represent standard deviation.)

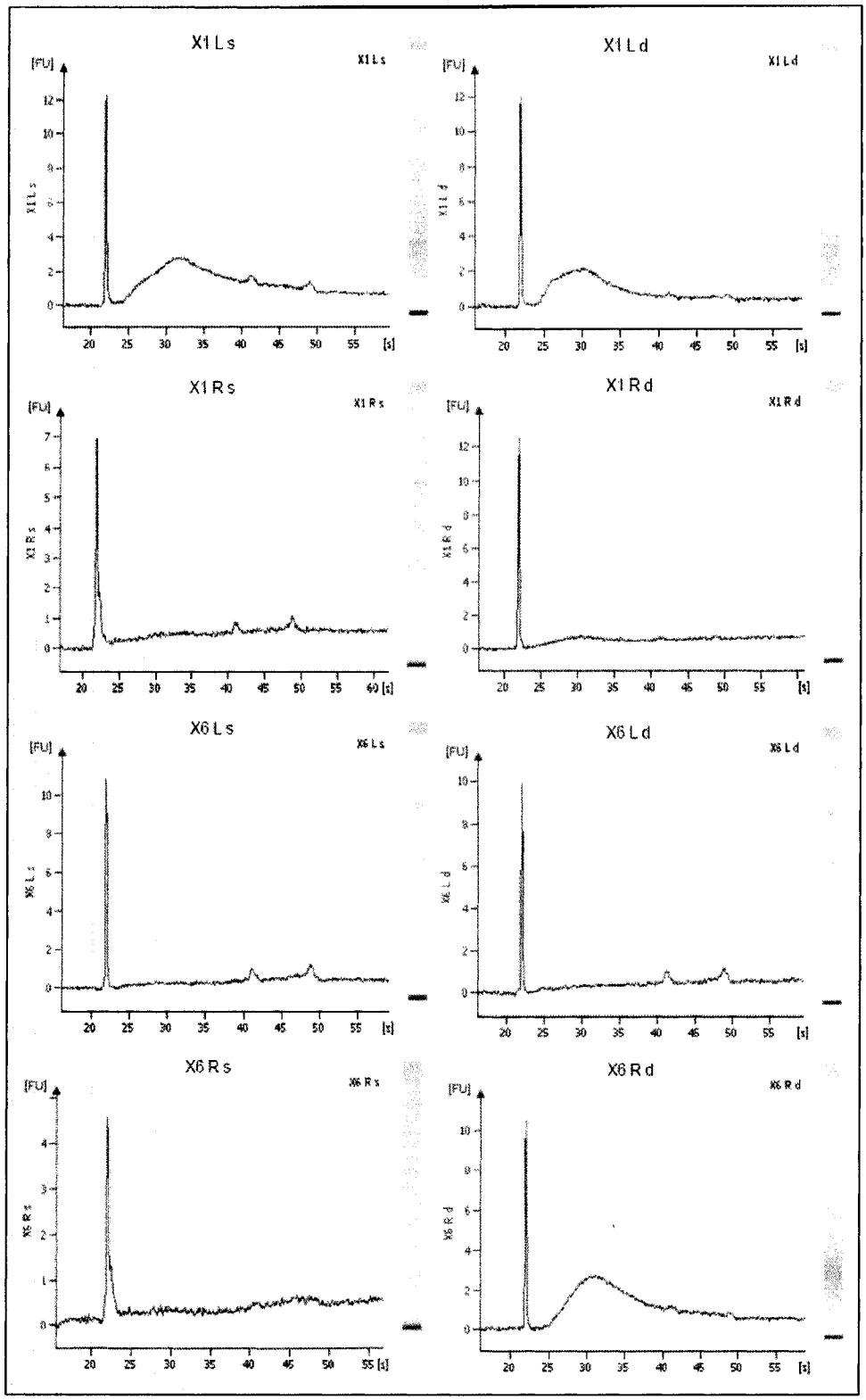


Figure 22a: Electropherograms from laser captured samples determined with the 2nd generation Pico LabChip® Kit (arrays 1-8). (The y-axis shows the intensity of fluorescence detected (a measure for RNA amount). The x-axis shows the time of detection.)

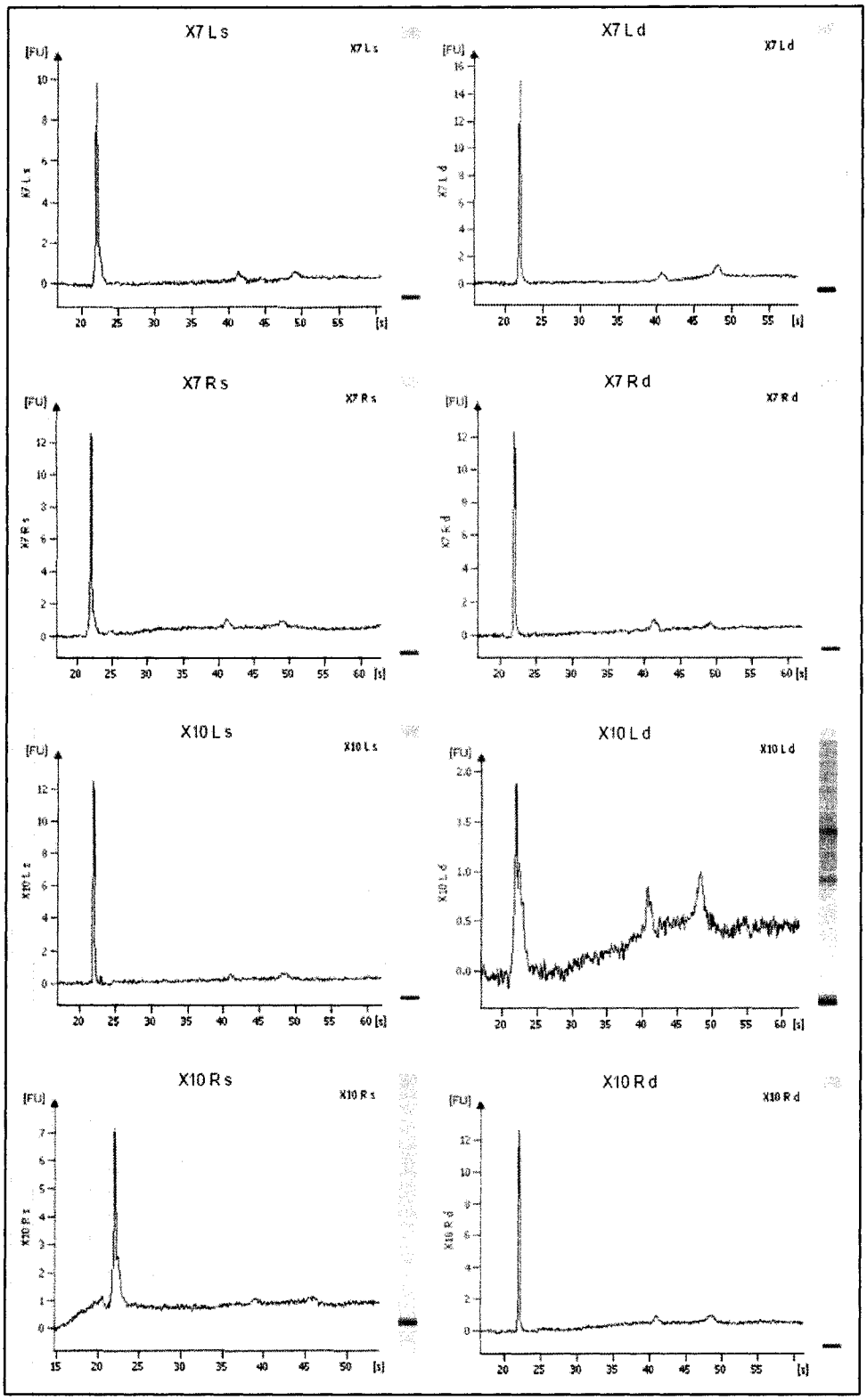


Figure 22b: Electropherograms from laser captured samples determined with the 2nd generation Pico LabChip® Kit (arrays 9-16). (The y-axis shows the intensity of fluorescence detected (a measure for RNA amount). The x-axis shows the time of detection.)

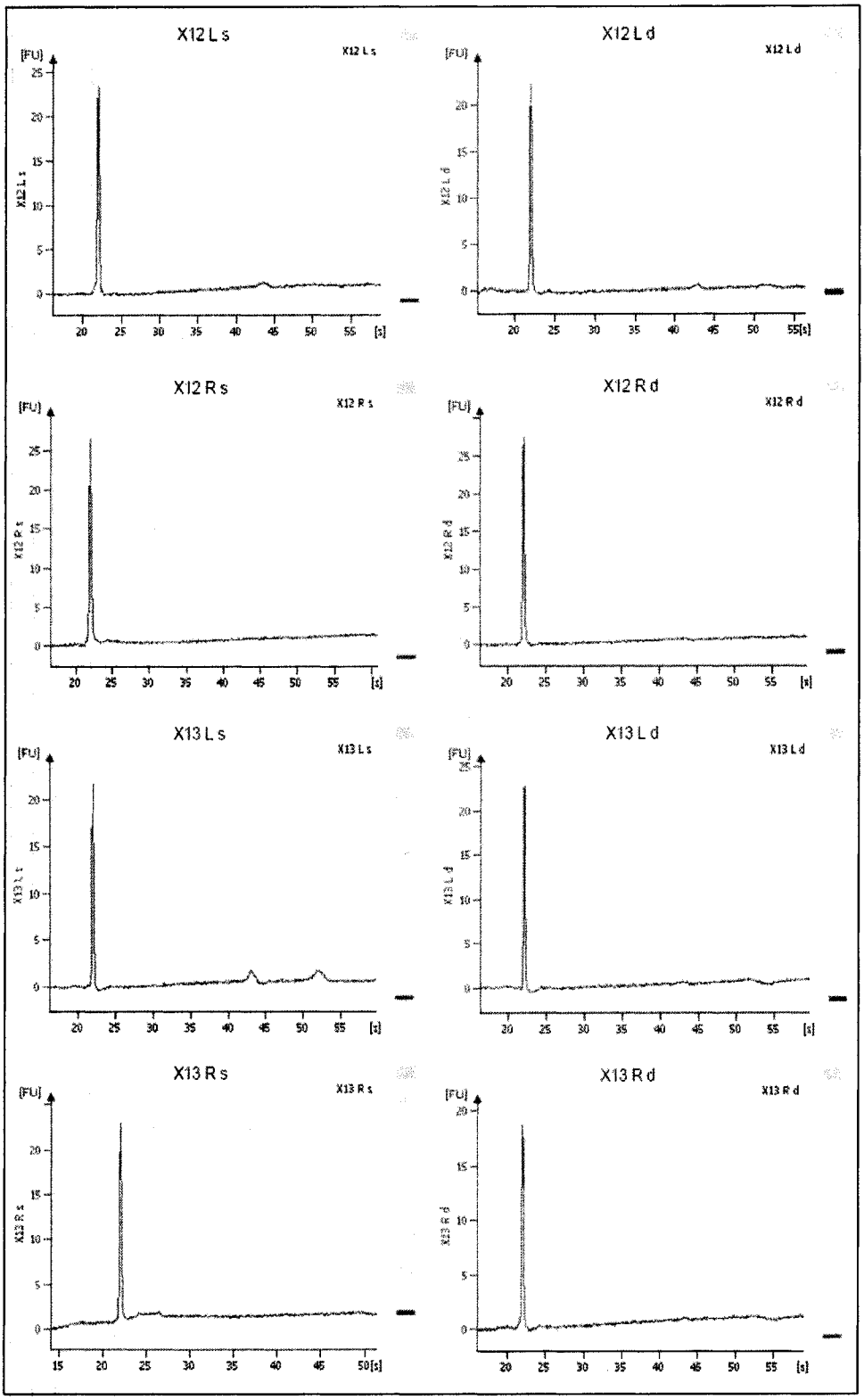


Figure 22c: Electropherograms from laser captured samples determined with the 2nd generation Pico LabChip® Kit (arrays 17-24). (The y-axis shows the intensity of fluorescence detected (a measure for RNA amount). The x-axis shows the time of detection.)

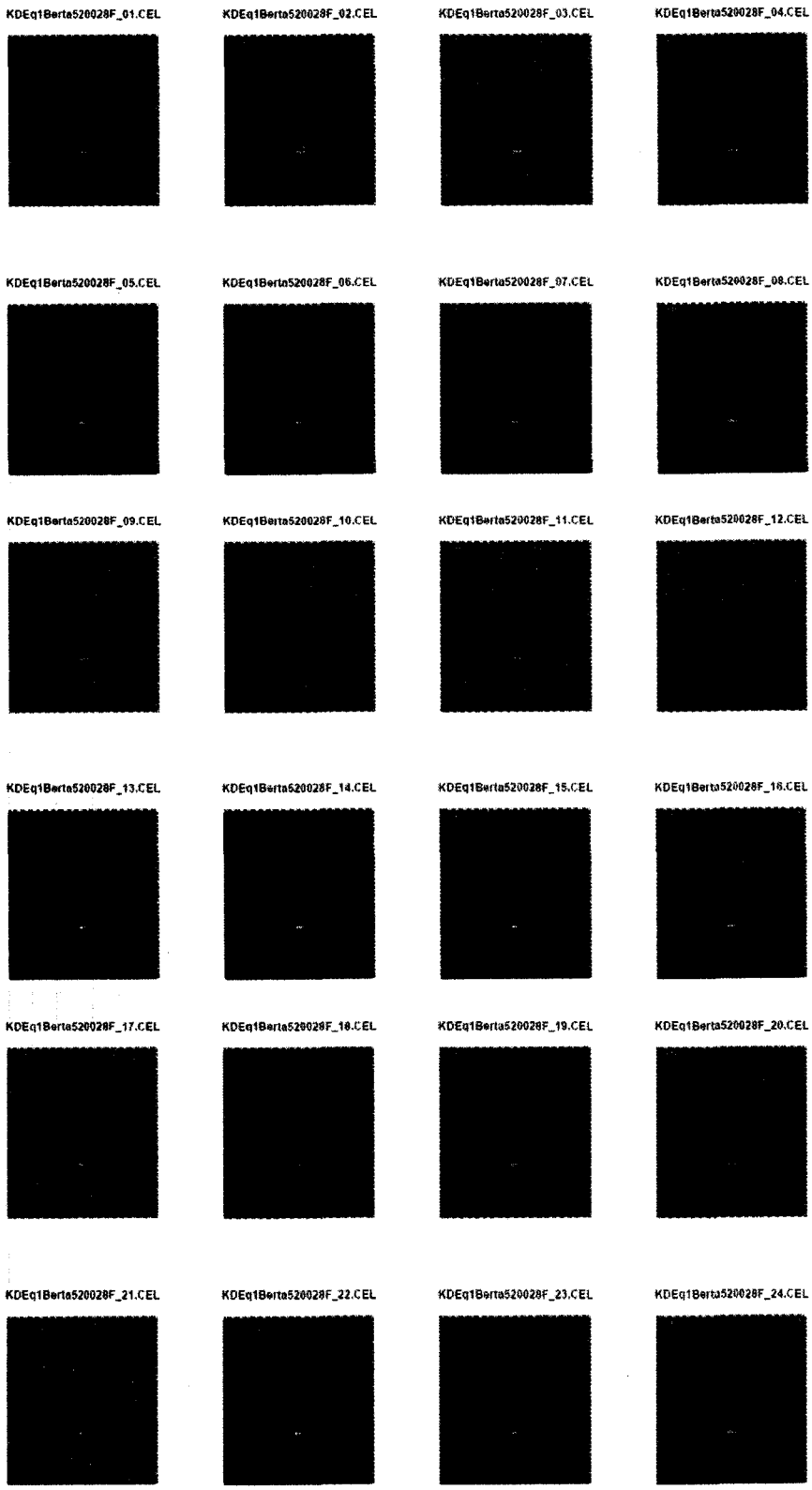


Figure 23: CEL file images of all arrays. Note that array 14 appears darker than all other arrays. (White spots represent present signals, black spots represent absent signal.)

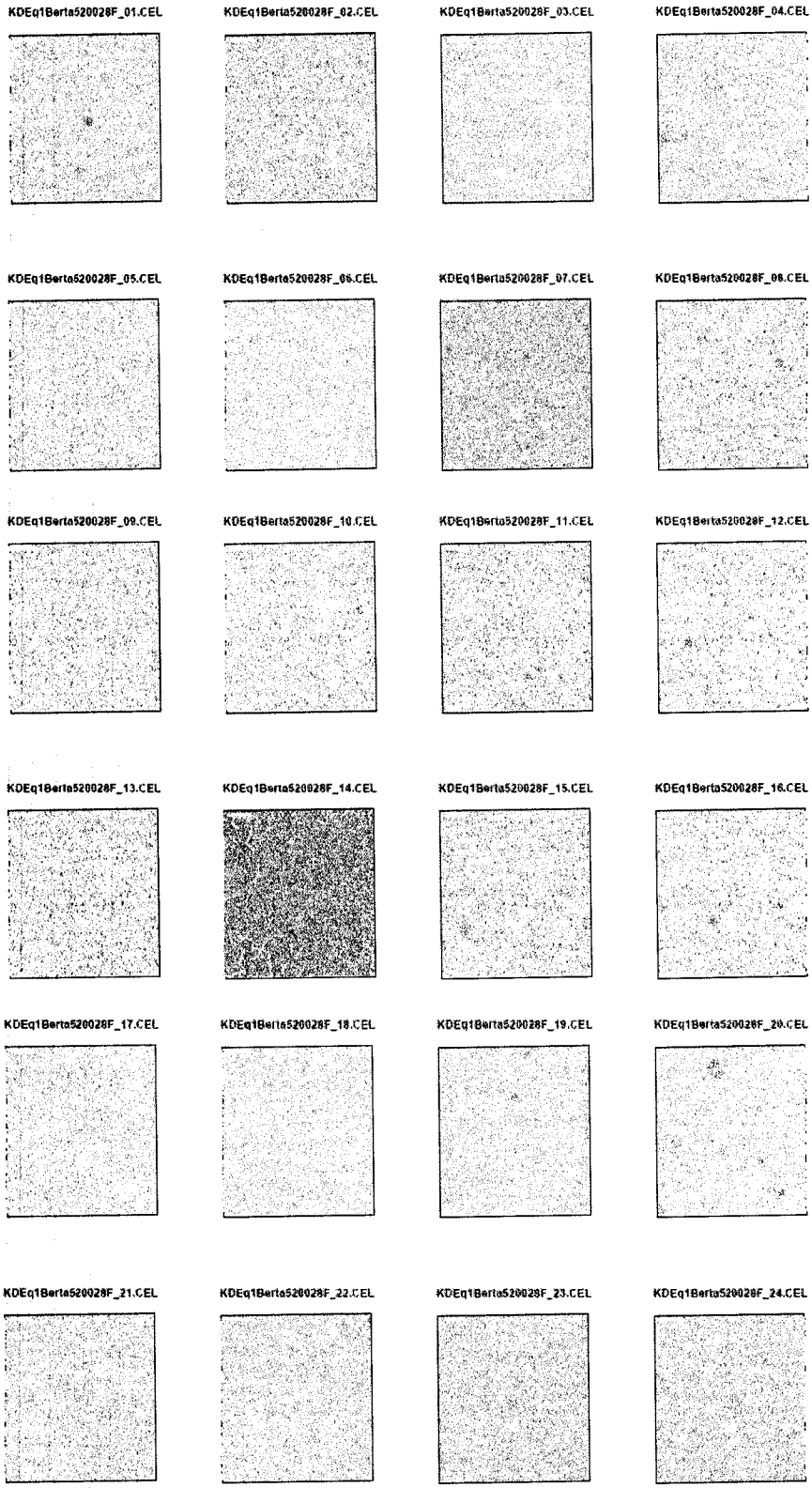


Figure 24: Residual plots of all arrays. Note that array 14 contains more red (larger positive residuals) and blue (larger negative residuals) cells compared to all other arrays. Further note the small circular areas of increased residual values in arrays 1, 7, 8 and 20.

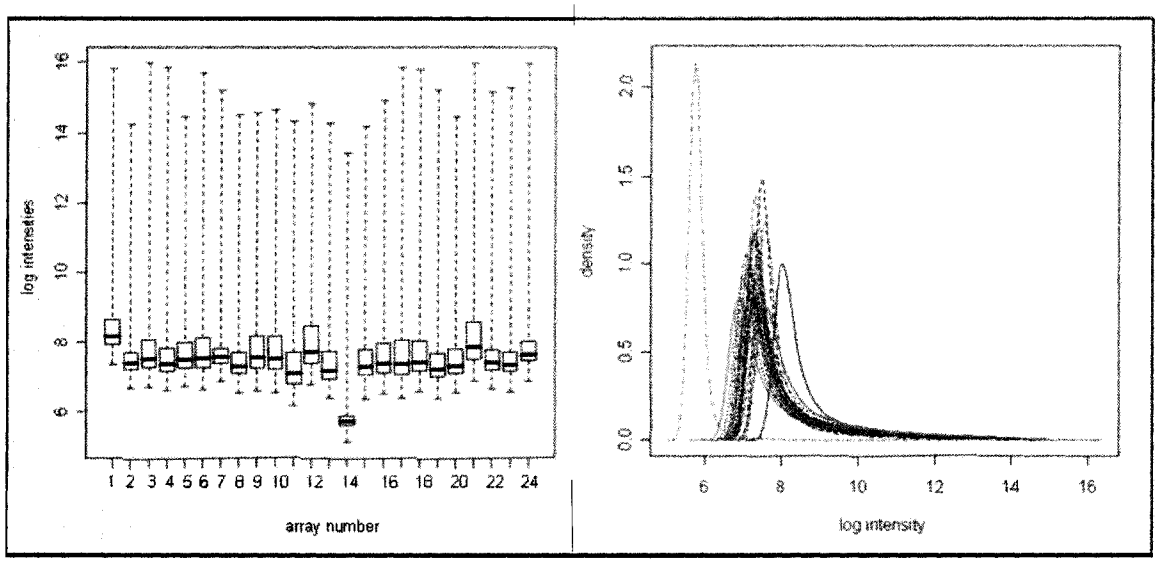


Figure 25: Box plot and histogram of $\log_2$ transferred probe intensities for all arrays. (Represented by the y-axis in the box plot and by the x-axis in the histogram.) In the histogram, array 14 is shown in red and has the lowest probe intensity. Array 1 is shown in black and has the highest intensity. (

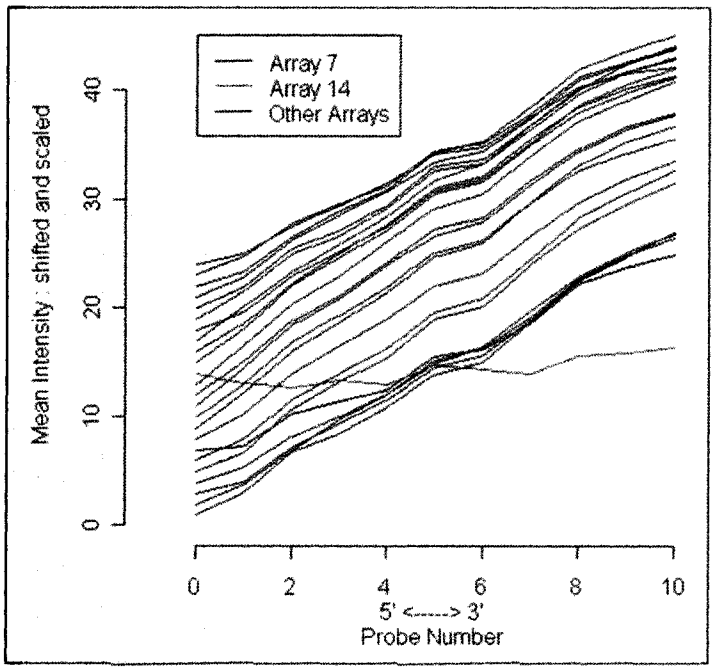


Figure 26: RNA digestion plot for all arrays. Note that array 14 has a markedly different digestion pattern compared to the other arrays. Array 7 also has a slightly different digestion pattern. (The y-axis shows the detected, shifted and scaled signal intensity. The x-axis represents the 10 different probes that make up each probe set. Notice that probe number 10 represents the most 3' probe and probe number 1 represents the most 5' probe for each gene. 0 represents background signal.)

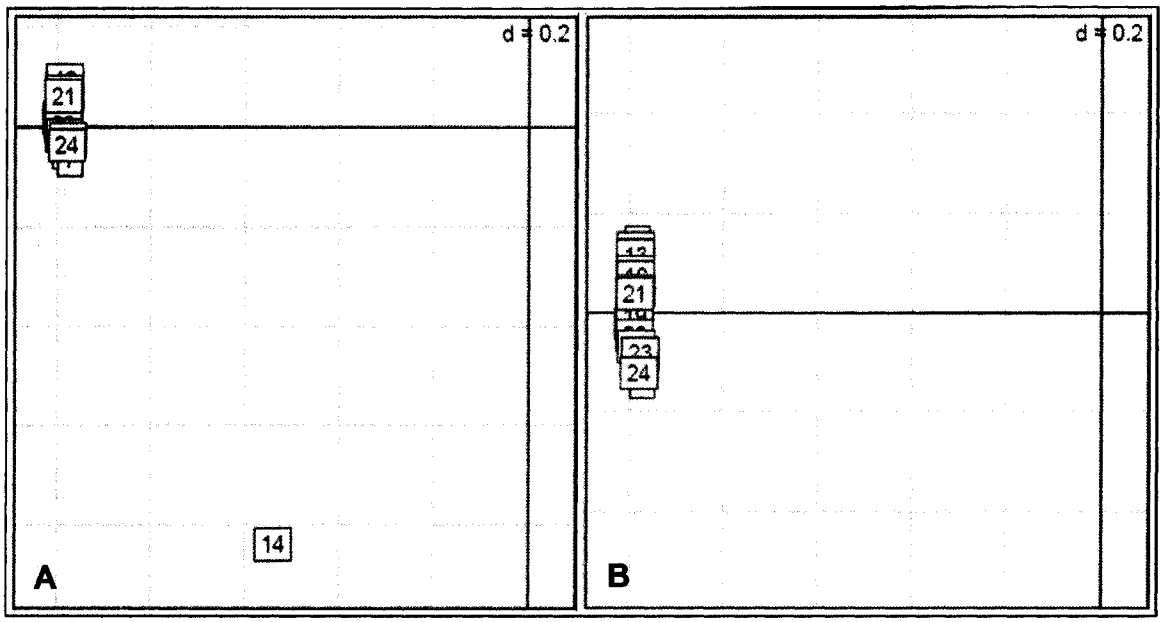


Figure 27: Principal Component Analysis plots. (**A**) Note array 14 appearing to be an extreme outlier. (**B**) PCA plot without array 14. The remaining arrays are tightly clustered. (Both axes represent one principal component, a summary variable chosen based on their ability to explain the variability in the data set)

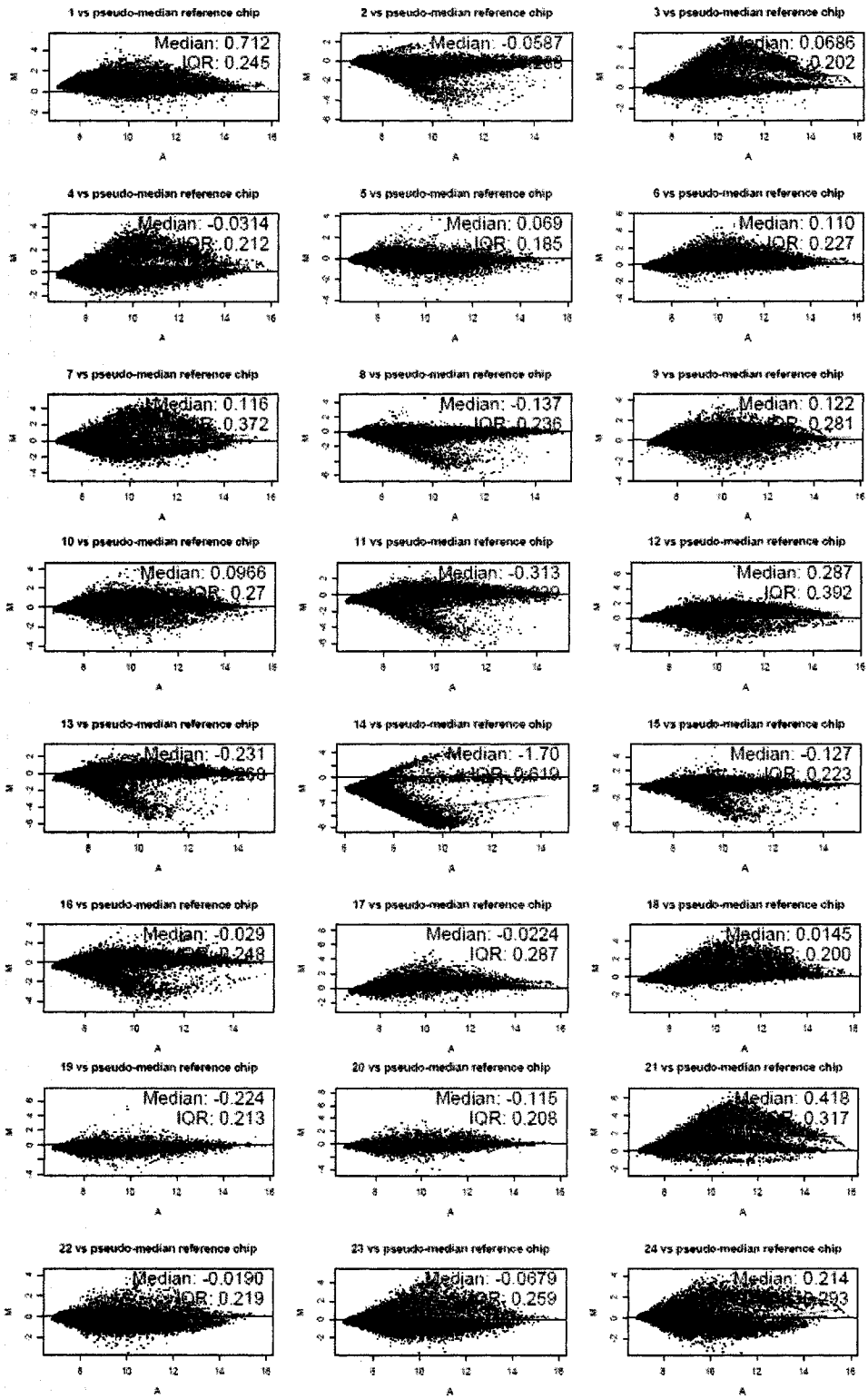


Figure 28: MVA plots for all arrays. Note the extreme curvature for array 14. (The y-axis shows the in $\log_2$-fold differences in probe intensity between each probe minus the $\log_2$ intensity of that probe of a hypothetical median array. The x-axis shows the average $\log_2$ intensitiesof each probe plus the $\log_2$ intensity of that probe of the hypothetical median array.)

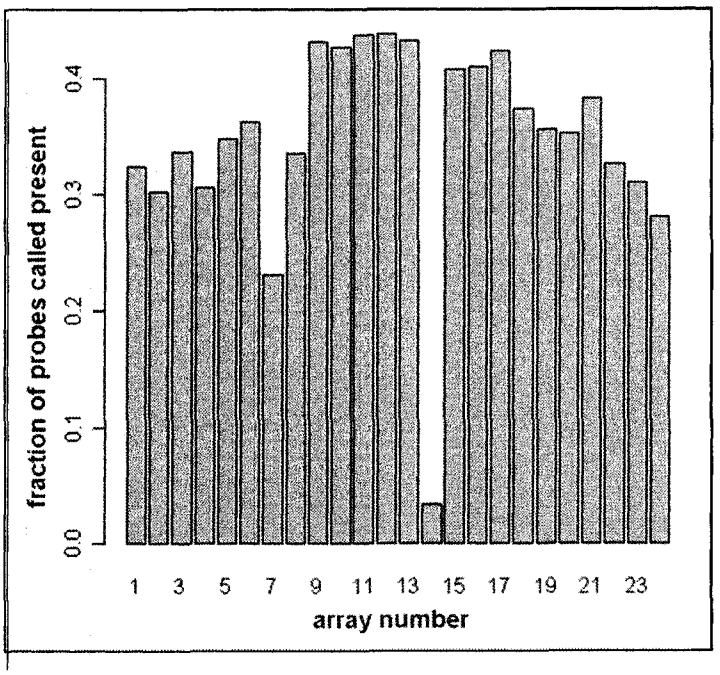


Figure 29: Fraction of probe sets called present for each array. Note the significantly lower number of present calls for array 14. (The y-axis represents the fraction of probes that were called present on the array. The x-axis represents the array number.)

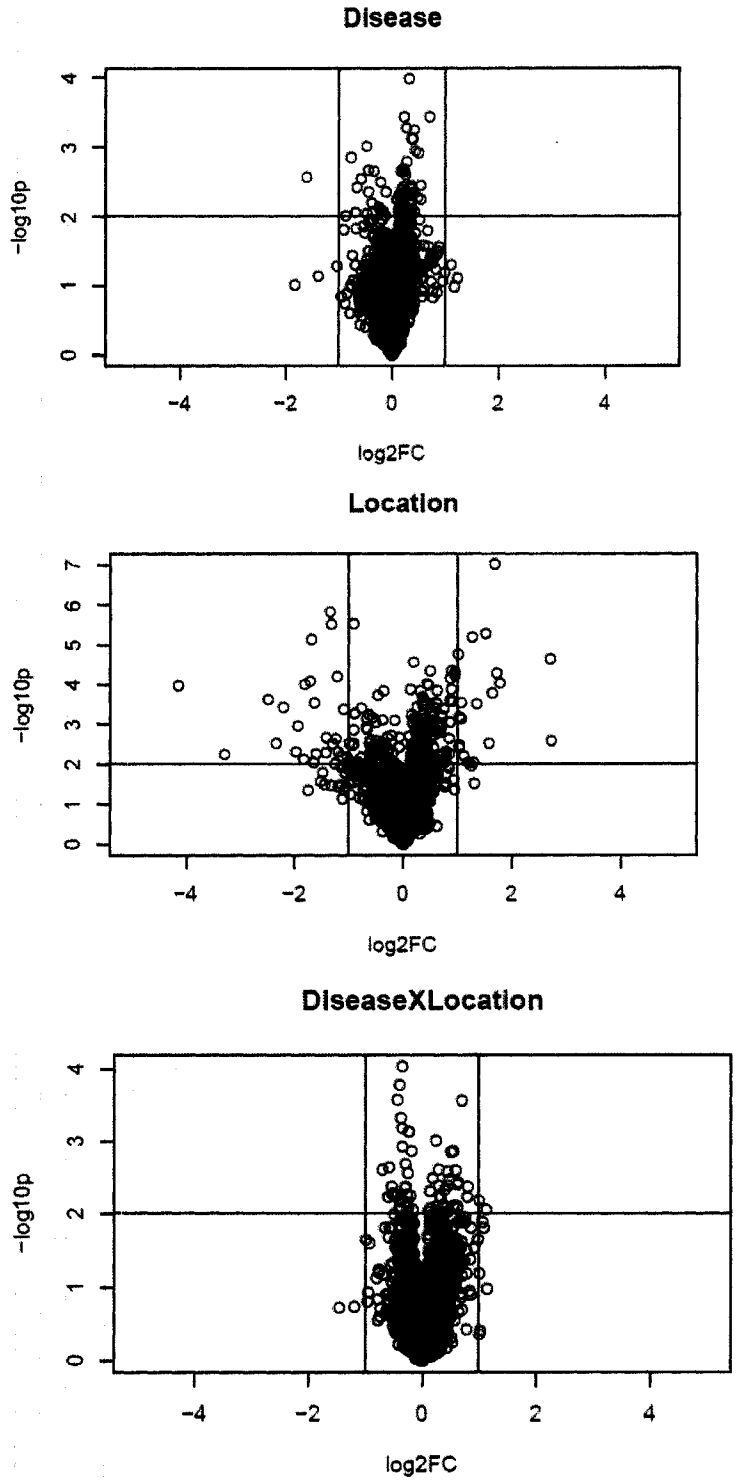


Figure 30: Venn diagrams for comparisons of interest. (Disease: osteoarthritic vs. control cartilage, Location: tangential vs. radial layer, DiseaseXLocation: osteoarthritic vs. control, dependent on cartilage layer) log2FC: $\log_2$ fold change, -log10p: $-\log_{10}$ of the p-values. (The y-axis represents the $\log_{10}$ transformed raw p-values for each gene, whereas the x-axis represents the $\log_2$ transformed fold change for each gene for the respective comparison.)

## 5 *Tables*

Table 1: Sequences or source for TaqMan® primers and probes.

| Equine Gene | Forward Primer | Probe | Reverse Primer |
|---|---|---|---|
| **GAPDH** | AAGTGGATATTGTCGCCA TCAAT | ACCTCAACTACATGGTCTA CATGTTTCAGTATGATTCC | AACTTGCCATGGGTGGAA TC |
| **aggrecan** | Primers and probe purchased from the Lucy Whittier Molecular & Diagnostic Core Facility, University of California Davis (sequences proprietary) | | |
| **collagen type II** | CGCTGTCCTTCGGTGTCA C | CCAGGATGTCCGGCAGCC AGG | TTTGGGTCCTACAATATCC TTGATG |
| **MMP3** | AACACTGGACGAAGGATG CAT | AGGGATCAATTTTCTCCTT GTTGCTGCTCA | ACCCAGGGAATGACCAAG TTC |
| **TGF-β** | GCCTGAGGCGGACTACTA CA | ATAGATTTCGTTTTCCTTT TCCACCATTAGCA | TGAGCCGGTCTCCACAGT CT |

Table 2: Original concentration, purity and RNA quality of 4 macroscopic samples used to produce several dilution series (Tables 3 and 4). All 4 samples were of good purity (260/280>1.8) and quality (RIN>8.0).

| Sample | RNA Concentration (ng/µl) | 260/280 | RIN (Nano LabChip®) |
|---|---|---|---|
| **M1** | 220.8 | 2.03 | 8.3 |
| **M2** | 431.4 | 2.01 | 8.4 |
| **M3** | 90.8 | 1.99 | 8.5 |
| **M4** | 158.6 | 2.01 | 8.5 |

Table 3: Dilution series used to determine a possible relationship between RNA concentration and RIN determined with the Nano LabChip® Kit. Notice the high RINs in the samples with concentrations above the lower limit of detection for the assay (500pg/µl).

| Sample | RNA Concentration (ng/µl) | RIN (Nano LabChip®) |
|---|---|---|
| **M1** | 200 | 9.1 |
| **M1** | 100 | 9.0 |
| **M1** | 50 | 8.0 |
| **M1** | 25 | 8.5 |
| **M1** | 12.5 | 1.0 |
| **M1** | 0 | 1.0 |
| **M2** | 350 | 8.8 |
| **M2** | 175 | 8.8 |
| **M2** | 87.5 | 8.9 |
| **M2** | 43.75 | 9.4 |
| **M2** | 21.88 | 7.9 |
| **M2** | 0 | 1.0 |
| **M3** | 90.8 | 8.5 |
| **M3** | 45.4 | 7.7 |
| **M3** | 22.7 | 7.6 |
| **M3** | 11.35 | 7.2 |
| **M3** | 5.68 | 1 |
| **M3** | 0 | 1.0 |
| **M4** | 158.6 | 8.6 |
| **M4** | 79.3 | 8.9 |
| **M4** | 39.65 | 8.4 |
| **M4** | 19.83 | 8.0 |
| **M4** | 9.91 | 8.1 |
| **M4** | 0 | 1.0 |

Table 4: Dilution series used to determine a possible relationship between RNA concentration and RIN determined with the Pico LabChip® Kit. Note the higher RINs in samples with higher RNA concentrations and the large number of samples without an assigned RIN.

| Sample | RNA Concentration (pg/µl) | RIN (Pico LabChip®) | |
|---|---|---|---|
| **M1** | 5078 | N/A | 9.2 |
| **M1** | 2539 | N/A | 9.1 |
| **M1** | 1270 | N/A | 8.4 |
| **M1** | 635 | 7.8 | N/A |
| **M1** | 317 | 8.1 | N/A |
| **M1** | 159 | 1.7 | N/A |
| **M1** | 79 | N/A | N/A |
| **M1** | 40 | 4.0 | 1.9 |
| **M1** | 20 | 1.0 | N/A |
| **M1** | 10 | 1.0 | N/A |
| **M2** | 5177 | N/A | 8.9 |
| **M2** | 2588 | N/A | 8.9 |
| **M2** | 1294 | N/A | 8.6 |
| **M2** | 647 | N/A | N/A |
| **M2** | 324 | N/A | N/A |
| **M2** | 162 | N/A | 2.4 |
| **M2** | 81 | N/A | N/A |
| **M2** | 40 | N/A | 2.4 |
| **M2** | 20 | 1.1 | N/A |
| **M2** | 10 | 1.1 | N/A |
| **M3** | 4994 | 8.4 | |
| **M3** | 2497 | 8.8 | |
| **M3** | 1249 | 8.7 | |
| **M3** | 624 | 7.8 | |
| **M3** | 312 | N/A | |
| **M3** | 156 | N/A | |
| **M3** | 78 | N/A | |
| **M3** | 39 | N/A | |
| **M3** | 20 | N/A | |
| **M3** | 10 | N/A | |
| **M4** | 5012 | 8.6 | |
| **M4** | 2506 | 8.6 | |
| **M4** | 1253 | 8.7 | |
| **M4** | 627 | 8.6 | |
| **M4** | 313 | 8.2 | |
| **M4** | 157 | N/A | |
| **M4** | 78 | N/A | |
| **M4** | 39 | N/A | |

Table 4: (continued)

| Sample | RNA Concentration (pg/µl) | RIN (Pico LabChip®) |
|---|---|---|
| **M4** | 20 | N/A |
| **M4** | 10 | N/A |
| **M1** | 4990 | 8.2 |
| **M1** | 2495 | 8.5 |
| **M1** | 1996 | 8.3 |
| **M1** | 1497 | 8.8 |
| **M1** | 1198 | 8.4 |
| **M1** | 999 | 8.1 |
| **M1** | 799 | 8.1 |
| **M1** | 599 | 7.8 |
| **M1** | 399 | 7.2 |
| **M1** | 200 | 6.0 |
| **M2** | 5004 | 8.5 |
| **M2** | 2502 | 8.4 |
| **M2** | 2002 | 8.6 |
| **M2** | 1502 | 8.8 |
| **M2** | 1202 | 8.8 |
| **M2** | 1003 | 8.3 |
| **M2** | 802 | 8.4 |
| **M2** | 602 | 8.5 |
| **M2** | 401 | N/A |
| **M2** | 201 | N/A |
| **M3** | 4994 | 8.7 |
| **M3** | 2497 | 8.6 |
| **M3** | 1998 | 8.8 |
| **M3** | 1499 | 8.9 |
| **M3** | 1199 | N/A |
| **M3** | 1000 | N/A |
| **M3** | 800 | N/A |
| **M3** | 600 | N/A |
| **M3** | 400 | N/A |
| **M3** | 200 | N/A |
| **M4** | 5012 | 8.7 |
| **M4** | 2506 | 8.4 |
| **M4** | 2005 | N/A |
| **M4** | 1504 | 8.4 |
| **M4** | 1203 | N/A |
| **M4** | 1003 | N/A |
| **M4** | 802 | N/A |
| **M4** | 602 | 8.2 |
| **M4** | 401 | N/A |
| **M4** | 201 | N/A |

Table 5: Macroscopic samples with known RNA quality were used to determine differences in Ct values between aliquots that were reverse transcribed with oligo dT primers or with random hexamers prior to real-time PCR for the equine gene GAPDH. Asterisks indicate samples that were incubated at 65°C for varying times (10-35 minutes) to decrease their RNA quality.

| Sample | RNA Concentration (pg/ul) | RIN (Nano LabChip®) | Difference in Ct (oligo-dT – rand. hexamer; GAPDH) |
|---|---|---|---|
| **Q1** | 4990 | 8.2 | 1.33 |
| **Q2** | 999 | 8.1 | 1.45 |
| **Q3** | 399 | 7.2 | 1.66 |
| **Q4** | 5004 | 8.5 | 1.84 |
| **Q5** | 1003 | 8.7 | 1.84 |
| **Q6** | 401 | N/A | 1.39 |
| **Q7** | 4994 | 8.7 | 0.95 |
| **Q8** | 1000 | N/A | 1.74 |
| **Q9** | 400 | N/A | 2.01 |
| **Q10** | 5012 | 8.7 | 1.01 |
| **Q11** | 1003 | N/A | 1.31 |
| **Q12** | 401 | N/A | 0.29 |
| **Q13*** | 3595000 | 7.0 | -0.001 |
| **Q14*** | 92000 | 7.8 | 0.88 |
| **Q15*** | 184000 | 6.8 | 0.74 |
| **Q16*** | 179750 | 7.3 | 0.98 |
| **Q17*** | 37800 | 4.3 | 1.75 |
| **Q18*** | 66100 | 4.6 | 2.05 |

Table 6: Subjective observations and RINs of electropherograms from microscopic samples (scrape and LCM samples) obtained using the RNA 6000 Pico LabChip® on the 2100 Bioanalyzer (Agilent Technologies, Palo Alto, CA). Empty RIN cells signify that RIN was not attempted to be determined.

| Sample Type | Sample # | Electropherogram Comments | RIN |
|---|---|---|---|
| **scrape** | 1 | artifact: unexplainable large peak | N/A |
| **scrape** | 2 | artifact: unexplainable large peak | N/A |
| **scrape** | 3 | artifact: fluctuating baseline | N/A |
| **scrape** | 4 | small rRNA peaks (18S>28S), peak close to marker | 2.9 |
| **scrape** | 5 | small rRNA peaks (18S>28S), peak close to marker | 1.4 |
| **scrape** | 6 | small rRNA peaks (18S>28S), peak close to marker | 2.3 |
| **scrape** | 7 | small rRNA peaks (18S>28S), peak close to marker | 2.6 |
| **scrape** | 8 | artifacts: bad baseline | 1.7 |
| **scrape** | 9 | artifacts: rising baseline | N/A |
| **scrape** | 10 | artifacts: unexplainable high peak | N/A |
| **scrape** | 11 | artifacts: rising baseline | N/A |
| **scrape** | 12 | artifacts: rising baseline | 2.6 |
| **scrape** | 13 | artifacts: rising baseline | N/A |
| **scrape** | 14 | artifacts: rising baseline | N/A |
| **scrape** | 15 | artifacts: rising baseline | N/A |
| **scrape** | 16 | artifacts: rising baseline | N/A |
| **scrape** | 17 | artifacts: rising baseline | N/A |
| **LCM** | 18 | artifact: unexplainable large peaks | |
| **LCM** | 19 | artifact: unexplainable large peaks | |
| **LCM** | 20 | artifact: unexplainable large peaks | |
| **LCM** | 21 | below detectable level | |
| **LCM** | 22 | below detectable level | |
| **LCM** | 23 | diffuse, wide band close to marker peak: degradation? | |
| **LCM** | 24 | below detectable level | |
| **LCM** | 25 | below detectable level | |
| **LCM** | 26 | below detectable level | |
| **LCM** | 27 | below detectable level | |
| **LCM** | 28 | artifact | |
| **LCM** | 29 | below detectable level | |
| **LCM** | 30 | below detectable level | |
| **LCM** | 31 | below detectable level | |
| **LCM** | 32 | below detectable level | |
| **LCM** | 33 | below detectable level | |
| **LCM** | 34 | artifact | |

Table 6: (continued)

| Sample Type | Sample # | Electropherogram Comments | RIN |
|---|---|---|---|
| **LCM** | 35 | below detectable level | |
| **LCM** | 36 | below detectable level | |
| **LCM** | 37 | below detectable level | |
| **LCM** | 38 | below detectable level | |
| **LCM** | 39 | peak close to marker | 1 |
| **LCM** | 40 | artifact: undulating baseline | N/A |
| **LCM** | 41 | artifact: undulating baseline | N/A |
| **LCM** | 42 | artifact: undulating baseline | N/A |
| **LCM** | 43 | artifact: undulating baseline | N/A |
| **LCM** | 44 | artifact: undulating baseline | N/A |
| **LCM** | 45 | artifact: undulating baseline | N/A |

Table 7: Microscopic samples with unknown RNA quality used to determine differences in Ct values between aliquots that were reverse transcribed with oligo dT primers or with random hexamers prior to real-time PCR for the equine gene GAPDH.

| Sample | Difference in Ct (oligo-dT – rand. hexamer; GAPDH) |
|---|---|
| **1q** | 1.61 |
| **2q** | 2.20 |
| **3q** | 2.29 |
| **4q** | 1.66 |
| **5q** | 4.59 |
| **6q** | 2.14 |
| **7q** | 3.41 |
| **8q** | 2.87 |
| **9q** | 3.19 |

Table 8: RNA yields and purity for the macroscopic samples used to validate the isolation and amplification of RNA from laser captured articular chondrocytes.

| Sample | Tissue Wet Weight (mg) | RNA Concentration (ng/ul) | RNA Yield (ng/mg cartilage) | 260/280 |
|---|---|---|---|---|
| **M1** | 224.8 | 47.815 | 6.38 | 2.08 |
| **M2** | 296.7 | 26.66 | 2.70 | 1.91 |
| **M3** | 390.9 | 167.15 | 12.83 | 2.10 |
| **M4** | 297.5 | 228.96 | 23.09 | 2.08 |
| **M5** | 170.2 | 145.885 | 25.71 | 2.02 |
| **M6** | 176.8 | 122.87 | 20.85 | 2.07 |

Table 9: Estimated RNA yields (prior and after amplification) and observations from electropherograms (prior to amplification) for the LCM samples used to validate the isolation and amplification of RNA from laser captured articular chondrocytes.

| Sample | Estimated Total RNA Yield (pg/8caps) | Electropherogram Comments | Total RNA Post Amplification (µg) |
|---|---|---|---|
| **L1** | 3000 | 28S rRNA peak lower than 18S rRNA peak, baseline mildly elevated in-between peaks | 90.24 |
| **L2** | artifacts in electropherogram: electropherogram not legible | | 62.61 |
| **L3** | artifacts in electropherogram: electropherogram not legible | | 59.24 |
| **L4** | 3000 | 28S rRNA peak higher than 18S rRNA peak, but baseline rising from 45 to 70 seconds | 74.16 |
| **L5** | 4000 | 28S rRNA peak lower than 18S rRNA peak, baseline mildly elevated in-between peaks | 75.55 |
| **L6** | 8000 | 28S rRNA peak lower than 18S rRNA peak, baseline mildly elevated in-between peaks | 87.62 |

Table 10: Horses used in the gene array analysis experiment.

| Horse | Treatment | Limb with Osteochondral Fragment | Control Limb |
|---|---|---|---|
| **1** | Diclofenac | right | left |
| **6** | None | left | right |
| **7** | Diclofenac | left | right |
| **10** | None | right | left |
| **12** | Diclofenac | left | right |
| **13** | None | left | right |

Table 11: Controlled exercise program (imposed 5 days/week on all horses from day 14 until day 70 post-operatively).

| Time interval | Speed | Gait |
|---|---|---|
| 2 minutes | 8-12 miles/h | trot |
| 2 minutes | 25-33 miles/h | gallop |
| 2 minutes | 8-12 miles/h | trot |

Table 12: Estimated numbers of cells captured per slide and resulting estimated cell numbers per sample (8 caps pooled into 1 sample).

| Array | Slide 1 | Slide 2 | Slide 3 | Slide 4 | Slide 5 | Slide 6 | Slide 7 | Slide 8 | Total Cells /Sample |
|---|---|---|---|---|---|---|---|---|---|
| **1** | 114 | 220 | 175 | 123 | 100 | 100 | 156 | 124 | 1112 |
| **2** | 271 | 229 | 272 | 291 | 270 | 236 | 232 | 160 | 1961 |
| **3** | 229 | 329 | 162 | 212 | 150 | 154 | 174 | 206 | 1616 |
| **4** | 256 | 180 | 186 | 289 | 195 | 207 | 224 | 242 | 1779 |
| **5** | 220 | 218 | 180 | 150 | 160 | 170 | 200 | 216 | 1514 |
| **6** | 200 | 203 | 200 | 230 | 200 | 200 | 214 | 228 | 1675 |
| **7** | 179 | 179 | 140 | 157 | 180 | 170 | 180 | 150 | 1335 |
| **8** | 124 | 191 | 200 | 136 | 190 | 162 | 193 | 179 | 1375 |
| **9** | 124 | 108 | 178 | 164 | 162 | 111 | 135 | 145 | 1127 |
| **10** | 272 | 212 | 201 | 323 | 191 | 213 | 206 | 189 | 1807 |
| **11** | 203 | 128 | 174 | 192 | 199 | 177 | 192 | 168 | 1433 |
| **12** | 271 | 220 | 267 | 176 | 207 | 279 | 221 | 230 | 1871 |
| **13** | 219 | 263 | 235 | 244 | 200 | 189 | 270 | 200 | 1820 |
| **14** | 248 | 286 | 242 | 289 | 256 | 290 | 292 | 240 | 2143 |
| **15** | 264 | 230 | 198 | 228 | 300 | 293 | 275 | 228 | 2016 |
| **16** | 236 | 225 | 155 | 234 | 278 | 280 | 216 | 230 | 1854 |
| **17** | 150 | 176 | 156 | 188 | 139 | 140 | 140 | 105 | 1194 |
| **18** | 239 | 269 | 295 | 246 | 232 | 234 | 216 | 216 | 1947 |
| **19** | 103 | 132 | 140 | 107 | 120 | 268 | 121 | 157 | 1148 |
| **20** | 166 | 163 | 141 | 127 | 181 | 163 | 167 | 161 | 1269 |
| **21** | 196 | 217 | 285 | 246 | 230 | 182 | 230 | 184 | 1770 |
| **22** | 167 | 114 | 148 | 98 | 162 | 153 | 153 | 100 | 1095 |
| **23** | 279 | 247 | 220 | 250 | 256 | 280 | 217 | 200 | 1949 |
| **24** | 200 | 166 | 150 | 150 | 179 | 150 | 120 | 120 | 1235 |

Table 13: Time periods and average time in minutes (8 caps pooled per sample) between thawing of the section and covering the captured cells with extraction buffer.

| Array | Slide 1 | Slide 2 | Slide 3 | Slide 4 | Slide 5 | Slide 6 | Slide 7 | Slide 8 | Average Time For Capture |
|---|---|---|---|---|---|---|---|---|---|
| **1** | 13 | 13 | 11 | 12 | 11 | 11 | 12 | 11 | 11.75 |
| **2** | 15 | 14 | 13 | 14 | 15 | 14 | 15 | 12 | 14 |
| **3** | 15 | 15 | 12 | 12 | 11 | 11 | 12 | 11 | 12.38 |
| **4** | 15 | 14 | 14 | 14 | 12 | 13 | 14 | 13 | 13.63 |
| **5** | 13 | 15 | 13 | 12 | 12 | 12 | 14 | 13 | 13 |
| **6** | 14 | 14 | 13 | 13 | 14 | 14 | 12 | 13 | 13.38 |
| **7** | 13 | 12 | 11 | 13 | 12 | 12 | 15 | 11 | 12.38 |
| **8** | 13 | 13 | 13 | 14 | 13 | 11 | 13 | 14 | 13 |
| **9** | 11 | 11 | 11 | 11 | 11 | 11 | 11 | 11 | 11 |
| **10** | 15 | 14 | 12 | 15 | 13 | 13 | 13 | 12 | 13.38 |
| **11** | 13 | 12 | 12 | 12 | 12 | 11 | 12 | 13 | 12.13 |
| **12** | 15 | 13 | 14 | 12 | 13 | 15 | 13 | 14 | 13.63 |
| **13** | 15 | 14 | 13 | 13 | 13 | 13 | 14 | 12 | 13.38 |
| **14*** | 15 | 15 | 15 | 15 | 14 | 14 | 13 | 15 | 14.5 |
| **15** | 15 | 13 | 13 | 12 | 15 | 15 | 14 | 12 | 13.63 |
| **16** | 15 | 14 | 12 | 13 | 14 | 15 | 15 | 12 | 13.75 |
| **17** | 11 | 11 | 11 | 13 | 11 | 11 | 11 | 10 | 11.13 |
| **18** | 14 | 15 | 15 | 13 | 12 | 14 | 12 | 12 | 13.38 |
| **19** | 10 | 13 | 11 | 11 | 11 | 14 | 11 | 11 | 11.5 |
| **20** | 13 | 12 | 12 | 14 | 12 | 11 | 11 | 11 | 12 |
| **21** | 14 | 12 | 13 | 12 | 13 | 12 | 12 | 13 | 12.63 |
| **22** | 14 | 14 | 14 | 15 | 14 | 15 | 14 | 12 | 14 |
| **23** | 14 | 15 | 14 | 14 | 14 | 14 | 15 | 12 | 14 |
| **24** | 15 | 14 | 12 | 12 | 12 | 14 | 12 | 13 | 13 |

Table 14: Summary table of RNA quality control and estimation of RNA yield, as determined with the 2nd generation Pico LabCip® Kit. In cases where the RNA concentration of the sample was greater than 1000 pg/µl, it was assumed that this was a falsely high estimate, which is indicated as "non-credible estimate" in the table.

| Array | RIN | Estimated RNA Yield (pg) | Subjective Assessment Of Electropherogram | RIN Of corresponding Scrape Sample | Estimated RNA Yield Of Scrape Sample (pg) |
|---|---|---|---|---|---|
| **1** | 2.0 | non-credible estimate | 18S & 28S peaks present, mound at 30 sec | 8.4 | 40400 |
| **2** | 1.7 | non-credible estimate | 18S & 28S peaks small, mound at 30 sec | 8.4 | 40400 |
| **3** | N/A | 6100 | 18S & 28S peaks present, widened marker peak | 8.6 | 46770 |
| **4** | 1.0 | 5510 | small mound at 30 sec, 18S & 28S peaks barely visible | 8.6 | 46770 |
| **5** | 3.7 | 3770 | 18S & 28S peaks present | 7.8 | 16050 |
| **6** | 4.1 | 3280 | 18S & 28S peaks present | 7.8 | 16050 |
| **7** | N/A | 2150 | widened marker peak | 8.7 | 31270 |
| **8** | 2.1 | non-credible estimate | small mound at 30 sec, 18S & 28S peaks small | 8.7 | 31270 |
| **9** | 1.0 | 930 | 18S & 28S peaks present | 8.6 | 28300 |
| **10** | 7.6 | 2120 | 18S & 28S peaks present | 8.6 | 28300 |
| **11** | 2.5 | 6310 | 18S & 28S peaks present, barely visible peak at 25 sec | 8.3 | 24290 |
| **12** | 3.2 | 2020 | 18S & 28S peaks present | 8.3 | 24290 |

Table 14: (continued)

| Array | RIN | Estimated RNA Yield (pg) | Subjective Assessment Of Electropherogram | RIN Of corresponding Scrape Sample | Estimated RNA Yield Of Scrape Sample (pg) |
|---|---|---|---|---|---|
| **13** | 1.0 | 160 | 18S & 28S peaks small | 8.3 | 34930 |
| **14** | N/A | 3740 | 18S & 28S peaks small | 8.3 | 34930 |
| **15** | N/A | non-credible estimate | 18S & 28S peaks barely visible, shifted baseline | 8 | 17120 |
| **16** | 2.8 | 3280 | 18S & 28S peaks present | 8 | 17120 |
| **17** | 1.0 | 2020 | barely visible peak at 44 sec (18S peak?) | 7.5 | 53440 |
| **18** | 1.0 | 740 | 18S & 28S peaks barely visible | 7.5 | 53440 |
| **19** | 1.0 | 1660 | even baseline, barely visible peak at 25 sec | 8.9 | 20320 |
| **20** | 1.0 | 910 | even baseline | 8.9 | 20320 |
| **21** | 1.0 | 4020 | 18S & 28S peaks present | 8.4 | 29830 |
| **22** | 1.0 | 320 | even baseline | 8.4 | 29830 |
| **23** | N/A | non-credible estimate | even baseline, barely visible peak at 25 sec | 8.9 | 33090 |
| **24** | 1.0 | 2670 | even baseline | 8.9 | 33090 |

Table 15: Total RNA yields and 260/280 absorption ratios after 1 and 2 rounds of *in-vitro* transcription amplification.

| Array | Sample | RNA Yield (µg) post 1st IVT | 260/280 | RNA Yield (µg) post 2nd IVT | 260/280 |
|---|---|---|---|---|---|
| **1** | 1 L r C t | 1.675 | 2.11 | 63.8 | 1.802 |
| **2** | 1 L r C r | 1.499 | 1.65 | 61.6 | 1.851 |
| **3** | 1 R d OA t | 1.587 | 2.14 | 62.5 | 1.817 |
| **4** | 1 R d OA r | 1.339 | 2.26 | 55.8 | 1.821 |
| **5** | 6 L n OA t | 0.768 | 2.41 | 56.5 | 1.815 |
| **6** | 6 L n OA r | 1.419 | 2.19 | 51.0 | 1.871 |
| **7** | 6 R n C t | 1.404 | 2.10 | 55.3 | 1.825 |
| **8** | 6 R n C r | 1.547 | 1.88 | 64.5 | 1.939 |
| **9** | 7 L d OA t | 0.512 | 2.16 | 86.6 | 1.828 |
| **10** | 7 L d OA r | 0.376 | 2.11 | 65.2 | 1.877 |
| **11** | 7 R r C t | 0.474 | 1.84 | 83.2 | 1.974 |
| **12** | 7 R r C r | 0.393 | 2.07 | 69.2 | 1.919 |
| **13** | 10 L n C t | 0.516 | 1.99 | 72.1 | 1.858 |
| **14** | 10 L n C r | 0.694 | 1.63 | 5.0 | 3.288 |
| **15** | 10 R n OA t | 1.073 | 1.71 | 63.1 | 1.865 |
| **16** | 10 R n OA r | 0.763 | 1.68 | 68.3 | 1.901 |
| **17** | 12 L d OA t | 0.827 | 2.24 | 63.3 | 1.827 |
| **18** | 12 L d OA r | 1.154 | 2.16 | 62.0 | 1.905 |
| **19** | 12 R r C t | 0.997 | 2.25 | 64.6 | 1.833 |
| **20** | 12 R r C r | 0.966 | 2.06 | 56.4 | 1.914 |
| **21** | 13 L n OA t | 1.231 | 2.27 | 64.6 | 1.798 |
| **22** | 13 L n OA r | 0.836 | 2.15 | 56.5 | 1.931 |
| **23** | 13 R n C t | 1.400 | 2.03 | 57.0 | 1.844 |
| **24** | 13 R n C r | 1.681 | 2.18 | 57.1 | 1.877 |

Table 16: Correlations of $\log_2$ perfect match probe intensity values between arrays.

| Array | 2 | 3 | 4 | 5 | 6 | 7 | 8 | 9 | 10 | 11 | 12 | 13 |
|---|---|---|---|---|---|---|---|---|---|---|---|---|
| 1 | 0.90 | 0.96 | 0.96 | 0.95 | 0.96 | 0.91 | 0.89 | 0.91 | 0.89 | 0.86 | 0.88 | 0.87 |
| 2 | | 0.85 | 0.88 | 0.94 | 0.90 | 0.80 | 0.97 | 0.91 | 0.91 | 0.91 | 0.90 | 0.92 |
| 3 | | | 0.96 | 0.91 | 0.94 | 0.92 | 0.83 | 0.86 | 0.85 | 0.81 | 0.83 | 0.82 |
| 4 | | | | 0.91 | 0.95 | 0.93 | 0.86 | 0.85 | 0.86 | 0.80 | 0.84 | 0.81 |
| 5 | | | | | 0.96 | 0.84 | 0.94 | 0.95 | 0.95 | 0.92 | 0.93 | 0.93 |
| 6 | | | | | | 0.88 | 0.90 | 0.92 | 0.93 | 0.88 | 0.91 | 0.88 |
| 7 | | | | | | | 0.77 | 0.76 | 0.75 | 0.70 | 0.72 | 0.71 |
| 8 | | | | | | | | 0.92 | 0.94 | 0.93 | 0.93 | 0.94 |
| 9 | | | | | | | | | 0.97 | 0.97 | 0.97 | 0.97 |
| 10 | | | | | | | | | | 0.96 | 0.98 | 0.96 |
| 11 | | | | | | | | | | | 0.98 | 0.98 |
| 12 | | | | | | | | | | | | 0.96 |

| Array | 14 | 15 | 16 | 17 | 18 | 19 | 20 | 21 | 22 | 23 | 24 |
|---|---|---|---|---|---|---|---|---|---|---|---|
| 1 | 0.32 | 0.88 | 0.88 | 0.95 | 0.96 | 0.95 | 0.95 | 0.93 | 0.95 | 0.94 | 0.93 |
| 2 | 0.39 | 0.93 | 0.93 | 0.89 | 0.89 | 0.93 | 0.93 | 0.80 | 0.91 | 0.85 | 0.84 |
| 3 | 0.32 | 0.83 | 0.83 | 0.93 | 0.95 | 0.91 | 0.91 | 0.96 | 0.92 | 0.95 | 0.93 |
| 4 | 0.36 | 0.82 | 0.85 | 0.92 | 0.96 | 0.92 | 0.94 | 0.93 | 0.95 | 0.94 | 0.95 |
| 5 | 0.31 | 0.94 | 0.94 | 0.94 | 0.93 | 0.95 | 0.95 | 0.89 | 0.94 | 0.89 | 0.88 |
| 6 | 0.30 | 0.89 | 0.90 | 0.95 | 0.96 | 0.94 | 0.95 | 0.93 | 0.95 | 0.91 | 0.91 |
| 7 | 0.40 | 0.73 | 0.74 | 0.85 | 0.90 | 0.87 | 0.87 | 0.88 | 0.90 | 0.93 | 0.93 |
| 8 | 0.34 | 0.95 | 0.96 | 0.89 | 0.88 | 0.92 | 0.92 | 0.80 | 0.89 | 0.82 | 0.82 |
| 9 | 0.23 | 0.96 | 0.96 | 0.94 | 0.90 | 0.93 | 0.91 | 0.86 | 0.89 | 0.83 | 0.81 |
| 10 | 0.23 | 0.95 | 0.97 | 0.93 | 0.91 | 0.92 | 0.93 | 0.87 | 0.90 | 0.83 | 0.82 |
| 11 | 0.21 | 0.97 | 0.96 | 0.91 | 0.87 | 0.91 | 0.89 | 0.81 | 0.85 | 0.78 | 0.76 |
| 12 | 0.20 | 0.95 | 0.97 | 0.93 | 0.90 | 0.92 | 0.92 | 0.85 | 0.88 | 0.80 | 0.80 |
| 13 | 0.24 | 0.98 | 0.97 | 0.92 | 0.88 | 0.91 | 0.89 | 0.81 | 0.86 | 0.80 | 0.77 |
| 14 | | 0.23 | 0.27 | 0.27 | 0.30 | 0.35 | 0.32 | 0.25 | 0.36 | 0.37 | 0.39 |
| 15 | | | 0.96 | 0.92 | 0.88 | 0.92 | 0.90 | 0.82 | 0.87 | 0.82 | 0.79 |
| 16 | | | | 0.91 | 0.90 | 0.92 | 0.92 | 0.83 | 0.89 | 0.81 | 0.81 |
| 17 | | | | | 0.96 | 0.96 | 0.94 | 0.92 | 0.93 | 0.92 | 0.89 |
| 18 | | | | | | 0.95 | 0.96 | 0.94 | 0.95 | 0.93 | 0.93 |
| 19 | | | | | | | 0.96 | 0.89 | 0.95 | 0.92 | 0.91 |
| 20 | | | | | | | | 0.90 | 0.96 | 0.91 | 0.92 |
| 21 | | | | | | | | | 0.91 | 0.92 | 0.91 |
| 22 | | | | | | | | | | 0.92 | 0.94 |
| 23 | | | | | | | | | | | 0.94 |

Table 17: Correlations between $log_2$ perfect match and $log_2$ mismatch probe intensity values. (L=left limb, R=right limb, r=possible remote effect of contralateral topical diclofenac treatment, d=topical diclofenac treatment, n=no treatment, C=control joint, OA=osteoarthritic joint, t=tangential cartilage layer, r=radial cartilage layer, *=array excluded from final data analysis)

| Array | Sample (horse, limb, medication, disease status, cartilage layer) | Correlation |
|---|---|---|
| **1** | 1 L r C t | 0.71 |
| **2** | 1 L r C r | 0.76 |
| **3** | 1 R d OA t | 0.71 |
| **4** | 1 R d OA r | 0.71 |
| **5** | 6 L n OA t | 0.76 |
| **6** | 6 L n OA r | 0.72 |
| **7** | 6 R n C t | 0.64 |
| **8** | 6 R n C r | 0.80 |
| **9** | 7 L d OA t | 0.76 |
| **10** | 7 L d OA r | 0.78 |
| **11** | 7 R r C t | 0.79 |
| **12** | 7 R r C r | 0.77 |
| **13** | 10 L n C t | 0.80 |
| **14*** | 10 L n C r | 0.72 |
| **15** | 10 R n OA t | 0.78 |
| **16** | 10 R n OA r | 0.77 |
| **17** | 12 L r OA t | 0.74 |
| **18** | 12 L r OA r | 0.71 |
| **19** | 12 R d C t | 0.72 |
| **20** | 12 R d C r | 0.73 |
| **21** | 13 L n OA t | 0.71 |
| **22** | 13 L n OA r | 0.68 |
| **23** | 13 R n C t | 0.70 |
| **24** | 13 R n C r | 0.69 |

Table 18: Differentially expressed genes between radial (reference group) and tangential cartilage layer, independent of disease status. Genes are ordered by functional categories. Some genes were represented by several probe sets on the array, thus, their (inferred) gene name may occur more than once in the same part of the table. Some genes have more than 1 function, thus, their (inferred) gene name may occur in several parts of the table. Positive $\log_2$ fold change values mean that the gene was upregulated in the radial layer compared to the tangential layer. Negative $\log_2$ fold change values mean that the gene was downregulated in the radial layer compared to the tangential layer. Genes were ranked according to their q-values (Rank #). Genes without homologue sequences with known gene names or known gene function were omitted from the table.

| **Cell cycle, cell proliferation, differentiation, apoptosis** | | | | | | | |
|---|---|---|---|---|---|---|---|
| **Rank #** | **Equine GenBank Accession Number and Description** | **Inferred Homology (Gene Name)** | **Biological Function** | **Present calls** | **$\log_2$ fold change** | **p-value** | **q-value** |
| 1 | CD535414\|LeukoN5_4_A01.b1_A027 Unstimulated peripheral blood leukocytes N5 | LIM domain only 4 | Pro cell proliferation, inhibiting cell differentiation | 21 | 1.694 | 0.0000001 | 0.0001 |
| 2 | BI961258\|MONO1_8_B03.b1_A005 Monocytes (MONO1) | ferritin, heavy polypeptide 1 | negative regulation of cell proliferation, intracellular sequestering of iron ions | 22 | -1.350 | 0.0000015 | 0.001 |
| 21 | CD535312\|LeukoN5_2_F11.b1_A027 Unstimulated peripheral blood leukocytes N5 | early growth response 1 | Transcription factor: pro cell proliferation, anti apoptosis, promotes collagen expression | 17 | -1.805 | 0.0001 | 0.006 |
| 38 | BI960801\|MONO1_1_A06.b1_A005 Monocytes (MONO1) | BTG family, member 2 | Anti cell proliferation | 16 | 0.397 | 0.0003 | 0.010 |
| 47 | CD465748\|LeukoN1_7_B02.b1_A023 Unstimulated peripheral blood leukocytes N1 | inhibitor of DNA binding 2, dominant negative helix-loop-helix protein | Pro cell proliferation, anti cell differentiation | 4 | -0.630 | 0.0006 | 0.016 |
| 51 | BM781091\|MLN1_4_F06.g1_A005 Mesenteric lymph node (MLN1) | cyclin G1 | Anti cell proliferation | 23 | 0.698 | 0.0006 | 0.016 |

| Cell cycle, cell proliferation, differentiation, apoptosis cont. | | | | | | | |
|---|---|---|---|---|---|---|---|
| **Rank #** | **Equine GenBank Accession Number and Description** | **Inferred Homology (Gene Name)** | **Biological Function** | **Present calls** | **$log_2$ fold change** | **p-value** | **q-value** |
| 55 | BM734744\|MONO1_12_D04.g1_A005 Monocytes (MONO1) | ferritin, heavy polypeptide 1 | negative regulation of cell proliferation, intracellular sequestering of iron ions | 2 | 0.278 | 0.0008 | 0.018 |
| 67 | CD467521\|LeukoS1_5_G10.b1_A023 Stimulated peripheral blood leukocytes S1 | heat shock 70kDa protein 1A | Molecular chaperone, protein stabilizing, anti apoptosis | 23 | 0.672 | 0.0010 | 0.020 |
| 73 | CD528299\|LeukoN3_1_G08.b2_A025 Unstimulated peripheral blood leukocytes N3 | HtrA serine peptidase 2 | Pro apoptosis | 23 | 0.361 | 0.0012 | 0.022 |
| 75 | BM735326\|MONO1_18_D01.g1_A005 Monocytes (MONO1) | lectin, galactoside-binding, soluble, 1 (galectin 1) | Anti cell proliferation, Pro apoptosis | 4 | -0.676 | 0.0013 | 0.023 |
| 97 | CD467520\|LeukoS1_5_F01.b1_A023 Stimulated peripheral blood leukocytes S1 | cyclin D2 | Pro cell proliferation | 19 | -1.247 | 0.0024 | 0.032 |
| 105 | CD536136\|LeukoN6_3_D08.b1_A028 Unstimulated peripheral blood leukocytes N6 | inhibitor of DNA binding 2, dominant negative helix-loop-helix protein | Pro cell proliferation, anti cell differentiation | 23 | -0.986 | 0.0030 | 0.037 |
| 108 | CD536618\|LeukoN6_5_G06.b1_A028 Unstimulated peripheral blood leukocytes N6 | cyclin D2 | Pro cell proliferation | 12 | -0.617 | 0.0031 | 0.037 |
| 129 | CD528325\|LeukoN3_1_H09.b2_A025 Unstimulated peripheral blood leukocytes N3 | dual specificity phosphatase 1 | Anti cell proliferation, stress response: anti apoptosis | 23 | -0.475 | 0.0043 | 0.043 |

| Cell cycle, cell proliferation, differentiation, apoptosis cont. | | | | | | | |
|---|---|---|---|---|---|---|---|
| **Rank #** | **Equine GenBank Accession Number and Description** | **Inferred Homology (Gene Name)** | **Biological Function** | **Present calls** | **$log_2$ fold change** | **p-value** | **q-value** |
| 131 | CD469338\|LeukoS2_3_H09.b1_A024 Stimulated peripheral blood leukocytes S2 | alpha tubulin | Intracellular structural protein, necessary for mitosis | 23 | -0.532 | 0.0044 | 0.044 |
| 137 | BM781280\|MLN1_6_C06.g1_A005 Mesenteric lymph node (MLN1) | cullin 1 | Anti cell proliferation, pro apoptosis | 23 | 0.366 | 0.0046 | 0.044 |
| 139 | BM780568\|APL1_4_E08.g1_A005 Liver (APL1) | protein phosphatase 2, catalytic subunit, beta isoform | Anti cell proliferation | 23 | 0.458 | 0.0049 | 0.046 |
| 152 | BM781438\|MLN1_8_B01.g1_A005 Mesenteric lymph node (MLN1) | cysteine rich transmembrane BMP regulator 1 (chordin-like) | Regulation of cell differentiation (cell type dependent) | 23 | -0.614 | 0.0058 | 0.050 |
| **Inflammatory mediator synthesis** | | | | | | | |
| **Rank #** | **Equine GenBank Accession Number and Description** | **Inferred Homology (Gene Name)** | **Biological Function** | **Present calls** | **$log_2$ fold change** | **p-value** | **q-value** |
| 71 | CD469696\|LeukoS2_8_G07.b1_A024 Stimulated peripheral blood leukocytes S2 | annexin A5 | Calcium ion channel, inhibitor of phospholipaseA, anticoagulant | 23 | 0.703 | 0.0012 | 0.022 |
| 96 | AF027335 REGION:\|Equus caballus prostaglandin G/H synthase-2 gene | N/A | Pro inflammation (prostaglandin synthesis) | 16 | -1.419 | 0.0023 | 0.031 |
| 110 | AF027335 REGION:\|Equus caballus prostaglandin G/H synthase-2 gene | N/A | Pro inflammation (prostaglandin synthesis) | 14 | -1.297 | 0.0033 | 0.038 |

| Inflammatory mediator synthesis cont. | | | | | | | |
|---|---|---|---|---|---|---|---|
| **Rank #** | **Equine GenBank Accession Number and Description** | **Inferred Homology (Gene Name)** | **Biological Function** | **Present calls** | **$log_2$ fold change** | **p-value** | **q-value** |
| 126 | BM780769\|APL1_8_B03.g1_A005 Liver (APL1) | microsomal glutathione S-transferase 2 | Pro inflammation (leukotriene synthesis) | 11 | 0.554 | 0.0040 | 0.041 |
| **Growth factors, transcription factors for growth factor expression** | | | | | | | |
| **Rank #** | **Equine GenBank Accession Number and Description** | **Inferred Homology (Gene Name)** | **Biological Function** | **Present calls** | **$log_2$ fold change** | **p-value** | **q-value** |
| 111 | AJ319906\|Equus caballus partial mRNA for fibroblast growth factor 2 (fgf2 gene). | N/A | Angiogenic, mechanical signal transduction | 20 | 1.036 | 0.0034 | 0.038 |
| 125 | BM781396\|MLN1_8_G02.g1_A005 Mesenteric lymph node (MLN1) | leucine rich repeat (in FLII) interacting protein 1 | Transcription repressor, possibly influencing TNF, EGFR, PDGFA transcription | 6 | -0.354 | 0.0039 | 0.041 |
| **Extracellular matrix proteins, their modifiers, extracellular matrix proteases and protease inhibitors, cell-matrix interaction proteins** | | | | | | | |
| **Rank #** | **Equine GenBank Accession Number and Description** | **inferred Homology (Gene Name)** | **Biological Function** | **Present calls** | **$log_2$ fold change** | **p-value** | **q-value** |
| 11 | AF040637\|Equus caballus aggrecan core protein | N/A | Extracellular matrix protein | 23 | 1.732 | 0.0001 | 0.005 |
| 18 | AF541975\| Equus caballus metalloproteinase (ADAMTS-1) | N/A | Extracellular matrix protease | 17 | -1.718 | 0.0001 | 0.006 |
| 21 | CD535312\|LeukoN5_2_F11.b1_A027 Unstimulated peripheral blood leukocytes N5 | early growth response 1 | Transcription factor: pro cell proliferation, anti apoptosis, promotes collagen expression | 17 | -1.805 | 0.0001 | 0.006 |

| Extracellular matrix proteins, their modifiers, extracellular matrix proteases and protease inhibitors, cell-matrix interaction proteins cont. | | | | | | | |
|---|---|---|---|---|---|---|---|
| **Rank #** | **Equine GenBank Accession Number and Description** | **Inferred Homology (Gene Name)** | **Biological Function** | **Present calls** | **$log_2$ fold change** | **p-value** | **q-value** |
| 29 | BM780462\|APL1_3_G02.g1_A005 Liver (APL1) | 3'-phosphoadenosine 5'-phosphosulfate synthase 2 | Sulfation of glycosaminoglycanes | 23 | 1.639 | 0.0002 | 0.008 |
| 31 | BM735254\|MONO1_17_B03.g1_A005 Monocytes (MONO1) | thrombospondin 1 | Cell-matrix interactions, anti angiogenesis | 17 | -2.493 | 0.0002 | 0.010 |
| 32 | AF325902\|Equus caballus cartilage oligomeric matrix protein (COMP) | N/A | Extracellular matrix protein | 23 | 0.863 | 0.0003 | 0.010 |
| 33 | AF041069\|Equus caballus fibronectin | N/A | Extracellular matrix protein | 23 | 1.369 | 0.0003 | 0.010 |
| 40 | BI961566\|MONO1_1_D07.g1_A005 Monocytes (MONO1) | beta-1,3-glucuronyltransferase 3 (glucuronosyltransferase I) | Proteoglycan synthesis | 6 | 0.359 | 0.0003 | 0.011 |
| 41 | BM734972\|MONO1_15_E07.g1_A005 Monocytes (MONO1) | thrombospondin 1 | Cell-matrix interactions, anti angiogenesis | 23 | -2.203 | 0.0004 | 0.012 |
| 63 | AF035934\|Equus caballus biglycan | N/A | Extracellular matrix protein | 23 | 0.649 | 0.0010 | 0.020 |
| 77 | BI961251\|MONO1_8_A07.b1_A005 Monocytes (MONO1) | thrombospondin 1 | Cell-matrix interactions, anti angiogenesis | 11 | -0.907 | 0.0014 | 0.024 |
| 92 | BM781037\|MLN1_3_B05.g1_A005 Mesenteric lymph node (MLN1) | Y box binding protein 1 | Transcription factor possibly modulating collagen I expression | 23 | 0.277 | 0.0021 | 0.030 |

Extracellular matrix proteins, their modifiers, extracellular matrix proteases and protease inhibitors, cell-matrix interaction proteins cont.

| Rank # | Equine GenBank Accession Number and Description | Inferred Homology (Gene Name) | Biological Function | Present calls | $log_2$ fold change | p-value | q-value |
|---|---|---|---|---|---|---|---|
| 101 | CD464887\|LeukoN4_5_A03.b1_A026 Unstimulated peripheral blood leukocytes N4 | CD44 molecule (Indian blood group) | Hyaluronic acid binding receptor, cell-matrix interactions | 7 | -0.473 | 0.0026 | 0.034 |
| 103 | AF034077 REGION:\|Equus caballus alpha-1-antitrypsin (Spi2) gene | N/A | Protease inhibitor (cathepsin G, among others) | 22 | 1.574 | 0.0030 | 0.037 |

**Angiogenesis**

| Rank # | Equine GenBank Accession Number and Description | Inferred Homology (Gene Name) | Biological Function | Present calls | $log_2$ fold change | p-value | q-value |
|---|---|---|---|---|---|---|---|
| 31 | BM735254\|MONO1_17_B03.g1_A005 Monocytes (MONO1) | thrombospondin 1 | Cell-matrix interactions, anti angiogenesis | 17 | -2.493 | 0.0002 | 0.010 |
| 41 | BM734972\|MONO1_15_E07.g1_A005 Monocytes (MONO1) | thrombospondin 1 | Cell-matrix interactions, anti angiogenesis | 23 | -2.203 | 0.0004 | 0.012 |
| 77 | BI961251\|MONO1_8_A07.b1_A005 Monocytes (MONO1) | thrombospondin 1 | Cell-matrix interactions, anti angiogenesis | 11 | -0.907 | 0.0014 | 0.024 |

**Cell protection under stress**

| Rank # | Equine GenBank Accession Number and Description | Inferred Homology (Gene Name) | Biological Function | Present calls | $log_2$ fold change | p-value | q-value |
|---|---|---|---|---|---|---|---|
| 17 | AB043676\|Equus caballus Hsp90beta | N/A | Molecular chaperone, protein stabilizing | 23 | 0.869 | 0.0001 | 0.006 |
| 67 | CD467521\|LeukoS1_5_G10.b1_A023 Stimulated peripheral blood leukocytes S1 | heat shock 70kDa protein 1A | Molecular chaperone, protein stabilizing, anti apoptosis | 23 | 0.672 | 0.0010 | 0.020 |

| Cell protection under stress cont. | | | | | | | |
|---|---|---|---|---|---|---|---|
| **Rank #** | **Equine GenBank Accession Number and Description** | **Inferred Homology (Gene Name)** | **Biological Function** | **Present calls** | **$log_2$ fold change** | **p-value** | **q-value** |
| 129 | CD528325\|LeukoN3_1_H09.b2_A025 Unstimulated peripheral blood leukocytes N3 | dual specificity phosphatase 1 | Anti cell proliferation, stress response: anti apoptosis | 23 | -0.475 | 0.0043 | 0.043 |
| 142 | BM734930\|MONO1_14_B06.g1_A005 Monocytes (MONO1) | superoxide dismutase 2, mitochondrial | Superoxide neutralization, anti apoptosis | 23 | -1.979 | 0.0051 | 0.047 |
| **Immune response proteins** | | | | | | | |
| **Rank #** | **Equine GenBank Accession Number and Description** | **Inferred Homology (Gene Name)** | **Biological Function** | **Present calls** | **$log_2$ fold change** | **p-value** | **q-value** |
| 7 | AF200416\| Equus caballus lipopolysaccharide receptor (CD14) | N/A | Cell surface receptor, modulating immune response | 17 | -1.681 | 0.0000074 | 0.001 |
| 19 | L07565\|Equus caballus (clone pHL5) productively rearranged Ig lambda chain mRNA, V3-J-C1 region | N/A | Immunoglobulin | 5 | 0.435 | 0.0001 | 0.006 |
| 27 | CD466971\|LeukoS1_1_E05.b1_A023 Stimulated peripheral blood leukocytes S1 | toll-like receptor 4 | Immune response to lipopolysaccharides | 1 | -0.357 | 0.0001 | 0.007 |
| 43 | CD465511\|LeukoN1_5_G10.b1_A023 Unstimulated peripheral blood leukocytes N1 | transporter 2, ATP-binding cassette, sub-family B (MDR/TAP) | Antigen processing and presentation | 8 | -0.766 | 0.0004 | 0.012 |
| 107 | BM780777\|APL1_8_A04.g1_A005 Liver (APL1) | beta-defensin 1 | Endogenous antimicrobial peptide | 16 | -2.333 | 0.0030 | 0.037 |
| 132 | BM780552\|APL1_4_F12.g1_A005 Liver (APL1) | Fc fragment of IgG, receptor, transporter, alpha | Membrane receptor recycling IgG and albumin | 2 | 0.330 | 0.0044 | 0.044 |

| **Proteins involved in cell communication** | | | | | | | |
|---|---|---|---|---|---|---|---|
| **Rank #** | **Equine GenBank Accession Number and Description** | **Inferred Homology (Gene Name)** | **Biological Function** | **Present calls** | **$log_2$ fold change** | **p-value** | **q-value** |
| 60 | BI961854\|MONO1_7_E01.g1 _A005 Monocytes (MONO1) | heparan sulfate (glucosamine) 3-O-sulfotransferase 3B1 | Matrix protein synthesis, cell surface receptor synthesis | 1 | 0.860 | 0.0009 | 0.020 |
| 68 | CD472170\|LeukoS6_1_A05.b 1_A028 Stimulated peripheral blood leukocytes S6 | Down syndrome critical region gene 1 | Inhibitor of calcineurin (upregulates IL-2 expression) | 21 | -1.937 | 0.0011 | 0.022 |
| 69 | CD471071\|LeukoS5_4_F07.b 1_A027 Stimulated peripheral blood leukocytes S5 | calmodulin 2 (phosphorylase kinase, delta) | Intracellular signaling, calcium-dependent | 23 | 0.455 | 0.0011 | 0.022 |
| **Proteins involved in the clotting cascade** | | | | | | | |
| **Rank #** | **Equine GenBank Accession Number and Description** | **Inferred Homology (Gene Name)** | **Biological Function** | **Present calls** | **$log_2$ fold change** | **p-value** | **q-value** |
| 14 | BI961094\|MONO1_6_A03.b1 _A005 Monocytes (MONO1) | vitamin K epoxide reductase complex, subunit 1 | Activator of Vitamin K | 21 | 0.958 | 0.00005 | 0.005 |
| **Intracellular structural proteins, proteins involved in cell movement** | | | | | | | |
| **Rank #** | **Equine GenBank Accession Number and Description** | **Inferred Homology (Gene Name)** | **Biological Function** | **Present calls** | **$log_2$ fold change** | **p-value** | **q-value** |
| 4 | CD464606\|LeukoN4_1_H11. b1_A026 Unstimulated peripheral blood leukocytes N4 | spectrin, beta, non-erythrocytic 1 | Intracellular structural protein | 22 | -1.325 | 0.00000 31 | 0.001 |
| 15 | BM781082\|MLN1_4_G08.g1_ A005 Mesenteric lymph node (MLN1) | myosin VI | Intracellular structural protein, intracellular movement | 23 | 0.954 | 0.0001 | 0.005 |
| 42 | CD465825\|LeukoN1_8_A08. b1_A023 Unstimulated peripheral blood leukocytes N1 | Enah-vasodilator stimulated phosphoprotein-like | Organization of intracellular structural proteins | 7 | 0.593 | 0.0004 | 0.012 |

| Intracellular structural proteins, proteins involved in cell movement cont. | | | | | | | |
|---|---|---|---|---|---|---|---|
| **Rank #** | **Equine GenBank Accession Number and Description** | **Inferred Homology (Gene Name)** | **Biological Function** | **Present calls** | **$log_2$ fold change** | **p-value** | **q-value** |
| 53 | CD465127\|LeukoN1_2_B06.b1_A023 Unstimulated peripheral blood leukocytes N1 | actin related protein 2/3 complex, subunit 5 | Organization of intracellular structural proteins | 23 | -0.671 | 0.0007 | 0.017 |
| 82 | CD466282\|LeukoN2_3_F06.b1_A024 Unstimulated peripheral blood leukocytes N2 | cofilin 2 (muscle) | Modification of intracellular structural proteins | 21 | 0.436 | 0.0016 | 0.025 |
| 131 | CD469338\|LeukoS2_3_H09.b1_A024 Stimulated peripheral blood leukocytes S2 | alpha tubulin | Intracellular structural protein, necessary for mitosis | 23 | -0.532 | 0.0044 | 0.044 |
| 133 | CD470381\|LeukoS4_4_E11.b1_A026 Stimulated peripheral blood leukocytes S4 | capping protein (actin filament) muscle Z-line, alpha 2 | Organization of intracellular structural proteins | 23 | -0.272 | 0.0045 | 0.044 |
| 153 | BM780678\|APL1_6_B11.g1_A005 Liver (APL1) | enabled homolog (Drosophila) | Intracellular structural protein, intracellular movement | 23 | 0.854 | 0.0057 | 0.050 |
| **Intracellular iron storage proteins** | | | | | | | |
| **Rank #** | **Equine GenBank Accession Number and Description** | **Inferred Homology (Gene Name)** | **Biological Function** | **Present calls** | **$log_2$ fold change** | **p-value** | **q-value** |
| 2 | BI961258\|MONO1_8_B03.b1_A005 Monocytes (MONO1) | ferritin, heavy polypeptide 1 | negative regulation of cell proliferation, intracellular sequestering of iron ions | 22 | -1.350 | 0.0000015 | 0.001 |
| 138 | D14523\|Equus caballus mRNA for ferritin light chain | N/A | intracellular sequestering of iron ions | 23 | -0.503 | 0.0048 | 0.046 |

| Proteins involved in intracellular signaling | | | | | | | |
|---|---|---|---|---|---|---|---|
| **Rank #** | **Equine GenBank Accession Number and Description** | **Inferred Homology (Gene Name)** | **Biological Function** | **Present calls** | **$log_2$ fold change** | **p-value** | **q-value** |
| 12 | CD464354\|LeukoN4_3_C06.b1_A026 Unstimulated peripheral blood leukocytes N4 | T-cell lymphoma invasion and metastasis 2 | Intracellular signal transduction | 21 | 0.492 | 0.00005 | 0.005 |
| 26 | CD467260\|LeukoS1_3_A12.b1_A023 Stimulated peripheral blood leukocytes S1 | guanine nucleotide binding protein (G protein), beta polypeptide 1 | Intracellular signal transduction | 23 | 0.322 | 0.0001 | 0.007 |
| 30 | CD536257\|LeukoN6_4_F04.b1_A028 Unstimulated peripheral blood leukocytes N6 | signal-induced proliferation-associated 1 like 1 | GTPase activator | 4 | -0.469 | 0.0002 | 0.008 |
| 34 | CD467406\|LeukoS1_4_F10.b1_A023 Stimulated peripheral blood leukocytes S1 | T-cell lymphoma invasion and metastasis 2 | Intracellular signal transduction | 23 | 0.610 | 0.0003 | 0.010 |
| 59 | BM735460\|MONO1_19_G12.g1_A005 Monocytes (MONO1) | c-src tyrosine kinase | Intracellular signal transduction | 23 | -0.510 | 0.0009 | 0.020 |
| 114 | BM735258\|MONO1_17_B07.g1_A005 Monocytes (MONO1) | hematological and neurological expressed sequence 1 | GTPase activator | 3 | 0.250 | 0.0033 | 0.038 |
| 130 | CD468559\|LeukoS3_4_D11.b1_A025 Stimulated peripheral blood leukocytes S3 | myotubularin related protein 6 | Phosphatase activity | 19 | 0.381 | 0.0043 | 0.043 |

| **Ion channels** | | | | | | | |
|---|---|---|---|---|---|---|---|
| **Rank #** | **Equine GenBank Accession Number and Description** | **Inferred Homology (Gene Name)** | **Biological Function** | **Present calls** | **$log_2$ fold change** | **p-value** | **q-value** |
| 48 | BM735319\|MONO1_18_D12.g1_A005 Monocytes (MONO1) | potassium channel tetramerisation domain containing 12 | Potassium channel activity | 11 | -0.895 | 0.0006 | 0.016 |
| 62 | BM781440\|MLN1_8_B03.g1_A005 Mesenteric lymph node (MLN1) | ATPase, H+ transporting, lysosomal 70kDa, V1 subunit A | Proton transport, transmembrane | 22 | 0.504 | 0.0009 | 0.020 |
| 71 | CD469696\|LeukoS2_8_G07.b1_A024 Stimulated peripheral blood leukocytes S2 | annexin A5 | Calcium ion channel, inhibitor of phospholipaseA, anticoagulant | 23 | 0.703 | 0.0012 | 0.022 |
| 106 | CD535176\|LeukoN5_1_B10.b1_A027 Unstimulated peripheral blood leukocytes N5 | ATPase, H+ transporting, lysosomal 16kDa, V0 subunit c | Proton transport, transmembrane | 23 | 0.272 | 0.0030 | 0.037 |
| **Transcription factors involved in skeletal development** | | | | | | | |
| **Rank #** | **Equine GenBank Accession Number and Description** | **Inferred Homology (Gene Name)** | **Biological Function** | **Present calls** | **$log_2$ fold change** | **p-value** | **q-value** |
| 124 | BI961347\|MONO1_4_D02.b1_A005 Monocytes (MONO1) | v-ets erythroblastosis virus E26 oncogene homolog 2 | Transcription factor, influencing skeletal development | 18 | -0.570 | 0.0038 | 0.040 |
| **Proteins involved in mRNA splicing** | | | | | | | |
| **Rank #** | **Equine GenBank Accession Number and Description** | **Inferred Homology (Gene Name)** | **Biological Function** | **Present calls** | **$log_2$ fold change** | **p-value** | **q-value** |
| 128 | BM735127\|MONO1_16_E08.g1_A005 Monocytes (MONO1) | splicing factor, arginine/serine-rich 1 | mRNA splice site selection, spliceosome assembly | 4 | 0.347 | 0.0041 | 0.042 |

| Proteins involved in mRNA splicing cont. | | | | | | | |
|---|---|---|---|---|---|---|---|
| **Rank #** | **Equine GenBank Accession Number and Description** | **Inferred Homology (Gene Name)** | **Biological Function** | **Present calls** | **$log_2$ fold change** | **p-value** | **q-value** |
| 151 | CD535760\|LeukoN5_8_A03.b1_A027 Unstimulated peripheral blood leukocytes N5 | heterogeneous nuclear ribonucleoprotein A2/B1 | mRNA splicing, via spliceosome | 23 | 0.448 | 0.0056 | 0.050 |
| **Transcription factors of unknown function** | | | | | | | |
| **Rank #** | **Equine GenBank Accession Number and Description** | **Inferred Homology (Gene Name)** | **Biological Function** | **Present calls** | **$log_2$ fold change** | **p-value** | **q-value** |
| 66 | BM781210\|MLN1_5_G12.g1_A005 Mesenteric lymph node (MLN1) | nuclear receptor subfamily 1, group D, member 2 | Transcription factor with unknown function | 23 | 0.711 | 0.0010 | 0.020 |
| 98 | BM780979\|MLN1_2_D01.g1_A005 Mesenteric lymph node (MLN1) | SERTA domain containing 2 | Transcription factor with unknown function | 23 | 0.847 | 0.0024 | 0.032 |
| 134 | BM781181\|MLN1_5_B12.g1_A005 Mesenteric lymph node (MLN1) | PHD finger protein 20-like 1 | Transcription factor with unknown function | 14 | 0.257 | 0.0045 | 0.044 |
| 148 | CD468682\|LeukoS3_5_H08.b1_A025 Stimulated peripheral blood leukocytes S3 | forkhead box P1 | Transcription factor with unknown function | 20 | -0.503 | 0.0056 | 0.049 |
| **Ribosomal proteins and other proteins necessary for translation** | | | | | | | |
| **Rank #** | **Equine GenBank Accession Number and Description** | **Inferred Homology (Gene Name)** | **Biological Function** | **Present calls** | **$log_2$ fold change** | **p-value** | **q-value** |
| 50 | BI961165\|MONO1_6_H03.b1_A005 Monocytes (MONO1) | ribosomal protein, large, P1 | Protein synthesis, translation | 23 | 0.558 | 0.0006 | 0.016 |

| Ribosomal proteins and other proteins necessary for translation cont. | | | | | | | |
|---|---|---|---|---|---|---|---|
| **Rank #** | **Equine GenBank Accession Number and Description** | **Inferred Homology (Gene Name)** | **Biological Function** | **Present calls** | **$log_2$ fold change** | **p-value** | **q-value** |
| 64 | CD536649\|LeukoN6_5_G09.b1_A028 Unstimulated peripheral blood leukocytes N6 | glycyl-tRNA synthetase | Amino acid charging of tRNAs | 16 | 0.464 | 0.0010 | 0.020 |
| 79 | BI961317\|MONO1_8_H06.b1_A005 Monocytes (MONO1) | ribosomal protein, large, P0 | Protein synthesis, translation | 23 | 0.428 | 0.0015 | 0.025 |
| 81 | CD469699\|LeukoS2_8_E07.b1_A024 Stimulated peripheral blood leukocytes S2 | eukaryotic translation elongation factor 1 gamma | Aminoacyl tRNA delivery to ribosomes | 23 | 0.368 | 0.0016 | 0.025 |
| 87 | CD466099\|LeukoN2_2_G10.b1_A024 Unstimulated peripheral blood leukocytes N2 | ribosomal protein L4 | Protein synthesis, translation | 23 | 0.342 | 0.0017 | 0.026 |
| 94 | CD528909\|LeukoN3_8_E07.b1_A025 Unstimulated peripheral blood leukocytes N3 | ribosomal protein, large, P0 | Protein synthesis, translation | 23 | 0.380 | 0.0022 | 0.031 |
| 104 | CD536386\|LeukoN6_7_B08.b1_A028 Unstimulated peripheral blood leukocytes N6 | eukaryotic translation elongation factor 1 delta (guanine nucleotide exchange protein) | Aminoacyl tRNA delivery to ribosomes | 23 | 0.372 | 0.0030 | 0.037 |
| 150 | BM735084\|MONO1_23_B06.g1_A005 Monocytes (MONO1) | ribosomal protein L13 | Protein synthesis, translation | 23 | 0.271 | 0.0058 | 0.050 |

| **Amino acid synthesis and transport proteins** | | | | | | | |
|---|---|---|---|---|---|---|---|
| **Rank #** | **Equine GenBank Accession Number and Description** | **Inferred Homology (Gene Name)** | **Biological Function** | **Present calls** | **$log_2$ fold change** | **p-value** | **q-value** |
| 44 | BM780648\|APL1_6_E08.g1_A005 Liver (APL1) | argininosuccinate synthetase 1 | Arginine synthesis, decreasing NO toxicity | 14 | -1.098 | 0.0004 | 0.012 |
| 112 | CD535752\|LeukoN5_8_A09.b1_A027 Unstimulated peripheral blood leukocytes N5 | solute carrier family 7 (cationic amino acid transporter, y+ system), member 7 | Amino acid transporter (transmembrane) | 17 | -0.938 | 0.0033 | 0.038 |
| 140 | BM780336\|APL1_1_A07.g1_A005 Liver (APL1) | glutamate-ammonia ligase (glutamine synthetase) | Glutamine synthesis | 23 | -1.200 | 0.0049 | 0.046 |
| **Intracellular protein transport** | | | | | | | |
| **Rank #** | **Equine GenBank Accession Number and Description** | **Inferred Homology (Gene Name)** | **Biological Function** | **Present calls** | **$log_2$ fold change** | **p-value** | **q-value** |
| 65 | BM734690\|MONO1_11_H03.g1_A005 Monocytes (MONO1) | ATG9 autophagy related 9 homolog A | Protein transport | 3 | 0.174 | 0.0010 | 0.020 |
| 91 | BM781193\|MLN1_5_B01.g1_A005 Mesenteric lymph node (MLN1) | vesicle docking protein p115 | Intracellular protein transport, vesicular transport from ER to Golgi | 22 | 0.415 | 0.0021 | 0.030 |
| 119 | BI961352\|MONO1_4_D07.b1_A005 Monocytes (MONO1) | SEC22 vesicle trafficking protein homolog B | Intracellular protein transport, vesicular transport from ER to Golgi | 23 | 0.420 | 0.0035 | 0.039 |

| **Protein catabolism** | | | | | | | |
|---|---|---|---|---|---|---|---|
| **Rank #** | **Equine GenBank Accession Number and Description** | **Inferred Homology (Gene Name)** | **Biological Function** | **Present calls** | **$log_2$ fold change** | **p-value** | **q-value** |
| 149 | CD465752\|LeukoN1_7_E09.b1_A023 Unstimulated peripheral blood leukocytes N1 | ubiquitin-conjugating enzyme E2G 1 | Protein degradation via the ubiquitin cycle | 3 | 0.312 | 0.0058 | 0.050 |
| **Intracellular proteases and inhibitors** | | | | | | | |
| **Rank #** | **Equine GenBank Accession Number and Description** | **Inferred Homology (Gene Name)** | **Biological Function** | **Present calls** | **$log_2$ fold change** | **p-value** | **q-value** |
| 16 | BM780791\|APL1_9_D08.g1_A005 Liver (APL1) | cystatin B (stefin B) | Protease inhibitor, intracellular | 21 | -1.211 | 0.0001 | 0.005 |
| **Lipid and steroid metabolism** | | | | | | | |
| **Rank #** | **Equine GenBank Accession Number and Description** | **Inferred Homology (Gene Name)** | **Biological Function** | **Present calls** | **$log_2$ fold change** | **p-value** | **q-value** |
| 9 | BM780280\|APL1_1_F11.g1_A005 Liver (APL1) | apolipoprotein A-I | Lipid transport (in plasma), cholesterol esterification, prostacyclin stabilization | 13 | 2.716 | 0.0000232 | 0.003 |
| 25 | CD535462\|LeukoN5_4_E08.b1_A027 Unstimulated peripheral blood leukocytes N5 | degenerative spermatocyte homolog 1, lipid desaturase | Fatty acid desaturation | 20 | 0.879 | 0.0001 | 0.007 |
| 143 | CD466976\|LeukoS1_1_A11.b1_A023 Stimulated peripheral blood leukocytes S1 | farnesyl diphosphate synthase | Necessary for cholesterol/steroid synthesis | 15 | -0.281 | 0.0052 | 0.047 |

| Carbohydrate metabolism | | | | | | | |
|---|---|---|---|---|---|---|---|
| **Rank #** | **Equine GenBank Accession Number and Description** | **Inferred Homology (Gene Name)** | **Biological Function** | **Present calls** | **$log_2$ fold change** | **p-value** | **q-value** |
| 37 | BI961111\|MONO1_6_B10.b1_A005 Monocytes (MONO1) | aldo-keto reductase family 1, member B1 (aldose reductase) | Carbohydrate metabolism, protection against toxic aldehydes from lipid peroxidation | 23 | 0.900 | 0.0003 | 0.010 |
| 49 | CD469929\|LeukoS4_2_H06.b1_A026 Stimulated peripheral blood leukocytes S4 | enolase 1, (alpha) | Glycolysis | 23 | 0.361 | 0.0006 | 0.016 |
| **Oxidative phosphorylation** | | | | | | | |
| **Rank #** | **Equine GenBank Accession Number and Description** | **Inferred Homology (Gene Name)** | **Biological Function** | **Present calls** | **$log_2$ fold change** | **p-value** | **q-value** |
| 136 | CD468800\|LeukoS3_7_A05.b1_A025 Stimulated peripheral blood leukocytes S3 | phosphatidylglycerophosphate synthase 1 | Phospholipid synthesis (cardiolipin, supports oxidative phosphorylation) | 16 | 0.186 | 0.0045 | 0.044 |
| 142 | BM734930\|MONO1_14_B06.g1_A005 Monocytes (MONO1) | superoxide dismutase 2, mitochondrial | Superoxide neutralization, anti apoptosis | 23 | -1.979 | 0.0051 | 0.047 |

Table 19: Differentially expressed genes between control (reference group) and osteoarthritic cartilage. Genes are ordered by functional categories. Positive $log_2$ fold change values mean that the gene was downregulated in osteoarthritic cartilage compared to control cartilage. Negative $log_2$ fold change values mean that the gene was upregulated in osteoarthritic cartilage compared to control cartilage. When differences were dependent on cartilage layer, it is indicated so. In that case, positive $log_2$ fold change values mean that the gene was downregulated in osteoarthritic cartilage compared to control cartilage, and that this was more pronounced n the radial than the tangential cartilage layer.
Some genes were represented by several probe sets on the array, thus, their (inferred) gene name may occur more than once in the same part of the table. Some genes have more than 1 function, thus, their (inferred) gene name may occur in several parts of the table. Genes were ranked according to their raw p-values and their fold change (Rank #). Genes without homologue sequences with known gene names or known gene function were omitted from the table.

| **Cell cycle, cell proliferation, differentiation, apoptosis** | | | | | | | |
|---|---|---|---|---|---|---|---|
| Genes differentially expressed between osteoarthritic and control cartilage: | | | | | | | |
| **Rank #** | **Description** | **Inferred Homology (Gene Name)** | **Biological Function** | **Present calls** | **$log_2$ fold change** | **p-value** | **q-value** |
| 157 | CD467520\|LeukoS1_5_F01.b1_ A023 Stimulated peripheral blood leukocytes S1 | cyclin D2 | Pro cell proliferation | 19 | -0.763 | 0.0014 | 0.279 |
| 170 | CD528325\|LeukoN3_1_H09.b2_ A025 Unstimulated peripheral blood leukocytes N3 | dual specificity phosphatase 1 | Anti cell proliferation, response to oxidative stress | 23 | -0.692 | 0.009 | 0.332 |
| Genes differentially expressed between osteoarthritic and control cartilage, dependent on location within the cartilage of the sample (tangential and radial cartilage layer): | | | | | | | |
| **Rank #** | **Description** | **Inferred Homology (Gene Name)** | **Biological Function** | **Present calls** | **$log_2$ fold change** | **p-value** | **q-value** |
| 164 | CD471772\|LeukoS6_2_C01.b1_ A028 Stimulated peripheral blood leukocytes S6 | antizyme inhibitor 1 | Pro cell proliferation, anti apoptosis | 17 | 0.805 | 0.0043 | 0.424 |
| 165 | BM781203\|MLN1_5_H09.g1_A0 05 Mesenteric lymph node (MLN1) | heat shock 70kDa protein 5 (glucose-regulated) | Anti apoptosis, protein folding and assembly | 23 | 0.798 | 0.006 | 0.424 |

| **Extracellular matrix proteins, their modifiers, extracellular matrix proteases and protease inhibitors, cell-matrix interaction proteins** | | | | | | | |
|---|---|---|---|---|---|---|---|
| Genes differentially expressed between osteoarthritic and control cartilage: | | | | | | | |
| **Rank #** | **Description** | **Inferred Homology (Gene Name)** | **Biological Function** | **Present calls** | **$log_2$ fold change** | **p-value** | **q-value** |
| 159 | AF034077 \|Equus caballus alpha-1-antitrypsin (Spi2) gene | N/A | Protease inhibitor (cathepsin G, among others) | 22 | -1.602 | 0.0027 | 0.279 |
| **Cell protection under stress** | | | | | | | |
| Genes differentially expressed between osteoarthritic and control cartilage: | | | | | | | |
| **Rank #** | **Description** | **Inferred Homology (Gene Name)** | **Biological Function** | **Present calls** | **$log_2$ fold change** | **p-value** | **q-value** |
| 170 | CD528325\|LeukoN3_1_H09.b2_A025 Unstimulated peripheral blood leukocytes N3 | dual specificity phosphatase 1 | Anti cell proliferation, response to oxidative stress | 23 | -0.692 | 0.009 | 0.332 |
| **Immune response proteins** | | | | | | | |
| Genes differentially expressed between osteoarthritic and control cartilage: | | | | | | | |
| **Rank #** | **Description** | **Inferred Homology (Gene Name)** | **Biological Function** | **Present calls** | **$log_2$ fold change** | **p-value** | **q-value** |
| 156 | CD468301\|LeukoS3_2_D09.b1_A025 Stimulated peripheral blood leukocytes S3 | nuclear factor of kappa light polypeptide gene enhancer in B-cells inhibitor, alpha | Transcriptional regulation of immune response | 23 | 0.709 | 0.0004 | 0.225 |
| **Proteins involved in membrane transport** | | | | | | | |
| Genes differentially expressed between osteoarthritic and control cartilage: | | | | | | | |
| **Rank #** | **Description** | **Inferred Homology (Gene Name)** | **Biological Function** | **Present calls** | **$log_2$ fold change** | **p-value** | **q-value** |
| 160 | BM780973\|MLN1_2_E09.g1_A005 Mesenteric lymph node (MLN1) | transmembrane 9 superfamily member 3 | Protein transport, transmembrane | 12 | -0.576 | 0.003 | 0.279 |

| **Carbohydrate metabolism** | | | | | | | |
|---|---|---|---|---|---|---|---|
| Genes differentially expressed between osteoarthritic and control cartilage, dependent on location within the cartilage of the sample (tangential and radial cartilage layer): | | | | | | | |
| **Rank #** | **Description** | **Inferred Homology (Gene Name)** | **Biological Function** | **Present calls** | **$log_2$ fold change** | **p-value** | **q-value** |
| 168 | BM735100\|MONO1_16_H11.g1 _A005 Monocytes (MONO1) | UDP-glucose pyrophosphorylase 2 | Glucose metabolism | 23 | 0.616 | 0.009 | 0.424 |
| 166 | BI960802\|MONO1_1_A08.b1_A 005 Monocytes (MONO1) | pyruvate kinase, muscle | Glucose metabolism | 11 | 1.000 | 0.007 | 0.424 |

## 6 References

Adams ME, Huang DQ, Yao LY, Sandell LJ (1992): *Extraction and isolation of mRNA from adult cartilage.* Anal Biochem 202:89-95.

Aigner T, Vornehm SI, Zeiler G, Dudhia J, von der Mark K, Bayliss MT (1997): *Suppression of cartilage matrix gene expression in upper zone chondrocytes of osteoarthritic cartilage.* Arthritis Rheum 40:562-569.

Aigner T, Zien A, Gehrsitz A, Gebhard PM, McKenna L (2001): : *Anabolic and catabolic gene expression pattern analysis in normal versus osteoarthritic cartilage using complementary dna–array technology.* Arthritis Rheumatism 44:2777-2789.

Aigner T, Hemmel M, Neureiter D, Gebhard PM, Zeiler G, Kirchner T, McKenna L (2001b): *Apoptotic cell death is not a widespread phenomenon in normal aging and osteoarthritic human articular knee cartilage.* Arthritis Rheumatism 44:1304-1312.

Aigner T, McKenna L (2002): *Molecular pathology and pathobiology of osteoarthritic cartilage.* Cell Mol Life Sci 59:5-18.

Aigner T, Dudhia J (2003): *Genomics of osteoarthritis.* Curr Opin Rheumatol 15:634-640.

Aigner T, Zien A, Hanisch D, Zimmer R (2003): *Gene expression in chondrocytes assessed with use of microarrays.* J Bone Joint Surg 85-A, Suppl 2:117-123.

Aigner T, Bartnik E, Sohler F, Zimmer R (2004): *Functional genomics of osteoarthritis.* Clin Orthop rel Res 427S:S138-S143.

Altschul SF, Madden TL, Schäffer AA, Zhang J, Zhang Z, Miller W, Lipman DJ (1997): *Gapped BLAST and PSI-BLAST: a new generation of protein database search programs.* Nucleic Acids Res 25:3389-3402.

Apweiler R, Bairoch A, Wu CH, Barker WC, Boeckmann B, Ferro S, Gasteiger E, Huang H, Lopez R, Magrane M, Martin MJ, Natale DA, O'Donovan C, Redaschi N, Yeh LS (2004): *UniProt: the Universal Protein Knowledgebase.* Nucleic Acids Res. 32:D115-D119.

Attur MG, Dave MN, Tsunoyama K, Akamatsu M, Kobori M, Miki J, Abramson SB, Katoh M, Amin AR (2002a): *"A system biology" approach to bioinformatics and functional genomics in complex human diseases: arthritis.* Curr Issues Mol Biol 4:129-146.

Attur MG, Dave M, Akamatsu M, Katoh M, Amin AR (2002b): *Osteoarthritis or osteoarthrosis: the definition of inflammation becomes a semantic issue in the genomic era of molecular medicine.* Osteoarthritis Cartilage 10:1-4.

Baugh LR, Hill AA, Brown EL, Hunter CP (2001): *Quantitative analysis of mRNA amplification by in vitro transcription.* Nucleic Acids Res 29:E29.

Benedek TG (2006): *A history of the understanding of cartilage.* Osteoarthritis Cartilage 14:203-209.

Benoyahu D, Akavia UD, Socher R, Shur I (2005): *Gene expression in skeletal tissues: application of laser capture microdissection.* J Microsc 220:1-8.

Bruyere O, Collette J, Kothari M, Zaim S, White D, Genant H, Peterfy C, Burlet N, Ethgen D, Montague T, Dabrowski C, Reginster JY (2006): *Osteoarthritis, magnetic resonance imaging, and biochemical markers: a one year prospective study.* Ann Rheum Dis 65:1050-1054.

Buckwalter JA, Saltzman C, Brown T (2004): *The impact of osteoarthritis.* Clin Orthop Rel Res 427S:S6-S15.

Caterson B, Flannery CR, Hughes CE, Little CB (2000): *Mechanisms involved in cartilage proteoglycan catabolism.* Matrix Biol 19:333-344.

Chomczinski P, Sacchi N (1987): *Single-step method of RNA isolation by acid guanidinium thiocyanate-phenol-chloroform extraction.* Anal Biochem 162:156-159.

Chow G, Nietfeld J, Knudson CB, Knudson W (1998): *Antisense inhibition of chondrocyte CD44 expression results in cartilage chondrolysis.* Arthritis Rheum 41:1411-1419.

Collins D, McElligott T (1960): *Sulphate ($^{35}SO_4$) uptake by chondrocytes in relation to histological changes in osteoarthritic human articular cartilage.* Ann Rheum Dis 19:318-330.

Dingle JT, Page Thomas DP, Hazleman B (1987): *The role of cytokines in arthritic diseases: in vitro and in vivo measurements of cartilage degradation.* Int J Tissue React 9:349-354.

Dodge GR, Poole AR (1989): *Immunohistochemical detection and immunochemical analysis of type II collagen degradation in human normal, rheumatoid, and osteoarthritic articular cartilage and in explants of bovine articular cartilage cultured with interleukin 1.* J Clin Invest 83:647-661.

Eberwine J, Yeh H, Miyashiro K, Cao Y, Nair S, Finnell R, Zettel M, Coleman P (1992): *Analysis of gene expression in single live neurons.* Proc Natl Acad Sci U S A 89:3010-3014.

Ehrlich MG, Armstrong L, Treadwell BB, Mankin HJ (1986): *Degradative enzyme systems in cartilage.* Clin Orthop 213:62-68.

Emmert-Buck MR, Bonner RF, Smith PD, Chuaqui RF, Zhuang Z, Goldstein SR, Weiss RA, Liotta LA (1996): *Laser Capture Microdissection.* Science 274:998-1001.

Eurell JA (2004): *Joints.* In: Eurell JA Veterinary Histology pp.74-75.

Eyre DR, McDevitt CA, Billingham MEJ, Muir H (1980): *Biosynthesis of collagen and other matrix proteins by articular cartilage in experimental osteoarthrosis.* Biochem J 188:823-837.

Finger F, Schörle C, Zien A, Gebhard P, Goldring MB, Aigner T (2003): *Molecular phenotyping of human chondrocytes cell lines T/C-28a2, T/C-28a4, and C-28/I2.* Arthritis Rheum 48:3395-3403.

Firestein GS, Pisetsky DS (2002): *DNA microarrays: Boundless technology or bound by technology? Guidelines for studies using microarray technology.* Arthritis Rheumatism 46:859-861.

Firth EC, Wensing T, Seuren F (1987): *An induced synovitis disease model in ponies.* Cornell Vet 77:107-118.

Foland JW, McIlwraith CW, Trotter GW, Powers BE, Lamar CH (1994): *Effect of betamethasone and exercise on equine carpal joints with osteochondral fragments.* Vet Surg 23:369-376.

Frisbie DD, Kawcak CE, Trotter GW, Powers BE, Walton RM, McIlwraith CW (1997): *Effects of triamcinolone acetonide on an in vivo equine osteochondral fragment exercise model.* Equine Vet J. 29, 349-59

Frisbie DD, Kawcak CE, Baxter GM, Trotter GW, Powers BE, Lassen ED, McIlwraith CW (1998): *Effects of 6alpha-methylprednisolone acetate on an equine osteochondral fragment exercise model.* Am J Vet Res. 59, 1619-1628

Frisbie DD, Trotter GW, Powers BE, Rodkey WG, Steadman JR, Howard RD, Park RD, McIlwraith CW (1999): *Arthroscopic subchondral bone plate microfracture technique augments healing of large chondral defects in the radial carpal bone and medial femoral condyle of horses.* Vet Surg. 28, 242-255

Frisbie DD, Ghivizzani SC, Robbins PD, Evans CH, McIlwraith CW (2002): *Treatment of experimental equine osteoarthritis by in vivo delivery of the equine interleukin-1 receptor antagonist gene.* Gene Ther. 9, 12-20

Frisbie DD, Oxford JT, Southwood L, Trotter GW, Rodkey WG, Steadman JR, Goodnight JL, McIlwraith CW (2003): *Early events in cartilage repair after subchondral bone microfracture.* Clin Orthop. 407, 215-227

Gebauer M, Saas J, Haag J, Dietz U, Takigawa M, Bartnik E, Aigner T (2005): *Repression of anti-proliferative factor Tob1 in osteoarthritic cartilage.* Arthritis Res Ther 7:R274-284.

Gentleman RC, Carey VJ, Bates DM, Bolstad B, Dettling M, Dudoit S, Ellis B, Gautier L, Ge Y, Gentry J, Hornik K, Hothorn T, Huber W, Iacus S, Irizarry R, Leisch F, Li C, Maechler M, Rossini AJ, Sawitzki G, Smith C, Smyth G, Tierney L, Jean Y. H. Yang JYH, Zhang J (2004): *Bioconductor: open software development for computational biology and bioinformatics.* Genome Biol 5:R80.

Ginsberg SD (2005): *RNA amplification strategies for small sample populations.* Methods 37:229-237.

Goldring MB (2006): *Update on the biology of the chondrocyte and new approaches to treating cartilage diseases.* Best Pract Res Clin Rheumatol 20:1003-1025.

Goldring MB, Berenbaum F (2004): *The regulation of chondrocyte function by proinflammatory mediators: prostaglandins and nitric oxide.* Clin Orthop Relat Res 427 (Suppl):S37-46.

Goodrich LR, Nixon AJ (2006). *Medical treatment of osteoarthritis in the horse - a review.* Vet J 171:51-69.

Grant EP, Pickard MD, Briskin MJ, Guiterrez-Ramos J-C (2002): *Gene expression profiles. Creating new perspectives in arthritis research.* Arthritis Rheumatism 46:874-884.

Gu W, Bertone AL (2004): *Generation and performance of an equine-specific large-scale gene expression microarray.* Am J Vet Res 65:1664-1673.

Guilak F, Fermor B, Keefe FJ, Kraus Vb, Olson SA, Pisetsky FJ, Setton LA, Weinberg JB (2004): *The role of biomechanics and inflammation in cartilage injury and repair.* Clin Orthop Rel Res, 423,17-26.

Gustafson SB, Trotter GW, Norrdin RW, Wrigley RH, Lamar C (1992): *Evaluation of intra-articularly administered sodium monoiodoacetate-induced chemical injury to articular cartilage of horses.* Am J Vet Res 53:1193-1202.

Hargrove JL, Schmidt FH (1989): *The role of mRNA and protein stability in gene expression.* FASEB J 3:2360-2370.

Henson FMD, Bowe EA, Davies ME (2005): *Promotion of the intrinsic damage-repair response in articular cartilage by fibroblastic growth factor-2.* Osteoarthritis Cartilage 13:537-544.

Hernandez J, Hawkins DL (2001): *Training failure among yearling horses.* Am J Vet Res 62:1418-1422.

Horton Jr WE, Yagi R, Laverty D, Weiner S (2005): *Overview of studies comparing human normal cartilage with minimal and advanced osteoarthritic cartilage.* Clin Exp Rheumatol 23:103-112.

Imbeaud S, Graudens E, Boulanger V, Barlet X, Zaborski P, Eveno E, Mueller O, Schroeder A, Auffray C (2005): *Towards standardization of RNA quality assessment using user-independent classifiers of microcapillary electrophoresis traces.* Nucleic Acids Res 33:e56.

Irizarry RA, Hobbs B, Collin F, Beazer-Barclay YD, Antonellis KJ, Scherf U, Speed TP (2003): *Exploration, normalization, and summaries of highdensity oligonucleotide array probe level data.* Biostatistics 4:249-264.

Ishiguro N, Kojima T, Poole AR (2002): *Mechanism of cartilage destruction in osteoarthritis.* Nagoya J Med Sci 65:73-84.

Islam S, Kermode T, Sultana D, Moskowitz RW, Mukhtar H, Malemud CJ, Goldberg VM, Haqqi TM (2001): *Expression profile of protein tyrosine kinase genes in human osteoarthritic chondrocytes.* Osteoarthritis Cartilage 9:684-693.

Jacquet R, Hillyer J, Landis WJ (2005): *Analysis of connective tissues by laser capture microdissection and reverse transcriptase-polymerase chain reaction.* Anal Biochem 337:22-34.

Jeffcott LB, Rossdale PD, Freestone J, Frank CJ, Towers-Clark PF (1982): *An assessment of wastage in Thoroughbred racing from conception to 4 years of age.* Equine vet. J. 14:185-198

Kawcak CE, Frisbie DD, Trotter GW, McIlwraith CW, Gillette SM, Powers BE, Walton RM (1997): *Effects of intravenous administration of sodium hyaluronate on carpal joints in exercising horses after arthroscopic surgery and osteochondral fragmentation.* Am J Vet Res. 58, 1132-1140

Kawcak CE, Norrdin RW, Frisbie DD, Trotter GW, Mcilwraith CW (1998): *Effects of osteochondral fragmentation and intra-articular triamcinolone acetonide treatment on subchondral bone in the equine carpus.* Equine Vet J. 30, 66-71

Kerman IA, Buck BJ, Evans SJ, Akil H, Watson SJ (2005): *Combining laser capture microdissection with quantitative real-time PCR: effects of tissue manipulation on RNA quality and gene expression.* J Neurosci Methods 153:71-85.

Kim HA, Cho M-L, Choi HY, Yoon CS, Jhun JY, Oh HJ, Kim H-Y (2006): *The catabolic pathway mediated by toll-like receptors in human osteoarthritic chondrocytes.* Arthritis Rehum 54:2152-2163.

Knorr T, Obermayr F, Bartnik A, Aigner T (2003): *YKL-39 (chitinase 3-like protein 2), but not YKL-40 (chitinase 3-like protein 1), is upregulated in osteoarthritic chondrocytes.* Ann Rheum Dis 62:995-998.

Knudson W, Casey B, Nishida Y, Eger W, Kuettner KE, Knudson CB (2000): *Hyaluronan oligosaccharides perturb cartilage matrix homeostasis and induce chondrogenic chondrolysis.* Arthritis Rheum 43:1165-1174.

Knudson W, Loeser RF (2002): *DC44 and integrin matrix receptors participate in cartilage homeostasis.* Cell Mol Life Sci 59:36-44.

Kurz B, Lemke AK, Fay J, Pufe T, Grodzinsky AJ, Schunke M (2005): *Pathomechanisms of cartilage destruction by mechanical injury.* Ann Anat 187:473-485.

Landis WJ, Jacquet R, Hillyer J, Zhang J (2003): *Analysis of osteopontin in mouse growth plate cartilage by application of laser capture microdissection and rt-PCR.* Connect Tissue Res 44 (Suppl 1), 28-32

Langelier E, Suetterlin R, Aebi U, Buschmann MD (1999): *Zonal dependence of the chondrocyte cytoskeleton and in vitro response to load.* Trans Orthop Res Soc 24:631.

Lawrence RC, Helmick CG, Arnett FC, Deyo RA, Felson DT, Giannini EH, Heyse SP, Hirsch R, Hochberg MC, Hunder GG, Liang MH, Pillemer SR, Steen VD, Wolfe F (1999): *Estimates of the prevalence of arthritis and selected musculoskeletal disorders in the United States.* Arthritis Rheum 41:778–799.

Little CB, Mittaz L, Belluoccio D, Rogerson FM, Campbell IK, Meeker CT, Bateman JF, Pritchard MA, Fosang AJ (2005): *ADAMTS-1-knockout mice do not exhibit abnormalities in aggrecan turnover in vitro or in vivo.* Arthritis Rheum 52:1461-1472.

Loeser RF Jr, Wallin R (1991): *Vitamin K-dependent carboxylation in articular chondrocytes.* Connect Tissue Res 26:135-144.

Loeser RF (2006): *Molecular mechanisms of cartilage destruction: mechanics, inflammatory mediators, and aging collide.* Arthritis Rheum 54:1357-1360.

Maglott D, Ostell J, Pruitt KD, Tatusova T (2005): *Entrez Gene: gene-centered information at NCBI.* Nucleic Acids Res 33(Database Issue):D54–D58.

Malfait A-M, Lui R-Q, Ijiri K, Komiya S, Tortorella MD (2002): *Inhibition of ADAM-TS4 and ADAM-TS5 prevents aggrecan degradation in osteoarthritic cartilage.* J Biol Chem 277:22201-22208.

Mallein-Gerin F, Gouttenoire J (2004): *RNA extraction from cartilage.* Methods Mol Med 100:101-104.

Mankin HJ, Dorfman H, Lipiello L, Zarins A (1971): *Biochemical and metabolic abnormalities in articular cartilage from osteo-arthritic human hips.* J Bone Joint Surg 53A:523-537.

Martel-Pelletier J (1998): *Pathophysiology of osteoarthritis.* Osteoarthritis Cartilage 6:374-376.

Martel-Pelletier J, Mineau F, Fahmi H, Laufer S, Reboul P, Boileau C, Lavigne M, Pelletier JP (2004): *Regulation of the expression of 5-lipoxygenase-activating protein/5-lipoxygenase and the synthesis of leukotriene B(4) in osteoarthritic chondrocytes: role of transforming growth factor beta and eicosanoids.* Arthritis Rheum 50:3925-33.

Martin JA, Buckwalter JA (2006): *Post-traumatic osteoarthritis: the role of stress induced chondrocyte damage.* Biorheology 43:517-521.

Matyas JR, Adams ME, Huang D, Sandell LJ (1995): *Discoordinate gene expression of aggrecan and type II collagen in experimental osteoarthritis.* Arthritis Rheum 38:420-425.

McIlwraith CW, Fessler JF, Blevins WE, Page EH, Rebar AH, Van Sickle DC, Coppoc GL (1979): *Experimentally induced arthritis of the equine carpus: clinical determinations.* Am J Vet Res 40:11-20.

McIlwraith CW, Van Sickle DC (1981): *Experimentally induced arthritis of the equine carpus: histologic and histochemical changes in the articular cartilage.* Am J Vet Res 42:209-217.

McIlwraith CW, Vachon AM (1988): *Review of pathogenesis and treatment of degenerative joint disease.* Equine Vet J Suppl 6:3-11.

McIlwraith CW (1996): *General Pathobiology of the joint and response to injury.* In: McIlwraith CW, Trotter GW (Eds.): Joint disease of the horse pp. 40-70, WB Saunders, Philadelphia

McIlwraith CW (1998): *Diseases of joints, tendons, ligaments, and related structures.* In: Stashak TS (Ed.): Adams' lameness in horses pp. 459-488, Lippincott Williams & Wilkins, Baltimore

McIlwraith CW (2005): *From arthroscopy to gene therapy – 30 years of looking in joints.* Proc Am Assoc Equine Pract 51:65-113.

Mukherjee P, Pasinetti GM (2002): *Altered gene expression during nimesulide-mediated inhibition of apoptotic death in human chondrocytes.* IJCP Supplement 128:20-23.

Nagase H, Kashiwagi M (2003): *Aggrecanases and cartilage matrix degradation.* Arthritis Res Ther 5:94-103.

Norrdin RW, Kawcak CE, Capwell BA, McIlwraith CW (1998): *Subchondral bone failure in an equine model of overload arthrosis.* Bone 22:133-139.

Oegema Jr TR, Johnson SL, Meglitsch T, Carpenter RJ (1996): *Prostaglandins and the zone of calcified cartilage in osteoarthritis.* Am J Therapeutics 3:139-149.

Owens JG, Kamerling SG, Stanton SR, Keowen ML, Prescott-Mathews JS (1996): *Effects of pretreatment with ketoprofen and phenylbutazone on experimentally induced synovitis in horses.* Am J Vet Res 57:866-874.

Parmigiani G, Garrett ES, Irizarry RA, Zeger SL (2003): *The analysis of gene expression data: an overview of methods and software.* In: Parmigiani G, Garrett ES, Irizarry RA, Zeger SL (Eds.): The analysis of gene expression data. pp. 1-45, Springer, New York

Patel OV, Suchyta SP, Sipkovsky SS, Yao J, Ireland JJ, Coussens PM, Smith GW (2005): *Validation and application of a high fidelity mRNA linear amplification procedure for profiling gene expression.* Vet Immun Immunopath 105:331-342.

Peng BG, Hou SX, Shi Q, Jia LS (2001): *The relationship between cartilage end-plate calcification and disc degeneration: an experimental study.* Chin Med J 114: 308-312.

Peri S, Navarro JD, Amanchy R, Kristiansen TZ, Jonnalagadda CK, Surendranath V, Niranjan V, Muthusamy B, Gandhi TK, Gronborg M, Ibarrola N, Deshpande N, Shanker K, Shivashankar HN, Rashmi BP, Ramya MA, Zhao Z, Chandrika KN, Padma N, Harsha HC, Yatish AJ, Kavitha MP, Menezes M, Choudhury DR, Suresh S, Ghosh N, Saravana R, Chandran S, Krishna S, Joy M, Anand SK, Madavan V, Joseph A, Wong GW, Schiemann WP, Constantinescu SN, Huang L, Khosravi-Far R, Steen H, Tewari M, Ghaffari S, Blobe GC, Dang CV, Garcia JG, Pevsner J, Jensen ON, Roepstorff P, Deshpande KS, Chinnaiyan AM, Hamosh A, Chakravarti A, Pandey A (2003): *Development of human protein reference database as an initial platform for approaching systems biology in humans.* Genome Res 13:2363-2371.

Pfander D, Cramer T, Deuerling D, Weseloh G, Swoboda B (2000): *Expression of thrombospondin-1 and its receptor CD36 in human osteoarthritic cartilage.* Ann Rheum Dis 59:448-54.

Pool RR (1996): *Pathologic manifestations of joint disease in the athletic horse.* In: McIlwraith CW, Trotter GW (Eds.): Joint Disease of the horse pp. 87-104, WB Saunders, Philadelphia

Poole AR, Ionescu M, Swan A, Dieppe PA (1994): *Changes in cartilage metabolism in arthritis are reflected by altered serum and synovial fluid levels of the cartilage proteoglycan aggrecan.* Implications for pathogenesis. J Clin Invest 94:25-33.

Raynauld J-P, Martel-Pelletier J, Berthiaume M-J, Beaudoin G, Choquette D, Haraoui B, Tannenbaum H, Meyer JM, Beary JF, Cline GA, Pelletier J-P (2006): *Long term evaluation of disease progression through the quantitative magnetic resonance imaging of symptomatic knee osteoarthritis patients: correlation with clinical symptoms and radiographic changes.* Arthritis Res Ther 8:R21.

Richardson DW, Dodge GR (2003): *Dose-dependent effects of corticosteroids on the expression of matrix-related genes in normal and cytokine-treated articular chondrocytes.* Inflamm Res 52:39-49.

Roshak AK, Callahan JF, Blake SM (2002): *Small-molecule inhibitors of NF-kappaB for the treatment of inflammatory joint disease.* Curr Opin Pharmacol 2:316-321.

Rossdale PD, Hopes R, Wingfield Digby NJ, Offord K (1985): *Epidemiological study of wastage among racehorses 1982 and 1983.* Vet. Rec. 116:66-68

Rutsch F, Terkeltaub R (2005): *Deficiencies of physiologic calcification inhibitors and low-grade inflammation in arterial calcification: lessons for cartilage calcification.* Joint Bone Spine 72:110-118.

Sandy JD, Adams ME, Billingham MEJ, Plaas A, Muir H (1984): *In vivo and in vitro stimulation of chondrocyte biosynthetic activity in early experimental osteoarthritis.* Arthritis Rheum 27:388-397.

Sato T, Konomi K, Yamasaki S, Aratani S, Tsuchimochi K, Yokouchi M, Masuko-Hongo K, Yagishita N, Nakamura H, Komiya S, Beppu M, Aoki H, Nishioka K, Nakajima T (2006): *Comparative analysis of gene expression profiles in intact and damaged regions of human osteoarthritic cartilage.* Arthritis Rheumatism 54:808-817.

Scharschmidt T Jacquet R, Hillyer J, Weiner S, Flanagan P, Landis WJ (2001): *RNA retrieval from frozen and archival osteoarthritic tissue utilizing laser capture microdissection* (Abstract). J Bone Mineral Res 16:S235.

Shao YY, Wang L, Hicks DG, Ballock RT (2006): *Analysis of gene expression in mineralized skeletal tissues by laser capture microdissection and RT-PCR.* Proc 51st Ann Meet Orthop Res Soc 52:0297.

Shikhman AR, Brinson DC, Lotz MK (2004): *Distinct pathways regulate facilitated glucose transport in human articular chondrocytes during anabolic and catabolic responses.* Am J Physiol Endocrinol Metab 286:E980-985.

Smith KJ, Bertone AL, Weisbrode SE, Radmacher M (2006): *Gross, histologic, and gene expression characteristics of osteoarthritic articular cartilage of the metacarpal condyle of horses.* Am J Vet Res 67:1299-1306.

Storey JD, Tibshirani R (2003): *Statistical significance for genomewide studies.* Proc Natl Acad Sci U S A 100:9440–9445.

Sugasawa T, Lenzen G, Simon S, Hidaka J, Cahen A, Guillaume JL, Camoin L, Strosberg AD, Nahmias C (2001): *The iodocyanopindolol and SM-11044 binding protein belongs to the TM9SF multispanning membrane protein superfamily.* Gene 273:227-237.

Suominen MM, Tulamo RM, Puupponen LM, Sankari SM (1999): *Effects of intra-articular injection of bufexamac suspension on amphotericin B-induced aseptic arthritis in horses.* Am J Vet Res 60:1467-1473.

Sweet MB, Thonar EJ, Immelman AR, Solomon L (1977): *Biochemical changes in progressive osteoarthrosis.* Ann Rheum Dis 36:387-398.

Swift GH, Peyton MJ, MacDonald RJ (2000): *Assessment of RNA quality by semi-quantitative RT-PCR of multiple regions of a long ubiquitous mRNA.* Biotechniques 28:524-531.

Takafuji VA, McIlwraith CW, Howard RD (2002): *Effects of equine recombinant interleukin-1alpha and interleukin-1beta on proteoglycan metabolism and prostaglandin E2 synthesis in equine articular cartilage explants.* Am J Vet Res 63:551-558.

Takafuji VA, Howard RD, Ward DL, Sharova LV, Crisman MV (2005): *Modulation of equine articular messenger RNA levels following brief exposure to recombinant equine interleukin-1beta.* Vet Immunol Immunopathol 106:23-38.

Tattersall, AL, Browning JA, Wilkins RJ (2005): *Modulation of H+ transport mechanisms by interleukin-1 in isolated bovine articular chondrocytes.* Cell Physiol Biochem 16:43-50.

Temple MM, Xue Y, Chen MQ, Sah RL (2006): *Interleukin-1alpha induction of tensile weakeningassociated with collagen degradation in bovine articular cartilage.* Arthritis Rheum 54:3267-3276.

Terkeltaub R, Johnson K, Murphy A, Ghosh S (2002): *Invited review: the mitochondrion in osteoarthritis.* Mitochondrion 1:301-319.

The Gene Ontology Consortium (2000): *Gene Ontology: tool for the unification of biology.* Nature Genet 25:25-29.

Todhunter RJ (1990): *Pathophysiology of synovitis: clinical signs and examination in horses.* Comp. Cont. Education Pract. Vet. 12:988-991

Todhunter PG, Kincaid SA, Todhunter RJ, Kammermann JR, Johnstone B, Baird AN, Hanson RR, Wright JM, Lin HC, Purohit RC (1996): *Immunohistochemical analysis of an equine model of synovitis-induced arthritis.* Am J Vet Res 57:1080-1093.

Tyler JA (1985): *Chondrocyte-mediated depletion of articular cartilage proteoglycans in vitro.* Biochem J 225:493-507.

USDA (2000): *Lameness and laminitis in U.S. horses.* USDA:APHIS:VS, CEAH, National Animal Health Monitoring System. Fort Collins, CO. #N318.0400.

Van Gelder RN, von Zastrow ME, Yool A, Dement WC, Barchas JD, Eberwine JH (1990): *Amplified RNA synthesized from limited quantities of heterogeneous cDNA.* Proc Natl Acad Sci USA 87:1663-1667.

Vasan N (1980): *Proteoglycans in normal and severely osteoarthritic human cartilage.* Biochem J 187:781-787.

Vincent T, Saklatvala J (2006): *Basic fibroblast growth factor: an extracellular mechanotransducer in articular cartilage?* Biochem Soc Trans 34:456-457.

Vincenti MP, Brinckerhoff CE (2002): *Transcriptional regulation of collagenase (MMP-1, MMP-13) genes in arthritis: integration of complex signaling pathways for the recruitment of gene-specific transcription factors.* Arthritis Res 4:157-164.

Visco DM, Johnstone B, Hill MA, Jolly GA, Caterson B (1993): *Immunohistochemical analysis of 3-B-3(-) and 7-D-4 epitope expression in canine and human osteoarthritis.* Arthritis Rheum 36:1718-1725.

Wachsmuth L, Bau B, Fan Z, Pect A, Gerwin N, Aigner T (2004): *ADAMTS-1, a gene of articular chondrocytes in vivo and in vitro, is downregulated by interleukin 1beta.* J Rheumatol 31:315-320.

Wang Y, Middleton F, Horton JA, Reichel L, Farnum CE, Damron TA (2004): *Microarray analysis of proliferative and hypertrophic growth plate zones identifies differentiation markers and signal pathways.* Bone 35:1273-1293.

Wong M, Carter DR (2003): *Articular cartilage functional histomorphology and mechanobiology: a research perspective.* Bone 33:1-13.

Yoshida K, Suzuki Y, Saito A, Fukuda K, Hamanishi C, Munakata H (2005): Aggrecanase-1 (ADAMTS-4) interacts with α1-antitrypsin. Biochim Biophys Acta 1725:152-159.

Zhang H, Liew CC, Marshall KW (2002): *Microarray analysis reveals the involvement of beta-2 microglobulin (B2M) in human osteoarthritis.* Osteoarthritis Cartilage 10:950-960.

# 7 *Appendix: Detailed Protocols*

## 1. RNA Isolation from Macroscopic Cartilage Samples

(1) Pulverize cartilage in manual pulverizer:
(2) place frozen cartilage into sterilized pulverizer, hit plunger at least 10 times, add 500µl Trizol to powder to get a pellet, place pellet into 14ml Falcon tube on ice. *(#1 falcon tube)*
(3) Add more trizol (up to 0.025ml/mg)
(4) Homogenize with the tube in ice for 30 seconds
(5) Incubate for 5 minutes at room temperature
(6) Transfer liquid into microcentrifuge tubes (2ml/tube) *(#1 micro tube)*
(7) Centrifuge at 10,000xg (9500rpm in the Sorval centrifuge) for 10 minutes at 4°C
(8) Decant supernatant into new Falcon tube *(#2 falcon tube)*
(9) Add ½ volume of trizol to pellet, mix well, transfer into falcon tube *(#3 falcon tube)*
(10) Repeat homogenization
(11) Incubate for 5 minutes at room temperature
(12) Transfer liquid into microcentrifuge tubes (up to 2ml/tube) *(#2 micro tube)*
(13) Centrifuge at 10,000xg for 10 minutes at 4°C
(14) Decant supernatant into new #2 Falcon tube *(same as in step 5)*
*(15) OK to freeze here (-70°C, up to 6 months)*
(16) Add chloroform (0.2ml/ml trizol) to supernatant
(17) Vortex for 15 seconds
(18) Incubate for 3 minutes at room temperature
(19) Transfer liquid into microcentrifuge tubes (2ml/tube) *(#3 micro tube)*
(20) Centrifuge at 10,000xg for 15 minutes at 4°C
(21) Move aqueous phase to new Falcon tube, avoid the interphase! *(#4 falcon tube)*
(22) To the aqueous phase, add 400µl of chloroform
(23) Vortex for 15 seconds
(24) Incubate for 3 minutes at room temperature
(25) Transfer liquid into microcentrifuge tubes (2ml/tube) *(#4 micro tube)*
(26) Centrifuge at 10,000xg for 15 minutes at 4°C
(27) Move aqueous phase to new microcentrifuge tube (600µl/tube), avoid the interphase! *(#1 1.5ml micro tube – use clear conical tube so you can see the RNA pellet!)* Measure as you move!
(28) Add 1.05 volumes (630µl/tube) of isopropanol (100%) to aqueous phase

(29) Invert to mix – don't vortex!
(30) Incubate at room temperature for 10 minutes
(31) Centrifuge at 10,000xg for 10 minutes at 4°C
(32) Decant supernatant into falcon tube *(#5 falcon tube – keep in case pellet was loose)*
(33) Add 70% EtOH (0.8ml/mltrizol used = 1.3ml/tube)
(34) Vortex 15 seconds
*(35) OK to freeze here (-70°C, up to 12 months)*
(36) Centrifuge at 10,000xg for 10 minutes at 4°C
(37) Decant supernatant into falcon tube *(#6 falcon tube – keep in case pellet was loose)*
(38) Let microcentrifuge tube sit and dry thoroughly – hopefully you can see the pellet.
(39) Start RNA cleanup using the RNeasy mini kit (Qiagen) – start on page 80:
(40) Adjust the sample to a volume of 100µl with nuclease-free $H_2O$. Add 350µl Buffer RLT, vortex well. If you have 3 microcentrifuge tubes, use 33.3µl $H_2O$/tube and 116.7µl Buffer RLT/tube, then combine them into 1 tube.
(41) Add 250µl 100% EtOH, mix well by pipetting up and down.
(42) Pipet sample onto an RNeasy mini column.
(43) Centrifuge at 8000xg for 15 seconds.
(44) Reload flowthrough onto the same column.
(45) Centrifuge at 8000xg for 15 seconds.
(46) Discard flowthrough and collection tube, place column into new collection tube.
(47) Pipet 350µl Buffer RW1 onto column.
(48) Centrifuge at 8000xg for 15 seconds.
(49) Add 80µl DNase incubation mix directly onto the column.
(50) Incubate at room temperature for 15 minutes.
(51) Pipet 350µl Buffer RW1 onto column.
(52) Centrifuge at 8000xg for 15 seconds.
(53) Discard flowthrough.
(54) Pipet 500µl Buffer RPE onto column.
(55) Centrifuge at 8000xg for 15 seconds.
(56) Discard flowthrough.
(57) Pipet 500µl Buffer RPE onto column.
(58) Centrifuge at 8000xg for 2 minutes.
(59) Place column into new collection tube and centrifuge at full speed for 1 minute
(60) Place column into sample elution tube. Pipet 32µl nuclease-free $H_2O$ directly onto column.
(61) Centrifuge at 8000xg for 1 minute
(62) Reload flowthrough onto the same column.
(63) Centrifuge at 8000xg for 1 minute.

DNase incubation mix (/1sample):
10µl DNase stock
+70µl Buffer RDD
(Qiagen RNase-free DNase Set 79254)

(64) Quantitate and quality control RNA with a spectrophotometer and the Bioanalyzer Nano Chip.
(65) Store RNA at -80°C.

## 2. Laser Capture Microdissection of Adult Articular Cartilage

8 caps will be captured to be combined into 1 sample, the PicoPure RNA isolation kit (Arcturus) is used for RNA extraction.

**Preparations:**

(1) Store your slides in a slide box in the -80°C chest freezer.
(2) Preclean all surfaces with ethanol – be especially thorough if the workspace has not been used for a while – you will see why.... (dust, dust, dust).
(3) Start the computer and the Autopix program.
(4) Check that the incubator is actually at 42°C, get ice to cool the staining jars.
(5) Clean all surfaces and especially the forceps and glass Petri dish with RNaseZap. Also wipe off the tray of the Autopix – especially where the caps are unloaded!
(6) Make sure you have a timer, a rack for the staining jars in the hood, the forceps in the petri dish, some kimwipes, a sharpie, gloves, the cap handle (Arcturus), and double-sided tape, as well as the LCM log sheet.
(7) Place 4 staining jars into the ice cooler (submerged up to the lid)
(8) Use the HistoGene Kit (Arcturus) for the following:
(9) Fill the 1st jar with 75% EtOH, the 2nd with 95% EtOH, the 3rd with 100% EtOH, the 4th with xylene. (Open the xylene only under a hood – have the jar closed when on ice.)
(10) Prepare 8 tubes (0.5ml thin-walled PCR tubes, Applied Biosystems) by adding 35µl extraction buffer (PicoPure Kit, Arcturus) to each. Keep the tubes in a rack in a ziplock bag.
(11) Load the MacroCaps (8 total) into the Autopix.

**Actual Protocol** (wear gloves, RNaseZap them and change them frequently!!!):

(1) Take the 75%EtOH jar into the -80°C freezer.
(2) Place a slide into the jar.
(3) Start your 14 minute timer immediately!
(4) Walk back to the hood.
(5) Place jar in ice.
(6) Once your timer is at 13:30 minutes, move the slide with the forceps to the 95%EtOH.
(7) After 30 seconds, move the slide with the forceps to the 100%EtOH.
(8) After 30 seconds, move the slide with the forceps to the xylene. Do this under the hood! Move the slide up and down until the slide seems to not have any "streaks" anymore.
(9) After 1 minute, take the slide out of the xylene, close the xylene and place on ice again.

(10) Air and kimwipe dry the slide without touching a place that could be touched by the cap.
(11) Try to grossly locate the section on the slide and place it into the Autopix even before it is completely dry.
(12) Capture at 10x, start with these settings:
(13) Power: 100mW (that's the max)
(14) Pulse: 1500µsec (can go higher if you want a greater spot size or lower for smaller spot size)
(15) Hits: 1-5 (3 or 5 will increase the spot size and wetting) (you can go higher, but I expect more heat damage...)
(16) Delay: 20 µsec (If you use more than 5 hits, I would increase this, to allow for cooling between hits.)
(17) Intensity: 215mV
(18) You can use the counter to estimate cells you captured – if you do single cell capture.
(19) Stop capturing immediately once your 14 minute timer goes off!
(20) Get the cap out of the Autopix, using the cap handle, stick it to the double sided tape to remove any debris or unwanted cells, place it on top of a tube with extraction buffer. Turn the tube around and tap it gently on the counter to ascertain full coverage of the polymer membrane.
(21) Label the tube and cap.
(22) You can keep this cap at room temp for up to 2 hours, then it needs to be incubated at 42°C for 30 minutes.
(23) After incubation, centrifuge the tubes for 2 minutes at 800xg.
(24) Vortex the tubes well for 10 seconds, spin them down at 800xg for 10 seconds. (This will shear the longer DNA molecules and improves the DNase digestion later!)
(25) Freeze the tubes at -80°C until RNA extraction.

## 3. RNA Isolation from Laser Captured Samples

8 caps (35µl extraction buffer/cap) will be combined into 1 sample, double-loaded, DNase treated and double eluted. The PicoPure RNA isolation kit (Arcturus) is used.

(1) Place column in extra flowthrough tube, place lid on original flowthrough tube.
(2) Precondition the column with 250µl conditioning buffer.
(3) Incubate at room temp for 5 minutes.
(4) Centrifuge at 16,000xg for 1 minute.
(5) Place column back in original flowthrough tube, discard extra flowthrough tube.
(6) Thaw 4 of the 8 tubes and combine them into 1 tube.
(7) Add 140µl of 70% EtOH, pipette up and down.
(8) Pipette sample (280 µl) onto preconditioned column.
(9) Centrifuge column at 100xg for 2 minutes, followed by 16,000xg for 30 seconds.
(10) Reload flowthrough onto column.
(11) Centrifuge column at 100xg for 2 minutes, followed by 16,000xg for 30 seconds.
(12) Discard flowthrough.
(13) Thaw the remaining 4 tubes and combine them into 1 tube.
(14) Add 140µl of 70% EtOH, pipette up and down.
(15) Pipette sample (280 µl) onto column.
(16) Centrifuge column at 100xg for 2 minutes, followed by 16,000xg for 30 seconds.
(17) Reload flowthrough onto column.
(18) Centrifuge column at 100xg for 2 minutes, followed by 16,000xg for 30 seconds.
(19) Discard flowthrough.
(20) Add 100µl Wash Buffer 1 to column.
(21) Centrifuge at 8,000xg for 1 minute.

| DNase incubation mix (/1sample): |
| --- |
| 7µl DNase Stock + 35µl RDD Buffer |

(22) Add 40µl DNase incubation mix directly onto the column.
(23) Incubate at room temp for 15 minutes.
(24) Add 40µl Wash Buffer 1 to column.
(25) Centrifuge at 8,000xg for 15 seconds.
(26) Add 100µl Wash Buffer 2 to column.
(27) Centrifuge at 8,000xg for 1 minute.
(28) Add 100µl Wash Buffer 2 to column.
(29) Centrifuge at 16,000xg for 2 minutes.
(30) Make sure no buffer remains on or around column. (If so, place column in new flowthrough tube and centrifuge at 16,000xg for 1 minute.)
(31) Transfer column to new elution tube.
(32) Add 12µl Elution Buffer directly onto column.
(33) Incubate at room temp for 1 minute.
(34) Centrifuge at 1,000xg for 1 minute, followed by 16,000xg for 1 minute.

(35) Reload flowthrough onto column.
(36) Centrifuge at 1,000xg for 1 minute, followed by 16,000xg for 1 minute.
(37) Place on ice for capillary electrophoresis (Bioanalyzer Pico Chip, Agilent).
(38) Store RNA at -80°C.

## 4. 1st Strand cDNA Synthesis

(SuperScript™ III First-Strand Synthesis System, Cat. No: 18080-051, Invitrogen)

For the reverse transcription of 1pg-5µg of total RNA or 1pg-500ng of mRNA into 1st strand cDNA:

(1) Mix and spin down all solutions before use (__samples x __replicates = __Rxns)

(2) Combine the following: used:

(3) RNA up to 8 µl..... _____µl

(4) Primer* 1 µl..... _____µl

(5) dNTP 1 µl..... _____µl

(6) nuclease-free water to 10 µl..... _____µl

(7) Incubate at 65°C for 5 minutes

(8) Place on ice for at least 1 minute

(9) Prepare Mastermix in the exact order 1Rx 2Rxns __Rxns

(10) RT buffer 2 µl 5 µl _____µl

(11) $MgCl_2$ 4 µl 10 µl _____µl

(12) DTT 2 µl 5 µl _____µl

(13) RNaseOUT 1 µl 2.5 µl _____µl

(14) SuperScript III RT 1 µl 2.5 µl _____µl

(15) Add 10 µl of Mastermix to each RNA/primer mixture, mix gently, spin down

(16) Incubate at 25°C for 10 minutes if **random hexamers** used as primers (omit for **dTprimers**)

(17) Incubate at 50°C for 50 minutes

(18) Incubate at 85°C for 5 minutes

(19) Chill on ice

(20) Spin down

(21) Store at -20°C

## 5. Real-Time PCR

A total of 25µl (reaction mix plus sample) is used per well. All samples are run in triplicates. Following controls are used: (1) $H_2O$ instead of sample in reaction mix, (2) Not reverse transcribed (SSIII omitted during reverse transcription) sample in reaction mix. Keep all solutions, as well as the 96 well plate on ice.

(1) Make a template of sample and gene allocations for the 96 well plate.
(2) Start ABI 7000 (Applied Biosystems, Foster City, CA) to warm up the bulb and enter template into program.
(3) Per well, dilute 12.5µl Mastermix (TaqMan Mastermix, Applied Biosystems, Foster City, CA) with 6.3µl nuclease-free $H_2O$. Add extra for multiple wells (1 extra reaction per 10 wells).
(4) Per well, make up the primer and probe mix with 18.8µl diluted mastermix plus 1.2µl primer/probe stock (Lucy Whittier Molecular & Diagnostic Core Facility, UCDavis, Davis, CA). Add extra for multiple wells (1 extra reaction per 15 wells)
(5) Add 20µl of primer and probe mix into each designated well.
(6) Add 5µl sample cDNA into each designated well.
(7) Place adhesive cover over the 96 well plate. Make sure it seals 100%!
(8) Spin down plate briefly.
(9) Vortex plate for 10 seconds.
(10) Spin down plate briefly.
(11) Place plate into ABI 7000 and start PCR.

Cycle settings (40 cycles): 2 minutes at 50°C, 10 minutes at 95°C, 1 minute at 60°C.

## 6. *In-vitro* Transcription Amplification (2 rounds for subsequent qrtPCR)

(The RiboAmp HS RNA amplification kit (Arcturus Biosciences, Mountain View, CA) is used. The Poly(dIdC) (#27-7880-01, GE Healthcare, Piscataway, NJ) was reconstituted to a final concentration of 200 ng/µl: 2500µl of RNase-free water were added to the vial of 500µg (=10IU).

(1) Add 1µl polydIdC (=200ng) to the RNA sample (final volume 11-12µl)

(2) Add 1µl primer 1 (oligo dT/T7), incubate at 65°C for 5 min, then hold at 4°C for 1-5 min

(3) Add 9µl 1st strand synthesis mix, incubate at 42°C for 1h, then hold at 4°C for 1-30 min

1st strand synthesis mix (/1 sample): Add together 2µl HS enhancer, 5µl 1st strand mastermix, 2µl 1st strand enzyme mix

(4) Add 2µ 1st strand nuclease mix, incubate at 37°C for 30 min, then at 95°C for 5 min, then hold at 4°C for 1-30 min

(5) Add 1µl primer 2 (random hexamers), incubate at 95°C for 2 min, then hold at 4°C for 2-5 min

(6) Add 30µl 2nd strand synthesis mix, incubate at 25°C for 10 min, then at 37°C for 30 min, then at 70°C for 5 min, then hold at 4°C for 1-30 min

2nd strand synthesis mix (/1 sample): Add together 29µl 2nd strand mastermix, 1µl 2nd strand enzyme mix

(7) Precondition purification column with 250µl DNA binding buffer, incubate at room temp for 5 min, then spin at 16000xg for 1 min

(8) Place column into new collection tube

(9) Add 200µl DNA binding buffer to sample, mix, load onto column. Centrifuge at 100xg for 2 min, followed by 10000xg for 1 min.

(10) Reload flowthrough onto the same column, centrifuge at 100xg for 2 min, followed by 10000xg for 1 min.

(11) Load 250µl wash buffer onto column, centrifuge at 16000xg for 2 min

(12) Place column into new sample collection tube

(13) Add 11µl DNA elution buffer directly onto the column, incubate at room temp for 1 min, centrifuge at 1000xg for 1 min, then at 16000xg for 1 min.

(14) Reload flowthrough onto the same column, incubate at room temp for 1 min, centrifuge at 1000xg for 1 min, then at 16000xg for 1 min.

(15) Add 11µl IVT reaction mix, incubate at 42°C for 6h, then hold at 4°C for 1 min up to overnight

IVT reaction mix (/1 sample): Add together 2µl HS enhancer, 2µl IVT buffer, 6µl IVT mastermix, 2µl IVT enzyme mix

(16) Add 1µl DNase mix, incubate at 37°C for 15 min, then hold at 4°C for 1-15 min

(17) Precondition purification column with 250µl RNA binding buffer, incubate at room temp for 5 min, then spin at 16000xg for 1 min

(18) Place column into new collection tube

(19) Add 120µl RNA binding buffer to sample, mix, load onto column. Centrifuge at 100xg for 2 min, followed by 10000xg for 1 min.

(20) Reload flowthrough onto the same column, centrifuge at 100xg for 2 min, followed by 10000xg for 1 min.
(21) Load 200µl wash buffer onto column, centrifuge at 10000xg for 1 min
(22) Load 200µl wash buffer onto column, centrifuge at 16000xg for 2 min
(23) Place column into new sample collection tube
(24) Add 12µl RNA elution buffer directly onto the column, incubate at room temp for 1 min, centrifuge at 1000xg for 1 min, then at 16000xg for 1 min.
(25) Reload flowthrough onto the same column, incubate at room temp for 1 min, centrifuge at 1000xg for 1 min, then at 16000xg for 1 min.
(26) Add 1µl primer 2 (random hexamers) to eluted sample, incubate at 65°C for 5 min, then hold at 4°C for 1-5 min
(27) Add 9µl 1st strand synthesis mix, incubate at 25°C for 10 min, then at 37°C for 1h, then hold at 4°C for 1-30 min
1st strand synthesis mix (/1 sample): Add together 2µl HS enhancer, 5µl 1st strand mastermix, 2µl 1st strand enzyme mix
(28) Add 1µl primer 3 (oligo dT/T7), incubate at 95°C for 5 min, then hold at 4°C for 1-5 min
(29) Add 30µl 2nd strand synthesis mix, incubate at 37°C for 30 min, then at 70°C for 5 min, then hold at 4°C for 1-30 min
2nd strand synthesis mix (/1 sample): Add together 29µl 2nd strand mastermix, 1µl 2nd strand enzyme mix
(30) Precondition purification column with 250µl DNA binding buffer, incubate at room temp for 5 min, then spin at 16000xg for 1 min
(31) Place column into new collection tube
(32) Add 200µl DNA binding buffer to sample, mix, load onto column. Centrifuge at 100xg for 2 min, followed by 10000xg for 1 min.
(33) Reload flowthrough onto the same column, centrifuge at 100xg for 2 min, followed by 10000xg for 1 min.
(34) Load 250µl wash buffer onto column, centrifuge at 16000xg for 2 min
(35) Place column into new sample collection tube
(36) Add 11µl DNA elution buffer directly onto the column, incubate at room temp for 1 min, centrifuge at 1000xg for 1 min, then at 16000xg for 1 min.
(37) Reload flowthrough onto the same column, incubate at room temp for 1 min, centrifuge at 1000xg for 1 min, then at 16000xg for 1 min.
(38) Add 12µl IVT reaction mix, incubate at 42°C for 6h, then hold at 4°C for 1 min up to overnight
IVT reaction mix (/1 sample): Add together 2µl HS enhancer, 2µl IVT buffer, 6µl IVT mastermix, 2µl IVT enzyme mix
(39) Add 1µl DNase mix, incubate at 37°C for 15 min, then hold at 4°C for 1-15 min
(40) Precondition purification column with 250µl RNA binding buffer, incubate at room temp for 5 min, then spin at 16000xg for 1 min
(41) Place column into new collection tube
(42) Add 120µl RNA binding buffer to sample, mix, load onto column. Centrifuge at 100xg for 2 min, followed by 10000xg for 1 min.
(43) Reload flowthrough onto the same column, centrifuge at 100xg for 2 min, followed by 10000xg for 1 min.

(44) Load 200µl wash buffer onto column, centrifuge at 10000xg for 1 min
(45) Load 200µl wash buffer onto column, centrifuge at 16000xg for 2 min
(46) Place column into new sample collection tube
(47) Add 30µl RNA elution buffer directly onto the column, incubate at room temp for 1 min, centrifuge at 1000xg for 1 min, then at 16000xg for 1 min.
(48) Reload flowthrough onto the same column, incubate at room temp for 1 min, centrifuge at 1000xg for 1 min, then at 16000xg for 1 min.
(49) Store RNA at -80°C

## 7. *In-vitro* Transcription Amplification (2 rounds for subsequent gene array analysis)

(The RiboAmp HS RNA amplification kit (Arcturus Biosciences, Mountain View, CA) is used for the 1st round of amplification and generation of dscDNA. The Poly(dIdC) (#27-7880-01, GE Healthcare, Piscataway, NJ) was reconstituted to a final concentration of 200 ng/µl: 2500µl of RNase-free water were added to the vial of 500µg (=10IU). The GeneChip® IVT Labeling Kit (Affymetrix, Santa Clara, CA) is used for the second round of amplification. The Affymetrix sample cleanup module is used for labeled RNA purification.

(1) Add 1µl polydIdC (=200ng) to the RNA sample (final volume 11-12µl)

(2) Add 1µl primer 1 (oligo dT/T7), incubate at 65°C for 5 min, then hold at 4°C for 1-5 min

(3) Add 9µl 1st strand synthesis mix, incubate at 42°C for 1h, then hold at 4°C for 1-30 min

1st strand synthesis mix (/1 sample): Add together 2µl HS enhancer, 5µl 1st strand mastermix, 2µl 1st strand enzyme mix

(4) Add 2µ 1st strand nuclease mix, incubate at 37°C for 30 min, then at 95°C for 5 min, then hold at 4°C for 1-30 min

(5) Add 1µl primer 2 (random hexamers), incubate at 95°C for 2 min, then hold at 4°C for 2-5 min

(6) Add 30µl 2nd strand synthesis mix, incubate at 25°C for 10 min, then at 37°C for 30 min, then at 70°C for 5 min, then hold at 4°C for 1-30 min

2nd strand synthesis mix (/1 sample): Add together 29µl 2nd strand mastermix, 1µl 2nd strand enzyme mix

(7) Precondition purification column with 250µl DNA binding buffer, incubate at room temp for 5 min, then spin at 16000xg for 1 min

(8) Place column into new collection tube

(9) Add 200µl DNA binding buffer to sample, mix, load onto column. Centrifuge at 100xg for 2 min, followed by 10000xg for 1 min.

(10) Reload flowthrough onto the same column, centrifuge at 100xg for 2 min, followed by 10000xg for 1 min.

(11) Load 250µl wash buffer onto column, centrifuge at 16000xg for 2 min

(12) Place column into new sample collection tube

(13) Add 11µl DNA elution buffer directly onto the column, incubate at room temp for 1 min, centrifuge at 1000xg for 1 min, then at 16000xg for 1 min.

(14) Reload flowthrough onto the same column, incubate at room temp for 1 min, centrifuge at 1000xg for 1 min, then at 16000xg for 1 min.

(15) Add 11µl IVT reaction mix, incubate at 42°C for 6h, then hold at 4°C for 1 min up to overnight

IVT reaction mix (/1 sample): Add together 2µl HS enhancer, 2µl IVT buffer, 6µl IVT mastermix, 2µl IVT enzyme mix

(16) Add 1µl DNase mix, incubate at 37°C for 15 min, then hold at 4°C for 1-15 min

(17) Precondition purification column with 250µl RNA binding buffer, incubate at room temp for 5 min, then spin at 16000xg for 1 min

(18) Place column into new collection tube

(19) Add 120µl RNA binding buffer to sample, mix, load onto column. Centrifuge at 100xg for 2 min, followed by 10000xg for 1 min.
(20) Reload flowthrough onto the same column, centrifuge at 100xg for 2 min, followed by 10000xg for 1 min.
(21) Load 200µl wash buffer onto column, centrifuge at 10000xg for 1 min
(22) Load 200µl wash buffer onto column, centrifuge at 16000xg for 2 min
(23) Place column into new sample collection tube
(24) Add 12µl RNA elution buffer directly onto the column, incubate at room temp for 1 min, centrifuge at 1000xg for 1 min, then at 16000xg for 1 min.
(25) Reload flowthrough onto the same column, incubate at room temp for 1 min, centrifuge at 1000xg for 1 min, then at 16000xg for 1 min.
(26) Use 1µl sample to quantify RNA yield with the Nanodrop 1000
(27) Add the adequate amount of PolyA RNA controls (Affymetrix, Santa Clara, CA)
Add 2µl of 1:500000 (v/v) diluted PolyA RNA control per 1 ng of RNA to RNA sample.
(28) Add 1µl primer 2 (random hexamers) to sample, incubate at 65°C for 5 min, then hold at 4°C for 1-5 min
(29) Add 9µl 1st strand synthesis mix, incubate at 25°C for 10 min, then at 37°C for 1h, then hold at 4°C for 1-30 min
1st strand synthesis mix (/1 sample): Add together 2µl HS enhancer, 5µl 1st strand mastermix, 2µl 1st strand enzyme mix
(30) Add 1µl primer 3 (oligo dT/T7), incubate at 95°C for 5 min, then hold at 4°C for 1-5 min
(31) Add 30µl 2nd strand synthesis mix, incubate at 37°C for 30 min, then at 70°C for 5 min, then hold at 4°C for 1-30 min
2nd strand synthesis mix (/1 sample): Add together 29µl 2nd strand mastermix, 1µl 2nd strand enzyme mix
(32) Precondition purification column with 250µl DNA binding buffer, incubate at room temp for 5 min, then spin at 16000xg for 1 min
(33) Place column into new collection tube
(34) Add 200µl DNA binding buffer to sample, mix, load onto column. Centrifuge at 100xg for 2 min, followed by 10000xg for 1 min.
(35) Reload flowthrough onto the same column, centrifuge at 100xg for 2 min, followed by 10000xg for 1 min.
(36) Load 250µl wash buffer onto column, centrifuge at 16000xg for 2 min
(37) Place column into new sample collection tube
(38) Add 12µl DNA elution buffer directly onto the column, incubate at room temp for 1 min, centrifuge at 1000xg for 1 min, then at 16000xg for 1 min.
(39) Reload flowthrough onto the same column, incubate at room temp for 1 min, centrifuge at 1000xg for 1 min, then at 16000xg for 1 min.
(40) Store sample at -20°C until further amplification with the Affymetrix IVT labeling kit.
(41) Add 8µl $H_2O$, 4µl 10X IVT labeling buffer, 12µl IVT labeling NTP mix, 4µl labeling enzyme mix to sample. Mix gently and spin down very briefly.
(42) Incubate at 37°C for 16 hours.
(43) Add 60µl $H_2O$ to sample, vortex for 3 sec
(44) Add 350µl IVT cRNA Binding Buffer to sample, vortex for 3 sec

(45) Add 250µl EtOH (100%), mix by pipetting up and down
(46) Add sample onto the Spin column, centrifuge at 8000xg for 15 sec
(47) Discard flowthrough and collection tube, place column into new tube.
(48) Add 500µl cRNA wash buffer onto column, centrifuge at 8000xg for 15 sec
(49) Discard flowthrough
(50) Add 500µl EtOH (80% v/v) onto column, centrifuge at 8000xg for 15 sec
(51) Discard flowthrough
(52) Open the cap of the column, centrifuge at 16000xg for 5 min
(53) Discard flowthrough and collection tube, place column into new sample collection tube
(54) Add 11µl $H_2O$ directly onto the column, centrifuge at 16000xg for 1 minute
(55) Add 10µl $H_2O$ directly onto the column, centrifuge at 16000xg for 1 minute
(56) To determine RNA yield, dilute a sample aliquot 1:100 to 1:200 and use the Nanodrop 1000.
(57) Store labeled RNA at -80°C